NUREG/CR–4832
SAND92–0537
Vol. 7

Analysis of the LaSalle Unit 2 Nuclear Power Plant: Risk Methods Integration and Evaluation Program (RMIEP)

External Event Scoping Quantification

Prepared by
M. K. Ravindra, H. Banon

NTS/Structural Mechanics Associates

Sandia National Laboratories

Prepared for
U.S. Nuclear Regulatory Commission

AVAILABILITY NOTICE

Availability of Reference Materials Cited in NRC Publications

Most documents cited in NRC publications will be available from one of the following sources:

1. The NRC Public Document Room, 2120 L Street, NW., Lower Level, Washington, DC 20555
2. The Superintendent of Documents, U.S. Government Printing Office, P.O. Box 37082, Washington, DC 20013-7082
3. The National Technical Information Service, Springfield, VA 22161

Although the listing that follows represents the majority of documents cited in NRC publications, it is not intended to be exhaustive.

Referenced documents available for inspection and copying for a fee from the NRC Public Document Room include NRC correspondence and internal NRC memoranda; NRC bulletins, circulars, information notices, inspection and investigation notices; licensee event reports; vendor reports and correspondence; Commission papers; and applicant and licensee documents and correspondence.

The following documents in the NUREG series are available for purchase from the GPO Sales Program: formal NRC staff and contractor reports, NRC-sponsored conference proceedings, international agreement reports, grant publications, and NRC booklets and brochures. Also available are regulatory guides, NRC regulations in the *Code of Federal Regulations,* and *Nuclear Regulatory Commission Issuances*.

Documents available from the National Technical Information Service include NUREG-series reports and technical reports prepared by other Federal agencies and reports prepared by the Atomic Energy Commission, forerunner agency to the Nuclear Regulatory Commission.

Documents available from public and special technical libraries include all open literature items, such as books, journal articles, and transactions. *Federal Register* notices, Federal and State legislation, and congressional reports can usually be obtained from these libraries.

Documents such as theses, dissertations, foreign reports and translations, and non-NRC conference proceedings are available for purchase from the organization sponsoring the publication cited.

Single copies of NRC draft reports are available free, to the extent of supply, upon written request to the Office of Administration, Distribution and Mail Services Section, U.S. Nuclear Regulatory Commission, Washington, DC 20555.

Copies of industry codes and standards used in a substantive manner in the NRC regulatory process are maintained at the NRC Library, 7920 Norfolk Avenue, Bethesda, Maryland, for use by the public. Codes and standards are usually copyrighted and may be purchased from the originating organization or, if they are American National Standards, from the American National Standards Institute, 1430 Broadway, New York, NY 10018.

NUREG/CR-4832
SAND92-0537
Vol. 7
RX

Analysis of the LaSalle Unit 2 Nuclear Power Plant: Risk Methods Integration and Evaluation Program (RMIEP)

External Event Scoping Quantification

Manuscript Completed: February 1985
Date Published: July 1992

Prepared by
M. K. Ravindra[1], H. Banon[2]

NTS/Structural Mechanics Associates
5160 Birch Street
Newport Beach, CA 92660

Under Contract to:
Sandia National Laboratories
Albuquerque, NM 87185

Prepared for
Division of Safety Issue Resolution
Office of Nuclear Regulatory Research
U.S. Nuclear Regulatory Commission
Washington, DC 20555
NRC FIN A1386

[1]Currently with EQE, Inc., Costa Mesa, CA
[2]Currently with Exxon Production Research, Houston, TX

NRC FORM 335 (2-89) NRCM 1102, 3201, 3202

U.S. NUCLEAR REGULATORY COMMISSION

BIBLIOGRAPHIC DATA SHEET

(See instructions on the reverse)

1. REPORT NUMBER (Assigned by NRC. Add Vol., Supp., Rev., and Addendum Numbers, if any.)

NUREG/CR-4832
SAND92-0537
Vol. 7

2. TITLE AND SUBTITLE

Analysis of the LaSalle Unit 2 Nuclear Power Plant:
Risk Methods Integration and Evaluation Program (RMIEP)

External Event Scoping Quantification

3. DATE REPORT PUBLISHED

MONTH: July YEAR: 1992

4. FIN OR GRANT NUMBER

A1386

5. AUTHOR(S)

M.K. Ravindra, H. Banon

6. TYPE OF REPORT

Technical

7. PERIOD COVERED (Inclusive Dates)

8. PERFORMING ORGANIZATION – NAME AND ADDRESS (If NRC, provide Division, Office or Region, U.S. Nuclear Regulatory Commission, and mailing address. If contractor, provide name and mailing address.)

NTS/Structural Mechanics Associates
5160 Birch Street
Newport Beach, CA 92660

Under Contract to:
Sandia National Laboratories
Albuquerque, NM 87185

9. SPONSORING ORGANIZATION – NAME AND ADDRESS (If NRC, type "Same as above"; if contractor, provide NRC Division, Office or Region, U.S. Nuclear Regulatory Commission, and mailing address.)

Division of Safety Issue Resolution
Office of Nuclear Regulatory Research
US Nuclear Regulatory Commission
Washington, DC 20555

10. SUPPLEMENTARY NOTES

11. ABSTRACT (200 words or less)

This report is a description of the scoping quantification study which selected the external events to be included in the Level III PRA of the LaSalle County Nuclear Generating Station Unit 2. The study was performed by NTS/Structural Mechanics Associates (SMA) for Sandia National Laboratories as part of the Level I analysis being performed by the Risk Methods Integration and Evaluation Program (RMIEP). The methodology used is described in detail in a companion report, NUREG/CR-4839. In this report, we describe the process for selecting the external events, the screening analysis, and the detailed bounding calculations for those events not eliminated in the screening analysis. As a result of this analysis, it was concluded that only internal flooding, internal fire, and seismic events were potentially significant at LaSalle. Detailed analyses were performed for each of these and are reports in NUREG/CR-4832, Volumes 10, 9, and 8, respectively.

12. KEY WORDS/DESCRIPTORS (List words or phrases that will assist researchers in locating the report.)

External Events
PRA Methods
Risk Methods Integration and Evaluation Program (RMIEP)
Screening Procedures

13. AVAILABILITY STATEMENT

Unlimited

14. SECURITY CLASSIFICATION

(This Page) Unclassified

(This Report) Unclassified

15. NUMBER OF PAGES

16. PRICE

NRC FORM 335 (2-89)

ABSTRACT

This report is a description of the scoping quantification study which selected the external events to be included in the Level III PRA of the LaSalle County Nuclear Generating Station Unit II. The study was performed by NTS/Structural Mechanics Associates (SMA) for Sandia National Laboratories as part of the Level I analysis being performed by the Risk Methods Integration and Evaluation Program (RMIEP). The methodology used is described in detail in a companion report, NUREG/CR-4839. In this report, we describe the process for selecting the external events, the screening analysis, and the detailed bounding calculations for those events not eliminated in the screening analysis. As a result of this analysis, it was concluded that only internal flooding, internal fire, and seismic events were potentially significant at LaSalle. Detailed analyses were performed for each of these and are reports in NUREG/CR-4832, Volumes 10, 9, and 8, respectively.

CONTENTS

CONTENTS (Continued)

CONTENTS (Concluded)

LIST OF TABLES

LIST OF FIGURES

LIST OF FIGURES (Cont.)

FOREWORD

LaSalle Unit 2 Level III Probabilistic Risk Assessment

In recent years, applications of Probabilistic Risk Assessment (PRA) to nuclear power plants have experienced increasing acceptance and use, particularly in addressing regulatory issues. Although progress on the PRA front has been impressive, the usage of PRA methods and insights to address increasingly broader regulatory issues has resulted in the need for continued improvement in and expansion of PRA methods to support the needs of the Nuclear Regulatory Commission (NRC).

Before any new PRA methods can be considered suitable for routine use in the regulatory arena, they need to be integrated into the overall framework of a PRA, appropriate interfaces defined, and the utility of the methods evaluated. The LaSalle Unit 2 Level III PRA, described in this and associated reports, integrates new methods and new applications of previous methods into a PRA framework that provides for this integration and evaluation. It helps lay the bases for both the routine use of the methods and the preparation of procedures that will provide guidance for future PRAs used in addressing regulatory issues. These new methods, once integrated into the framework of a PRA and evaluated, lead to a more complete PRA analysis, a better understanding of the uncertainties in PRA results, and broader insights into the importance of plant design and operational characteristics to public risk.

In order to satisfy the needs described above, the LaSalle Unit 2, Level III PRA addresses the following broad objectives:

1) To develop and apply methods to integrate internal, external, and dependent failure risk methods to achieve greater efficiency, consistency, and completeness in the conduct of risk assessments;

2) To evaluate PRA technology developments and formulate improved PRA procedures;

3) To identify, evaluate, and effectively display the uncertainties in PRA risk predictions that stem from limitations in plant modeling, PRA methods, data, or physical processes that occur during the evolution of a severe accident;

4) To conduct a PRA on a BWR 5, Mark II nuclear power plant, ascertain the plant's dominant accident sequences, evaluate the core and containment response to accidents, calculate the consequences of the accidents, and assess overall risk; and finally

5) To formulate the results in such a manner as to allow the PRA to be easily updated and to allow testing of future improvements in methodology, data, and the treatment of phenomena.

The LaSalle Unit 2 PRA was performed for the NRC by Sandia National Laboratories (SNL) with substantial help from Commonwealth Edison (CECo) and its contractors. Because of the size and scope of the PRA, various related programs were set up to conduct different aspects of the analysis. Additionally, existing programs had tasks added to perform some analyses for the LaSalle PRA. The responsibility for overall direction of the PRA was assigned to the Risk Methods Integration and Evaluation Program (RMIEP). RMIEP was specifically responsible for all aspects of the Level I analysis (i.e., the core damage analysis). The Phenomenology and Risk Uncertainty Evaluation Program (PRUEP) was responsible for the Level II/III analysis (i.e., accident progression, source term, consequence analyses, and risk integration). Other programs provided support in various areas or performed some of the subanalyses. These programs include the Seismic Safety Margins Research Program (SSMRP) at Lawrence Livermore National Laboratory (LLNL), which performed the seismic analysis; the Integrated Dependent Failure Analysis Program, which developed methods and analyzed data for dependent failure modeling; the MELCOR Program, which modified the MELCOR code in response to the PRA's modeling needs; the Fire Research Program, which performed the fire analysis; the PRA Methods Development Program, which developed some of the new methods used in the PRA; and the Data Programs, which provided new and updated data for BWR plants similar to LaSalle. CECo provided plant design and operational information and reviewed many of the analysis results.

The LaSalle PRA was begun before the NUREG-1150 analysis and the LaSalle program has supplied the NUREG-1150 program with simplified location analysis methods for integrated analysis of external events, insights on possible subtle interactions that come from the very detailed system models used in the LaSalle PRA, core vulnerable sequence resolution methods, methods for handling and propagating statistical uncertainties in an integrated way through the entire analysis, and BWR thermal-hydraulic models which were adapted for the Peach Bottom and Grand Gulf analyses.

The Level I results of the LaSalle Unit 2 PRA are presented in: "Analysis of the LaSalle Unit 2 Nuclear Power Plant: Risk Methods Integration and Evaluation Program (RMIEP)," NUREG/CR-4832, SAND92-0537, ten volumes. The reports are organized as follows:

NUREG/CR-4832 - Volume 1: Summary Report.

NUREG/CR-4832 - Volume 2: Integrated Quantification and Uncertainty Analysis.

NUREG/CR-4832 - Volume 3: Internal Events Accident Sequence Quantification.

NUREG/CR-4832 - Volume 4: Initiating Events and Accident Sequence Delineation.

NUREG/CR-4832 - Volume 5: Parameter Estimation Analysis and Human Reliability Screening Analysis.

NUREG/CR-4832 - Volume 6: System Descriptions and Fault Tree Definition.

NUREG/CR-4832 - Volume 7: External Event Scoping Quantification.

NUREG/CR-4832 - Volume 8: Seismic Analysis.

NUREG/CR-4832 - Volume 9: Internal Fire Analysis.

NUREG/CR-4832 - Volume 10: Internal Flood Analysis.

The Level II/III results of the LaSalle Unit 2 PRA are presented in: "Integrated Risk Assessment For the LaSalle Unit 2 Nuclear Power Plant: Phenomenology and Risk Uncertainty Evaluation Program (PRUEP)," NUREG/CR-5305, SAND90-2765, 3 volumes. The reports are organized as follows:

NUREG/CR-5305 - Volume 1: Main Report

NUREG/CR-5305 - Volume 2: Appendices A-G

NUREG/CR-5305 - Volume 3: MELCOR Code Calculations

Important associated reports have been issued by the RMIEP Methods Development Program in: NUREG/CR-4834, Recovery Actions in PRA for the Risk Methods Integration and Evaluation Program (RMIEP); NUREG/CR-4835, Comparison and Application of Quantitative Human Reliability Analysis Methods for the Risk

Methods Integration and Evaluation Program (RMIEP); NUREG/CR-4836, Approaches to Uncertainty Analysis in Probabilistic Risk Assessment; NUREG/CR-4838, Microcomputer Applications and Modifications to the Modular Fault Trees; and NUREG/CR-4840, Procedures for the External Event Core Damage Frequency Analysis for NUREG-1150.

Some of the computer codes, expert judgement elicitations, and other supporting information used in this analysis are documented in associated reports, including: NUREG/CR-4586, User's Guide for a Personal-Computer-Based Nuclear Power Plant Fire Data Base; NUREG/CR-4598, A User's Guide for the Top Event Matrix Analysis Code (TEMAC); NUREG/CR-5032, Modeling Time to Recovery and Initiating Event Frequency for Loss of Off-Site Power Incidents at Nuclear Power Plants; NUREG/CR-5088, Fire Risk Scoping Study: Investigation of Nuclear Power Plant Fire Risk, Including Previously Unaddressed Issues; NUREG/CR-5174, A Reference Manual for the Event Progression Analysis Code (EVNTRE); NUREG/CR-5253, PARTITION: A Program for Defining the Source Term/Consequence Analysis Interface in the NUREG-1150 Probabilistic Risk Assessments, User's Guide; NUREG/CR-5262, PRAMIS: Probabilistic Risk Assessment Model Integration System, User's Guide; NUREG/CR-5331, MELCOR Analysis for Accident Progression Issues; NUREG/CR-5346, Assessment of the XXSOR Codes; and NUREG/CR-5380, A User's Manual for the Postprocessing Program PSTEVNT. In addition the reader is directed to the NUREG-1150 technical support reports in NUREG/CR-4550 and 4551.

Arthur C. Payne, Jr.
Principal Investigator
Phenomenology and Risk Uncertainty Evaluation Program and
Risk Methods Integration and Evaluation Program
Division 6412, Reactor Systems Safety Analysis
Sandia National Laboratories
Albuquerque, New Mexico 87185

ACKNOWLEDGMENT

The authors wish to acknowledge the guidance and technical support of Gregory J. Kolb and Kathleen Diegert.

1.0 INTRODUCTION

A full-scope Probabilistic Risk Assessment (PRA) of a nuclear power plant should consider all internal and external events that may pose a potential threat to the plant safety and contribute to the public risk. The detail to which the risk analysis is performed for each event depends on its frequency of occurrence and its effect on plant systems. In recent PRA studies, some external events (e.g., seismic, fire, internal flood, and extreme winds) have been treated in detail; other external events (e.g., turbine missiles, aircraft impact, and external flooding) have been dismissed as insignificant based on available data and judgment. Since PRA is a logical and formal procedure for examining all potential accidents, a logical and formal approach is needed for selection of important external events. The aim is to ensure that all potential external events are considered and that the significant ones are selected for more detailed studies. In fact, such a formal procedure has been developed in the PRA Procedures Guide, NUREG/CR-2300 (USNRC, 1983). This procedure also facilitates a complete documentation of the basis for selecting the external hazards which deserve further detailed attention. Because the PRA Procedures Guide only described detailed methods for seismic, flood, and fire events, a separate analysis was performed to develop scoping quantification methods for other external events (Ravindra and Banon, 1992).

This report is a description of the scoping quantification study which selected the external events to be included in the detailed PRA of the LaSalle County Nuclear Generating Station. The study was performed by NTS/Structural Mechanics Associates (SMA) for Sandia National Laboratories as part of the Risk Methods Integration and Evaluation Program (RMIEP). The study generally followed the procedures outlined in the PRA Procedures Guide (USNRC, 1983) as to methodology, presentation, and technical quality assurance, but was supplemented by scoping quantification methods developed and described in the report by Ravindra and Banon mentioned above.

1.1 Background

The Risk Methods Integration and Evaluation Program (RMIEP) performed by Sandia National Laboratories for the NRC selected the LaSalle County Station for application of the new methodologies developed as part of the full scope PRA. One task of the RMIEP plan was defined as an external event scoping quantification study which would select the external events to be included in a detailed external events analysis. For this purpose, NTS/Structural Mechanics Associates was

retained by Sandia National Laboratories to perform the scoping quantification study for the LaSalle County Station.

Although a general external event scoping study would consider all the possible events at the site; seismic, internal flood, and fire events were excluded from the present study. Based on the results of recent PRA studies, they were considered to be potential contributors to the plant risk and thus were included for a detailed study in the other tasks of RMIEP. The LaSalle County Station has been designed against the effects of extreme winds, tornadoes and tornado-generated missiles, and chlorine release. Examples of other external events which were considered in the LaSalle FSAR but were not specifically included in the design basis loads are external flooding, turbine missiles, and aircraft impact. The FSAR analysis was based on meeting the Regulatory Guide requirements rather than quantifying the plant risk from external events from a PRA standpoint.

The methods for performing an external event scoping quantification have been outlined in the PRA Procedures Guide (USNRC, 1983). However, the methods are described in a general fashion and the specific mathematical models and analytical techniques to be used are not described. The general methods described in the PRA Procedures Guide form the basis for the scoping procedures to be used in this study.

In addition to the PRA Procedures Guide, a review of the techniques and the mathematical models used to scope external events in other NRC and industry-sponsored studies was carried out. These models and techniques were examined for their applicability to the LaSalle scoping quantification study, including detailed bounding analyses, and the results were used to develop more detailed scoping quantification methods for use in this study (Ravindra and Banon, 1992).

1.2 Objective

The objective of this report was to perform a scoping quantification in order to define the additional external events, if any, that the LaSalle PRA should analyze in detail. As reported previously, the PRA analyzed seismic, fire, and internal flooding events in detail (see volumes 8, 9, and 10 respectively of this report).

1.3 Outline and Contents of Report

This report describes the external events scoping quantification performed for the LaSalle County Station (LSCS). This report is divided into four chapters. Chapter 1 is an overview of the study including background and

objectives. Chapter 2 describes the selection of methods for the external events risk analysis, identification of potential external events, and the general methodology for an external event bounding analysis. Also, Sections 2.6, 2.7, and 2.8 in Chapter 2 are general descriptions of the sources of information, technical quality assurance requirements, and the uncertainty analysis for external events. Chapter 3 describes the initial screening of the external events, and the more detailed bounding analysis performed for the events which could not be eliminated through the initial screening process. For each bounding analysis, a mathematical model is presented and sources of the data for estimation of parameters of the model are reported. The bounding analysis in Chapter 3 shows the significance of each external event to the plant risk. Therefore, events which require further detailed analysis are identified in Chapter 3. Chapter 4 summarizes the results of initial screening and bounding analyses. Also a set of recommendations based on these results is presented in Chapter 4.

2.0 EXTERNAL EVENT METHODOLOGY

An external event analysis in a PRA has three important goals. The first goal is that no significant events should be overlooked. The second goal is an optimal allocation of limited resources to the study of significant events, and the third goal is that the differences between external events and internal events (i.e., common-cause and fragility related failures) should be recognized and explicitly treated. Based on these goals, four tasks were identified for the present study.

1. Review of external event scoping quantification general techniques and mathematical models.

2. Identify potential external events.

3. Initial screening of external events.

4. Approximate bounding analysis to calculate risks from external events.

A general description of each task is given in the following sections.

2.1 Review of General Techniques and Mathematical Models

During the last four years, several Probabilistic Risk Assessments for nuclear power plants have been published. Aside from seismic, fire, and internal floods, other external events have not been treated in-depth in these PRAs. However, the general techniques and models for quantification of risk from external events have experienced much modification as more PRA studies were completed. Therefore, there is a need to study and compare these models and techniques before performing the LaSalle external event scoping quantification. It may be noted that not all of these models are applicable to the LaSalle site. For example, the Limerick PRA (PECO, 1983) which was performed by NUS Corporation studies the hazard from a chlorine explosion on site in great detail. However, information about chlorine stored at the LaSalle site indicates that only a small amount of liquid chlorine is stored on site. Therefore, it was judged that there is no possible risk from chlorine to the LaSalle County Station. On the other hand, reviews of the models and information which were carried out in this task would be used in developing the external event scoping quantification methods document.

2.2 Identification of Potential External Events

The PRA Procedures Guide (USNRC, 1983) was used as a guide for identification of potential external events at the LaSalle

site. Table 10-1 of the PRA Procedures Guide lists most of the possible external events for a plant site. This information was reviewed in the present study. Also, an extensive review of information on the site region and plant design was made to identify all external events to be considered. The data in the Final Safety Analysis Report (FSAR) regarding the geologic, seismologic, hydrologic, and meteorological characteristics of the site region as well as present and projected industrial activities (i.e., increases in the number of flights, construction of new industrial facilities) in the vicinity of the plant were reviewed for this purpose. A description of external events considered for the LaSalle site appears in Section 3.2.

2.3 Initial Screening of Events

At this stage, the external events identified as described above were screened in order to select the events for either approximate or detailed risk quantification. A set of screening criteria was formulated that should minimize the possibility of omitting significant risk contributors while reducing the amount of detailed analyses to manageable proportions. The set of screening criteria given by the PRA Procedures Guide used in this study is as follows.

An external event is excluded if:

1. The events for which the plant has been designed. This screening criterion is not applicable to events like earthquakes, floods, and extreme winds since their hazard intensities could conceivably exceed the plant design basis. An evaluation of plant design basis is made in order to estimate the resistance of plant structures and systems to a particular external event. For example, it is shown by Kennedy, Blejwas, and Bennett (1982) that safety-related structures designed for earthquake and tornado loadings in Zone 1 can safely withstand a 3.0 psi static pressure from explosions. Hence, if the PRA analyst demonstrates that the overpressure resulting from explosions at a source (e.g., railroad, highway, or industrial facility) can not exceed 3 psi, these postulated explosions need not be considered.

2. The event has a significantly lower mean frequency of occurrence than other events with similar uncertainties and could not result in worse consequences than those events. For example, the PRA analyst may exclude an event whose mean frequency of occurrence is less than some small fraction of those for other events. In this case, the uncertainty in the frequency estimate for the excluded

event is judged by the PRA analyst as not significantly influencing the total risk.

3. The event cannot occur close enough to the plant to affect it. This is also a function of the magnitude of the event. Examples of such events are landslides, volcanic eruptions, and earthquake fault ruptures.

4. The event is included in the definition of another event. For example, storm surges and seiches are included in external flooding; the release of toxic gases from sources external to the plant is included in the effects of either pipeline accidents, industrial or military facility accidents, or transportation accidents.

By this process of initial screening, a smaller set of external events is identified for risk assessment. A bounding analysis is then performed for these external events.

2.4 Bounding Analysis

Although the screening process has identified a set of external events for further risk analysis, it is still possible to perform simplified analyses to show that some of the events are not significant contributors to the risk. The bounding risk analysis is an essential step in the external event PRA as it minimizes the effort that is required for a detailed external events analysis. The key elements of a complete bounding risk analysis for an external event are:

- Hazard analysis
- Plant system and structure response analysis
- Evaluation of the fragility and vulnerability of plant structures and equipment
- Plant system and accident sequence analysis
- Consequence analysis

A hazard analysis estimates the frequency of occurrence of different intensities of an external event. These are called "hazard intensities." Typically, the output of hazard analysis is a hazard curve of exceedence frequency versus hazard intensity. Since there is normally a great deal of uncertainty in the parameter values and in the mathematical model of the hazard, the effects of uncertainty are represented through a family of hazard curves, and a probability value is assigned to each curve.

The purpose of structural response analysis is to translate the hazard input into responses of structures, piping systems,

and equipment. The fragility or vulnerability of a structure or equipment is the conditional frequency of its failure given a value of the response parameter. In some external event analyses, the response and fragility evaluation are combined and the fragility is expressed in terms of a global parameter of the hazard (e.g., tornado wind speed).

The analysis of plant systems and accident sequences consists of developing event trees and fault trees in which the initiating event can be the external hazard itself or a transient or LOCA initiating event induced by the external event. Various failure sequences that lead to core damage, containment failure, and a specific release category are identified and their conditional frequencies of occurrence are calculated. The unconditional frequency of core damage or of radionuclide release for a given release category is obtained by integrating over the entire range of hazard intensities. If the consequence analysis is carried out separately for the external event, the output would be curves of frequencies of damage (i.e., early fatalities, latent cancer deaths, or property damage).

After a bounding analysis is performed, an external event can be excluded from further risk assessment based on the same considerations as in the initial screening analysis. For example, calculation of the core damage frequency may be done using different bounding assumptions explained by the following example. Typically, nuclear power plants are sited such that the accidental impact of plant structures by aircraft is highly unlikely. For the purposes of an external event PRA, the risk from aircraft accidents may be assessed at different levels. The mean annual frequency of aircraft impacting the plant during take-off or landing, or in flight may be determined. If this hazard frequency is very low (e.g., $\leq 10^{-7}$ per year) then the aircraft impact as an external event may be eliminated from further study. This approach assumes that the aircraft impact results in damage of the structures leading to core damage or serious release. This assumption may or may not be highly conservative. The assessment of the conditional probability of core damage will determine the actual cutoff level used here. If the frequency of aircraft impacting the plant structures is estimated to be larger, the fragility of the structures may be evaluated to make a refined estimate of the frequency of core damage. Further refinements could include (1) elimination of certain structural failures as not resulting in core damage (e.g., damage to the diesel generator building may not result in core damage if offsite electrical power is available), and (2) performing a plant system and accident analysis to calculate the core damage frequency. This example shows that for some external events, it may be sufficient to perform only the

hazard analysis; for some others the hazard analysis and a simple fragility evaluation may be needed; only in rare cases, a plant-systems and accident sequence analysis may be necessary.

The procedure of screening out the external events in this stage consists of: (1) establishing an acceptably low mean frequency of core damage based upon simplifying conservative assumptions (i.e., $\leq 10^{-7}$ per year), (2) performing bounding calculations of the mean core damage frequency for each external event, and (3) eliminating from further consideration those events which have mean core damage frequencies less than the acceptable value (i.e., 10^{-7} per year).

As part of the licensing evaluation of nuclear power plants, probabilistic analyses are performed for a few external events, and the frequencies of unacceptable damage (i.e., exceedence of 10 CFR Part 100 guideline exposures) caused by these external events are shown to be very small. The information contained in the plant safety analysis reports and the analyses performed at the design stage in support of FSAR are reviewed and new information is gathered as part of this effort. Since the PRA attempts a realistic risk evaluation, the conservative bias introduced by the assumptions made in the licensing analysis are appropriately removed.

2.5 Detailed Analysis

For the external events that are not screened out by the initial screening process and the bounding analysis, a detailed risk analysis is necessary. Such an analysis is typically done for seismic events, internal flooding, and fire. The risk analysis methods for these events are described in Chapter 11 of the PRA Procedures Guide. Any other external events identified to be potentially significant contributors to the risk based on the results of this study would need to be studied in detail. However, such detailed PRA analysis is outside the scope of this report.

2.6 Information

Plant specific information for the present study was obtained from the LaSalle FSAR (CECO), and engineering drawings of the plant. This information was augmented by other information regarding the plant design basis provided to SMA by the Commonwealth Edison Company and Sargent and Lundy Engineers. Some of the generic data which were used in the external event bounding analysis were reported in previous PRA studies, e.g., the Limerick Severe Accident Risk Assessment (PECO, 1983) and the Midland PRA (CPCO, 1984). Also, a site visit was conducted by the SMA personnel. The objectives of the site

visit were to verify the information which was given in the FSAR and to gather new information concerning the effect of potential external events on the plant.

2.7 Technical Quality

This study conforms to the requirements of the assurance of technical quality as outlined in the PRA Procedures Guide, Chapters 2 and 10. The study was performed at the Newport Beach offices of NTS/Structural Mechanics Associates by the authors. The methods used, whether previously developed in a published PRA or developed as part of this study, were documented and internally reviewed. The results were internally reviewed by Dr. D. A. Wesley who is a senior consultant to the project. An external quality assurance audit of the project was also performed.

2.8 Uncertainty Analysis

Uncertainties exist in the hazard analysis and the fragility evaluation of plant structures and equipment. These arise from lack of data (i.e., parameter uncertainty) and in the use of analytical models to predict failure (i.e., model uncertainty). The uncertainty in frequency of the plant damage due to an external event is particularly important if the event is a potential contributor to the plant risk. Therefore, for these events, an attempt was made to address the question of model and parameter uncertainties, i.e., an integrated assessment of both parameter and model uncertainties was made to calculate the high confidence (95 percent) value of the annual frequency of plant damage. As will be described in Chapter 3, uncertainty analyses performed for these external events were in accordance with the methods and models used by SMA in previous Probabilistic Risk Assessment studies. An effort is currently underway at Sandia to develop new methods of uncertainty assessment as part of the RMIEP. Therefore, detailed information regarding the data which were used to estimate the parameters and choice of the models were provided to Sandia personnel to be used in an uncertainty assessment which is consistent with the RMIEP uncertainty methodology.

3.0 SCOPING QUANTIFICATION STUDY

This chapter describes the initial screening of external events and the bounding analyses which were performed as part of the LaSalle scoping quantification study. Section 3.1 is a general description of the plant structures, site characteristics, and transportation routes near the site. Section 3.2 lists all the external events which were identified for the LaSalle site. Also, the initial screening of these external events has been described in Section 3.2. Some of the events which required a more detailed screening analysis based on the LaSalle FSAR information are listed in Section 3.3. The external events which required a bounding analysis appear in Section 3.4, and those events which may require a detailed PRA analysis are identified in Section 3.5.

3.1 Plant Description

The LaSalle Nuclear Power Generating Station was designed in the early 1970's in accordance with criteria and codes in effect at that time (LaSalle FSAR). The station consists of two Boiling Water Reactors (BWR), each rated at 3323 Mwt and 1100 Mwe. The plant, with the exception of the Nuclear Steam Supply System (NSSS), was designed by Sargent & Lundy (S&L) Engineers. The NSSS was designed by the Nuclear Energy Division of the General Electric Company. The BWR Mark II containment design is used. The primary containment is a steel-lined, post-tensioned concrete structure enclosed in the reinforced concrete reactor building. The primary structure consists of a combined building which houses both NSSS units, the turbine buildings, an auxiliary building, the diesel generator buildings, a radwaste building, the service building, and the off-gas building. A lake screen house is located on the inlet flume but does not contain any critical equipment.

Seismic Category I structures and equipment were designed to withstand both a Safe Shutdown Earthquake (SSE) and an Operating Basis Earthquake (OBE). The maximum horizontal ground design accelerations at the foundation level were 20 percent of gravity for the SSE and 10 percent of gravity for the OBE. The corresponding maximum vertical design acceleration was two-thirds of horizontal for both the SSE and OBE. Plant structures and equipment important to safety were classed as Seismic Category I in the original design. Codes and standards used in the design and qualification of structures and equipment for the LaSalle Plant are listed in Table 3.1-1 (LaSalle FSAR). Figure 3.1-1 (LaSalle FSAR) shows the general arrangement of the LaSalle structures. It may be noted that the outside walls of LaSalle structures do not have the same thickness, e.g., the diesel generator walls are 12"

thick whereas the reactor building walls are 2'0" thick. Thickness of the outside walls is important in the analysis of structures for winds and tornadoes, tornado missiles, and turbine missiles. Figure 3.1-2 (LaSalle FSAR) shows a section of the plant structures including the reactor building, the auxiliary building, and the turbine building. Although the reactor building is enclosed by 2'0" walls below the refueling floor at Elevation 843'6", it is shielded by only metal siding above the refueling floor. The refueling floor of the reactor building in LaSalle does not contain any engineered safety features (ESF) equipment.

3.1.1 Site, Terrain, Meteorology

The LaSalle County Station Units 1 and 2 are located in northeastern Illinois. The Illinois River is approximately 5 miles north of the plant. Figure 3.1-3 (LaSalle FSAR) shows the general location of the site within the state of Illinois.

The LSCS site occupies approximately 3060 acres, of which 2058 acres comprise the cooling lake. There are no industries or residences on the site. There is a state fish hatchery associated with the plant. The general layout of the plant is shown in Figure 3.1-4 (LaSalle FSAR).

The major transportation routes near the site include the Illinois River, approximately 3.5 miles north of the northern boundary; Illinois State Highway 170, 0.5 mile east of the eastern boundary; and Interstate Highway 80, 8 miles north of the northern boundary of the site. The Chicago, Rock Island, and Pacific Railroad; approximately 3.25 miles north of the northern site boundary is the closest operating railroad line.

The LaSalle FSAR includes a description of existing and projected population centers near the site. The population within 10 miles of the site was 15,600 as of 1970 and it was relatively projected to grow to 24,300 by 2020. The most heavily populated areas near the site lie in the northeast direction towards the city of Chicago.

There are no storage facilities, mining and quarry operations, transportation facilities, tank farms, or oil and gas pipelines within 5 miles of the plant. There are no military bases, missile sites, military firing or bombing ranges, refineries, or underground gas storage facilities within 10 miles.

There are no products or materials regularly manufactured, stored, used, or transported within 5 miles of the site. The nearest industries are located in Seneca, Illinois, approximately 5.6 miles northeast of the site. There are no

commercial airports within 10 miles of the site, and there are no private airstrips within 5 miles.

At the present time, there are two airport site investigations in progress in the vicinity of the LSCS site. The LaSalle-Peru area approximately 23 miles west-northwest of the plant site is being studied as one possible site. The second airport study is being conducted in the area between the towns of Pontiac, Streator, and Dwight, approximately 18 miles south of the LSCS site. Both of these airports will be designed to handle commercial planes in addition to the single-engine and twin-engine planes common to the area. Also, the Continental Grain Company is developing a river terminal to handle both barge cargo and truck cargo, but there are no plans to handle hazardous or explosive materials.

The LSCS site experiences a high variability and a wide range of temperature extremes. For example, extreme temperatures recorded at nearby Ottawa, Illinois, range from 112° to -26°F. Temperature data recorded at Peoria Airport and Argonne National Laboratory as well as data from the LSCS meteorological tower were used in the plant design. Precipitation in the LSCS site area averages about 34 inches annually with monthly averages ranging from about 1.8 inches in January to 5.0 inches in July. Precipitation is not monitored at the LSCS site. Long term data from Peoria airport and Argonne National Laboratory were used in the plant design. Sleet or freezing rain can occur during the colder months of the year. Glaze storms with ice thickness of 0.75 inch or greater are expected to occur once every three years.

The LSCS site, located in mid-Illinois, experiences a wide spectrum of extreme winds. In addition, tornadoes have been historically observed in the State of Illinois. For the period 1916 through 1969, there were a total of 43 tornadoes in the ten county areas surrounding and including the LSCS site.

The terrain around the plant site is gently rolling, with ground surface elevations varying from 700 feet to 724 feet mean sea level (MSL) which is 217 feet above the normal pool elevation in the Illinois River. The river screen house and the outfall structure, both nonsafety-related structures, are the only plant facilities that are potentially affected by floods in the Illinois River.

3.1.2 Site Visit

A site visit was conducted in April 1984 by Drs. M. K. Ravindra and H. Banon (Structural Mechanics Associates) and

K. Campe (NRC, Site Analysis Branch). The purpose of the site visit was twofold: first to confirm the information in FSAR which is being used in the LaSalle scoping quantification study, and second to collect new information and look for possible changes in the plant and site conditions which could affect the risk from external hazards to the site. Therefore, the site visit included a tour of the plant structures as well as a survey of the plant boundary and surrounding areas. Following is a highlight of the issues which were resolved by the site visit.

1. No major changes or deviations from the information in LaSalle FSAR were observed in the plant or its surroundings. Since this study is concerned with the external events, the effort was concentrated on those factors which could affect the risk from these events.

2. A survey of the structures in LaSalle revealed that all the doors which open to the outside of the plant are leak-tight. Also, the ground floor in every structure has an adequate drainage system in case of flooding. This information was used for the external flooding analysis.

3. It was confirmed that the refueling floor of the reactor building as well as the top floor in the auxiliary building do not contain any ESF equipment. This information is needed in the analysis for wind and tornadoes.

4. During the site visit, a survey of the objects in the plant boundary which could potentially become tornado-generated missiles was carried out. The site visit confirmed that the potential number of missiles at the LaSalle site is less than the number which has been used in a tornado missile simulation study by Twisdale and Dunn (1981). Tornado missiles are discussed in Section 3.4.3.

5. It was observed that collapse of the stack under winds or tornado loads could affect the safety of category I structures in LaSalle. Further information from the Commonwealth Edison Company showed that the stack has been designed for the effects of the Design Basis Tornadoes. Therefore, the stack does not add to the risk from winds and tornadoes. This is described in more detail in Section 3.4.3.

6. The site visit confirmed that there are no industries, airports, pipelines, or major highways in the vicinity of the site. However, no attempt was made to find information regarding future construction of such

facilities near the site, i.e., this study would rely on the FSAR information for this purpose.

In addition to the site visit, the SMA personnel also visited the offices of Sargent and Lundy in Chicago, the Architect-Engineer for the LaSalle Plant to gather information for the scoping quantification study.

Table 3.1-1

Code Requirements for Components and Systems
Ordered After July 1, 1974

	QUALITY GROUP CLASSIFICATION			
	A	B	C	D
Pressure Vessels*	ASME Boiler and Pressure Vessel Code, Section III - 1974, Class 1.	ASME Boiler and Pressure Vessel Code, Section III - 1974, Class 2.	ASME Boiler and Pressure Vessel Code, Section III - 1974, Class 3.	ASME Boiler and Pressure Vessel Code, Section VIII, Div. 1-1974.
Piping	ASME Boiler and Pressure Vessel Code, Section III - 1974, Class 1.	ASME Boiler and Pressure Vessel Code, Section III - 1974, Class 2.	ASME Boiler and Pressure Vessel Code, Section III - 1974, Class 3.	ANSI B31.1 1973, Code for Pressure Piping.
Pumps and Valves	ASME Boiler and Pressure Vessel Code, Section III - 1974, Class 1.	ASME Boiler and Pressure Vessel Code, Section III - 1974, Class 2.	ASME Boiler and Pressure Vessel Code, Section III - 1974, Class 3.	ANSI B31.1 1973, Code for Pressure Piping.**
Low-Pressure Tanks	-	-	American Petroleum Institute, Recommended Rules for Design and Construction of Large Welded Low-Pressure Storage Tanks, API 620 1963 edition.	American Petroleum Institute, Recommended Rules for Design and Construction of Large Welded Low-Pressure Storage Tanks, API 620 1963
Atmospheric Storage Tanks	-	American Waterworks Association, Standard for Steel Tanks, Standpipes, Reservoirs and Elevated Tanks for Water Storage, AWWA-D100 1967 edition; or Welded Steel Tanks for Oil Storage, API-650 1964 edition.†	American Waterworks Association, Standard for Steel Tanks, Standpipes, Reservoirs and Elevated Tanks for Water Storage, AWWA-D100 1967 edition; or Welded Steel Tanks for Oil Storage, API-650 1964 edition.	American Waterworks Association, Standard for Steel Tanks, Standpipes, Reservoirs and Elevated Tanks for Water Storage, AWWA-D100 1967 edition; or Welded Steel Tanks for Oil Storage, API-650 1967 edition.
Heat Exchangers	ASME Boiler and Pressure Vessel Code, Section III - 1974, Class 1.	ASME Boiler and Pressure Vessel Code, Section III - 1974, Class 2.	ASME Boiler and Pressure Vessel Code, Section III - 1974, Class 3.	ASME Boiler and Pressure Vessel Code, Section VIII, Div. 1-1974, and Tubular Exchanger Manufacturers Association (TEMA) Class C.

*RPV and Containment Vessel excluded.

**For pumps operating above 150 psi and 212°F ASME Section VIII, Division 1, shall be used as a guide for calculating thickness of pressure retaining parts and in sizing cover bolting; below 150 psi and 212°F manufacturer's standards for service intended will be used.

†Supplementary NDE - 100% volumetric examination of the side wall for plates 3/16-inch thick and 100% surface examination of welds for plates 3/16-inch thick or less. Also, 100 percent surface examination for side-to-bottom welds.

Table 3.1-1

Code Requirements for Components and Systems
Ordered Prior to July 1, 1971

	QUALITY GROUP CLASSIFICATION			
	A**	B	C	D
Pressure Vessels†	ASME Boiler and Pressure Vessel Code, Section III, Class A - 1968 Addenda through Summer 1970.	ASME Boiler and Pressure Vessel Code, Section III, Class C - 1968 Addenda through Summer 1970.	ASME Boiler and Pressure Vessel Codes, Section VIII, Div. 1- 1968 Addenda through Summer 1970.	ASME Boiler and Pressure Vessel Codes, Section VIII, Div. 1- 1968 Addenda through Summer 1970.
Piping**	ANSI B31.7 Nuclear Power Piping, Class I - 1969.	ANSI B31.7 Nuclear Power Piping, Class II - 1969.	ANSI B31.7 Nuclear Piping, Class III - 1969.	ANSI B31.1.0 Code for Pressure Piping - 1967. Addendum - 1969.
Pumps and Valves**	ASME Code for Pumps and Valves for Nuclear Power, Class I - 1968 Draft Addenda March 1970.	ASME Codes for Pumps and Valves for Nuclear Power, Class II - 1968 Draft Addenda March 1970.	ASME Code for Pumps and Valves for Nuclear Power, Class III - 1968 Draft Addenda March 1970.	ANSI B31.1.0 Code for Pressure Piping* - 1967.
Low-Pressure Tanks	---	---	American Petroleum Institute, Recommended Rules for Design and Construction of Large Welded Low-Pressure Storage Tanks, API 620 1963 edition.	American Petroleum Institute, Recommended Rules for Design and Construction of Large Welded Low-Pressure Storage Tanks, API 620 1963 edition.
Atmospheric Storage Tanks	---	American Waterworks Association, Standard for Steel Tanks, Sandpipes, Reservoirs and Elevated Tanks for Water Storage, AWWA-D100 1967 edition; or Welded Steel Tanks for Oil Storage, API-650 1964 edition.††	American Waterworks Association, Standard for Steel Tanks, Sandpipes, Reservoirs and Elevated Tanks for Water Storage, AWWA-D100 1967 edition; or Welded Steel Tanks for Oil Storage, API-650 1964 edition.	American Waterworks Association, Standard for Steel Tanks, Sandpipes, Reservoirs and Elevated Tanks for Water Storage, AWWA-D100 1967 edition; or Welded Steel Tanks for Oil Storage, API-650 1964 edition.
Heat Exchangers	ASME Boiler and Pressure Vessel Code, Section III, Class A - 1968 Addenda through Summer 1970.	ASME Boiler and Pressure Vessel Code, Section III, Class C, 1968 Addenda through Summer 1970, and Tubular Exchanger Manufacturers Association (TEMA) Class C.	ASME Boiler and Pressure, Vessel Code, Section VIII, Div. 1, 1968 Addenda through Summer 1970, and Tubular Exchanger Manufacturers Association (TEMA) Class C.	ASME Boiler and Pressure, Vessel Code, Section Div. 1, 1968 Addenda through Summer 1970, and Tubular Exchanger Manufacturers Association (TEMA) Class C.

*Pumps operating above 150 psi and 212°F ASME Section VIII, Division 1 of the Boiler and Pressure Vessel Code shall be used as a guide for calculating the thickness of pressure retaining parts and in sizing cover bolting; below 150 psi and 212°F manufacturer's standards for service intended will be used.

**Group A nuclear piping, pumps and valves will meet the provisions of ASME Boiler and Pressure Vessel Code, Section III, Summer Addenda 1969, Paragraph N-153.

†RPV and Containment Vessel excluded.

††Supplementary NDE - 100% volumetric examination of the side wall for plates over 3/16-inch thick and 100% surface examination of welds for plates 3/16-inch thick or less. Also, 100% surface examination of side-to-bottom welds.

Table 3.1-1

Code Requirements for Components and Systems
Ordered After July 1, 1971

	QUALITY GROUP CLASSIFICATION			
	A	B	C	D
Pressure Vessels*	ASME Boiler and Pressure Vessel Code, Section III - 1971, Class 1.	ASME Boiler and Pressure Vessel Code, Section III - 1971, Class 2.	ASME Boiler and Pressure Vessel Code, Section III - 1971, Class 3.	ASME Boiler and Pressure Vessle Code, Section VIII, Div. 1-1968. Addenda through winter 1970.
Piping	ASME Boiler and Pressure Vessel Code, Section III - 1971, Class 1.	ASME Boiler and Pressure Vessel Code, Section III - 1971, Class 2.	ASME Boiler and Pressure Vessel Code, Section III - 1971, Class 3.	ANSI B31.1.0 - 1967, Code for Pressure Piping. Addendum B31.1.0a - 1969.
Pumps and Valves	ASME Boiler and Pressure Vessel Code, Section III - 1971, Class 1.	ASME Boiler and Pressure Vessel Code, Section III - 1971, Class 2.	ASME Boiler and Pressure Vessel Code, Section III - 1971, Class 3.	ANSI B31.1.0 - 1967, Code for Pressure Piping. Addendum B31.1.0a - 1969.**
Low-Pressure Tanks	-	-	American Petroleum Institute, Recommended Rules for Design and Construction of Large Welded Low-Pressure Storage Tanks, API 620 1963 edition.	American Petroleum Institute, Recommended Rules for Design and Construction of Large Welded Low-Pressure Storage Tanks, API 620 1963 edition.
Atmospheric Storage Tanks	-	American Waterworks Association, Standard for Steel Tanks, Standpipes, Reservoirs and Elevated Tanks for Water Storage, AWWA-D100 1967 edition; or Welded Steel Tanks for Oil Storage, API-650 1964 edition.†	American Waterworks Association, Standard for Steel Tanks, Standpipes, Reservoirs and Elevated Tanks for Water Storage, AWWA-D100 1967 edition; or Welded Steel Tanks for Oil Storage, API-650 1964 edition.	American Waterworks Association, Standard for Steel Tanks, Standpipes, Reservoirs and Elevated Tanks for Water Storage, AWWA-D100 1967 edition; or Welded Steel Tanks for Oil Storage, API-650 1964 edition.
Heat Exchangers	ASME Boiler and Pressure Vessel Code, Section III - 1971, Class 1.	ASME Boiler and Pressure Vessel Code, Section III - 1971, Class 2.	ASME Boiler and Pressure Vessel Code, Section III - 1971, Class 3.	ASME Boiler and Pressure Vessel Code, Section VIII, Div. 1-1968. Addenda through Winter 1970; and Tubular Exchanger Manufacturers Association (TEMA) Class C.

*RPV and Containment Vessel excluded.

**For pumps operating above 150 psi and 212°F ASME Section VIII, Division 1, shall be used as a guide for calculating thickness of pressure retaining parts and in sizing cover bolting; below 150 psi and 212°F manufacturer's standards for service intended will be used.

†Supplementary NDE - 100% volumetric examination of the side wall for plates 3/16-inch thick and 100% surface examination of welds for plates 3/16-inch thick or less. Also, 100% surface examination for side-to-bottom welds.

Reproduced from the LaSalle FSAR.

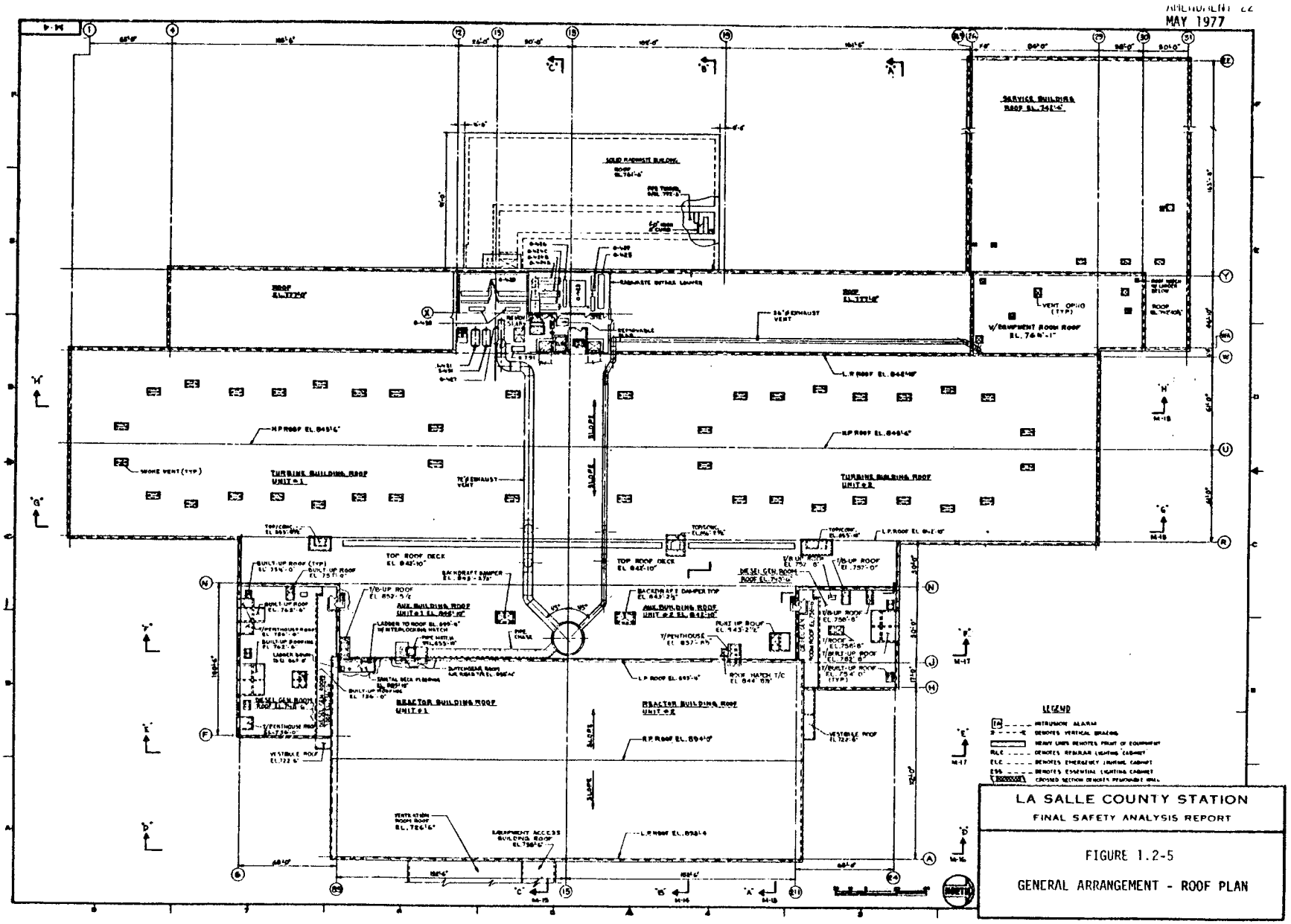

Figure 3.1-1. General Arrangement - Roof Plan

Reproduced from the LaSalle FSAR.

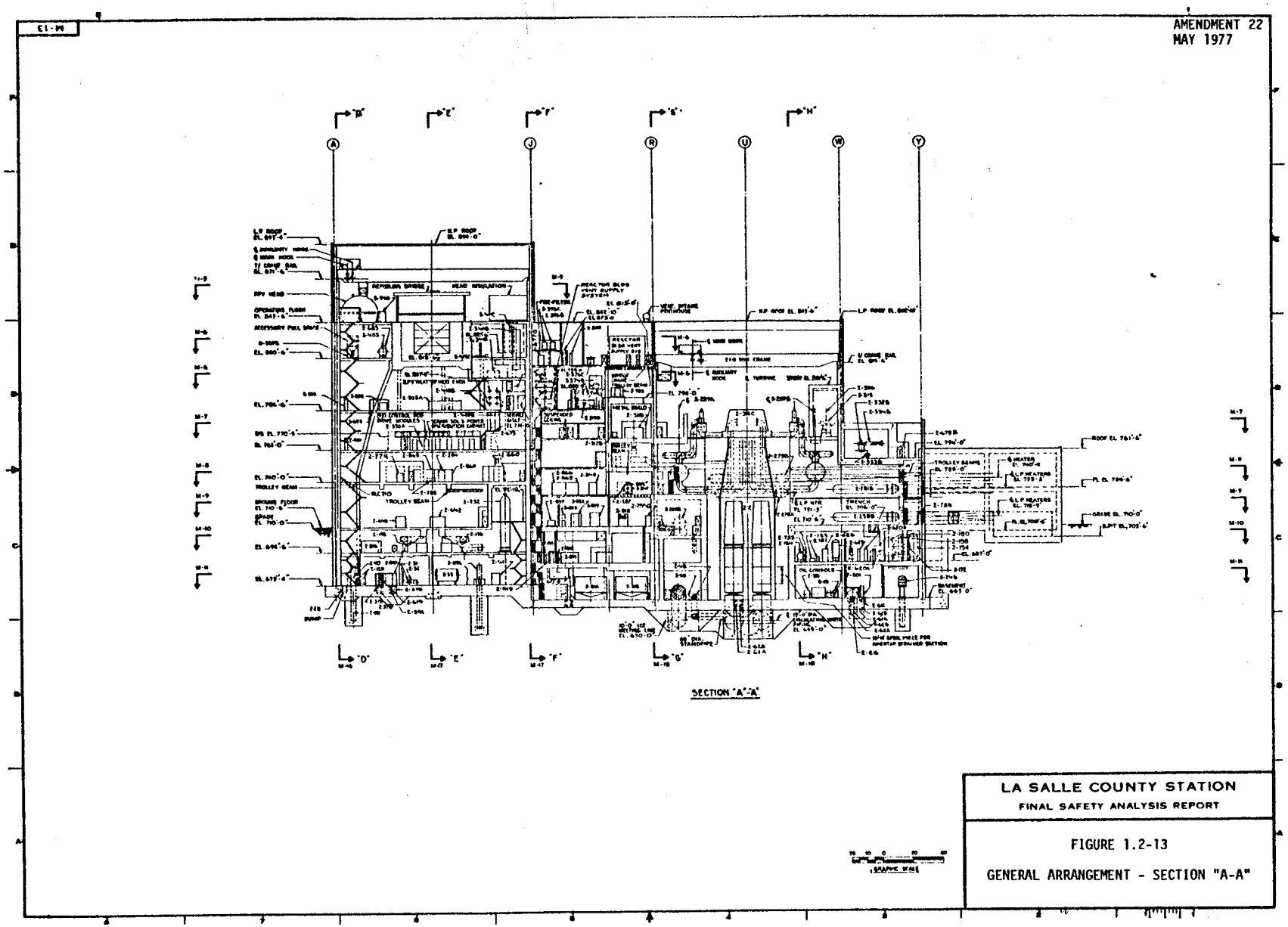

Figure 3.1-2. General Plant Arrangement

Reproduced from the LaSalle FSAR.

Reproduced from the LaSalle FSAR.

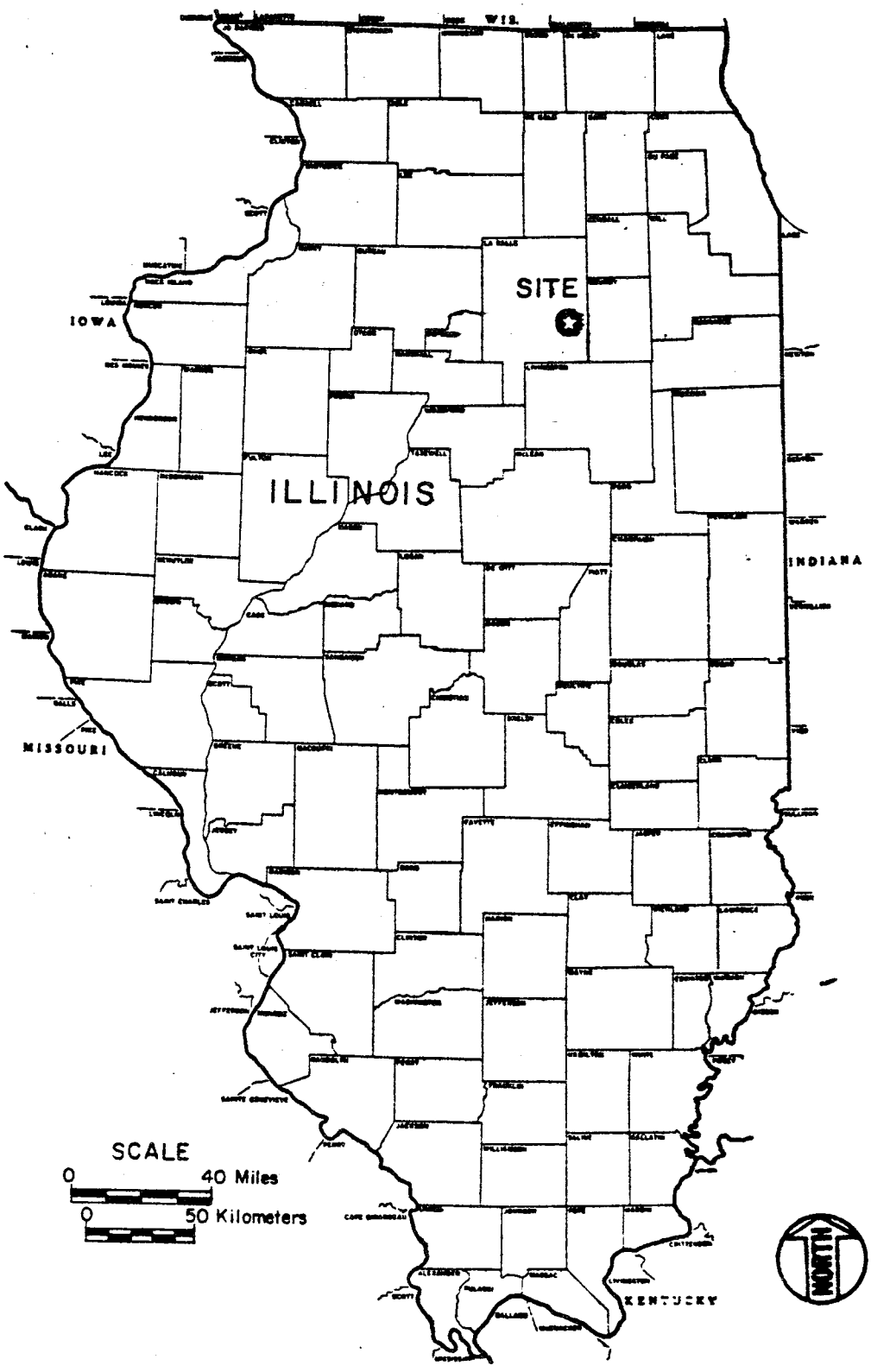

Figure 3.1-3. Location of the Site within the State of Illinois

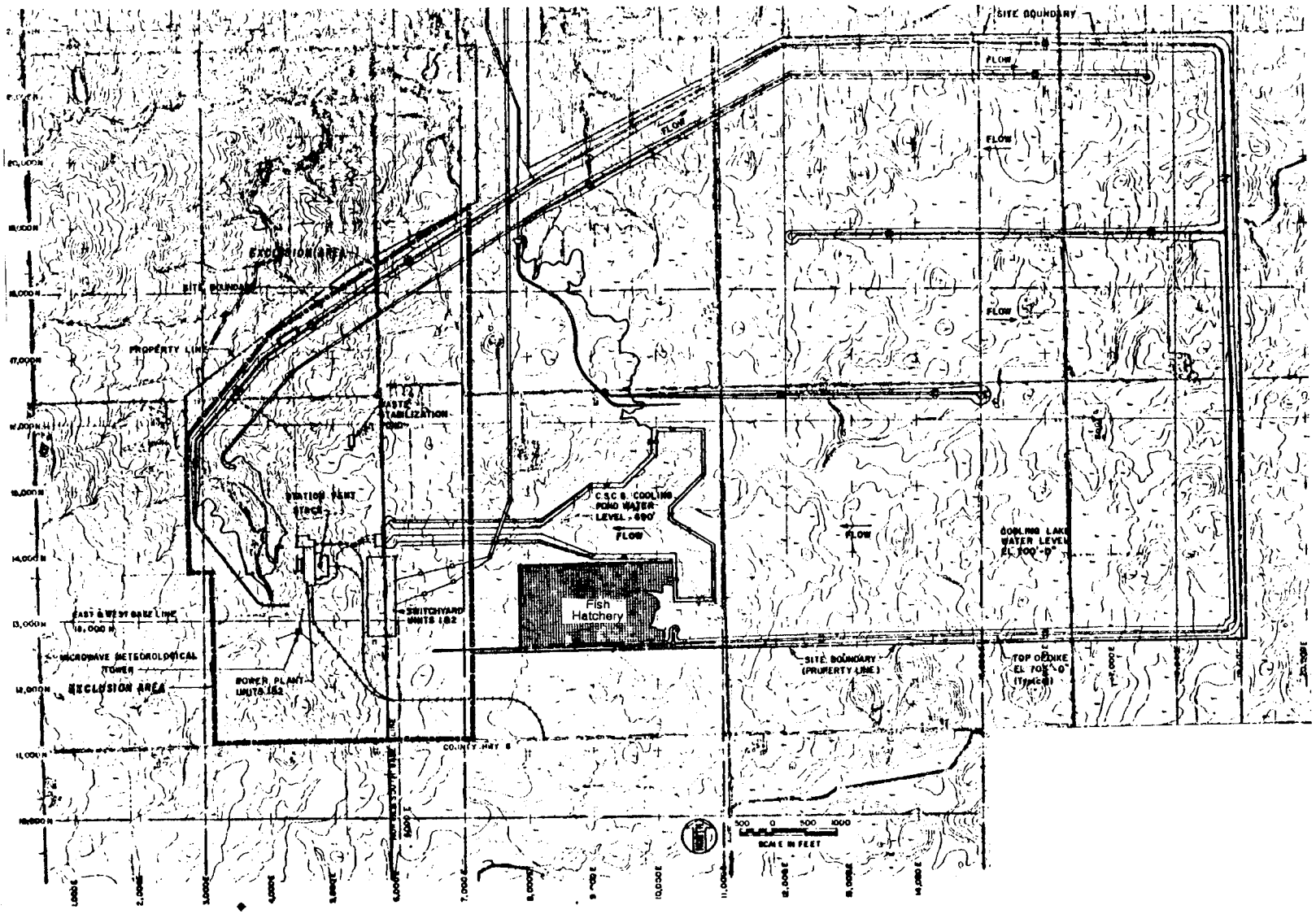

Figure 3.1-4. General Site Arrangement

Reproduced from the LaSalle FSAR.

3.2 Initial Screening of External Events

An extensive review of information on the site region and plant design was made to identify all external events to be considered. The data in the LaSalle Final Safety Analysis Report as well as other data obtained from the utility and the information gathered in the site visit were reviewed for this purpose. A general guide for this task is the PRA Procedures Guide (1983) which lists the possible external events for a nuclear power plant. Table 3.2-1 is a listing of external hazards for the LaSalle County Station. This table is similar to Table 10-1 of the PRA Procedures Guide. A set of screening criteria was developed which should minimize the possibility of omitting significant risk contributors while reducing the amount of analysis to manageable proportions. These screening criteria were described in Section 2.3 and are also listed at the end of Table 3.2-1. For each external event, the applicable screening criteria and a brief remark are included in the table.

In the following paragraphs, the external events in Table 3.2-1 are discussed in more detail. Also, the reasons for screening some of the events are presented.

Aircraft Impact

A bounding analysis is performed for this event.

Avalanche

LaSalle County Station is built on a gently rolling terrain where there are no mountains. Therefore, avalanches cannot occur near the site.

Biological Events

The only biological event which may affect safety of the plant is aquatic life in the cooling lake, i.e., fish may block flow of water from the lake to the plant. This event is not considered further because there would be adequate warning, and therefore remedial action can be taken.

Coastal Erosion

LaSalle County Station is located inland and therefore this event is not applicable to the site.

Drought

LSCS has been designed for the possible effects of droughts or low flow rates in the Illinois River. The total capacity of

the makeup pumps at the river screen house is 200 cfs which is much less than a 100-year low flow level of 1592 cfs in the Illinois River. In addition, loss of water from the Illinois River or from the cooling lake does not affect the ability of safety-related facilities to function adequately. The Ultimate Heat Sink (UHS) for the LaSalle is an excavated pond which is located under the southeast corner of the cooling lake area. In the unlikely event of unavailability of water from the cooling lake, emergency water supply would be obtained from the UHS. The UHS has a 30-day supply of water based on the worst period of recorded weather conditions at the site. Therefore, in case of a worst possible drought there would be enough time for remedial action to be taken.

External Flooding

A bounding analysis is performed for this event.

Extreme Winds and Tornadoes

A bounding analysis is performed for this event.

Fog

Fog can affect the frequency of occurrence of other hazards such as highway accidents or aircraft landing and take-off accidents. The effects of fog on highway, railway, or barge accidents are implicitly taken into account by assuming a worst possible transportation accident near the site. Transportation accidents are considered in detail for the present study. The effect of fog on aircraft landing of takeoff accident rates may be neglected because there are no airports within 5 miles of the site, i.e., only in-flight accidents contribute to aircraft hazard at the site.

Forest Fire

There are no forests in the vicinity of the LaSalle site, i.e., the site has been cleared. Therefore, this event is not applicable to the site.

Frost

Loads induced on LaSalle structures due to frost are much lower than snow and ice loads, i.e., frost loads can be safely neglected in the plant hazard analysis.

Hail

Hail was considered as one of the meteorological conditions in the design of LaSalle structures (LaSalle FSAR). However,

hail is less damaging than other missiles which are generated outside of the plant such as tornado missiles and turbine missiles. Therefore, hail is not considered further in the scoping study.

High Tide, High Lake Level or High River Stage

High tide is not applicable to the site because the plant is located inland. High lake level and high river stage are considered in the bounding analysis under external flooding.

High Summer Temperature

As mentioned under drought, the UHS is designed to provide a minimum of 30 days water supply for cooling taking into account evaporation, drift, seepage, and other water-loss mechanisms. Therefore, high record temperatures were indirectly included in the design of LaSalle under drought conditions.

Hurricane

LaSalle site is inland and thus is not affected by hurricanes.

Ice Cover

Ice loading is considered in the plant design along with snow loads. For this study, ice loads and snow loads are considered to act together (see snow loads).

Industrial or Military Facility Accident

This event is included in the scoping study.

Internal Flooding

This event is included in the detailed internal events analysis.

Landslides

The LaSalle plant is built on flat land where landslides are not possible.

Lightning

The plant structures and electrical systems are protected by lightning conductors against a current of 200 kilo-ampere (kA). In a study by the Electric Power Research Institute (NSAC, 1981), the range of predicted number of cloud-to-ground

lightning strikes of 25 kA or larger is estimated to be from 1.8 to 11.6 strikes per square kilometer per year. Of these strikes, only one percent have current amplitudes in excess of 200 kA. If the plant area is taken as 2,000' x 3,000', the annual frequency of lightning strikes damaging the plant systems is calculated to be from 10^{-3} to 6.4×10^{-2}. Therefore, lightning events cannot be screened out on the basis of their frequency of occurrence alone. Studies performed by Sandia National Laboratories under the NRC research program TAP A-45 have estimated the frequency of severe core damage may be as high as 1.7×10^{-6} per year due to lightning strikes for a plant in the vicinity of LaSalle with a minimum AC/DC system (i.e., two electrical divisions). The relevant scenario "station blackout" is the lightning strike results in the loss of offsite power and the onsite electric power is unavailable due to random causes. Since LaSalle has three electrical divisions, additional damaging lightning strikes or random electrical failures must occur in order for this scenario to happen. Inclusion of these additional events for LaSalle is judged to lower the scenario frequency below 10^{-7} per year. Since the lightning conductors are expected to sustain currents in excess of 200 kA, the above estimate of damage frequency is expected to be overly conservative. Also, the reactor building has metal siding permitting grounding of lightning strikes. Since the calculated frequency of damage is low, lightning is not expected to contribute to the plant core damage frequency and it will not be considered further in the current scoping study. The effects of lightning in inducing LOSP are included in the internal event quantification of LOSP and its time recovery curve.

Low Lake or River Water Level

This event is included under drought.

Low Winter Temperature

Low temperatures can affect the plant structures as well as the cooling lake or the Illinois River. Thermal stresses and embrittlement which are induced by low temperatures are insignificant compared to other design loads. In addition, these effects are covered by design codes and standards for plant design. Ice cover on the cooling lake or on the Illinois River does not affect the plant safety because of the availability of the ultimate heat sink. In case of an ice cover on the ultimate heat sink, there is adequate warning so that remedial action can be taken (provision for ice melting in lake screenhouse forebay).

Meteorite

This event has a very low probability of occurrence. A study by Solomon (1974) showed that the probability of a meteorite impacting a nuclear power plant is negligible, and therefore meteorites will not be considered in the scoping study.

Pipeline Accident

This event is included in the scoping study.

Intense Precipitation

This event is included under external flooding.

Release of Chemicals in Onsite Storage

This event is included in the scoping study.

River Diversion

The Illinois River is 5 miles away from the plant and the site is approximately 180 feet above the river elevation. Therefore, any river diversion could not become a hazard to the plant.

Sandstorm

This event is not relevant for the LaSalle site.

Seiche

This event is included under external flooding.

Seismic Activity

This event is included in the detailed external events analysis.

Snow

Snow and ice loads were considered in the design of category I structures. The following statistics were calculated for the design of structures due to local probable maximum precipitation (PMP) at the LaSalle site (FSAR):

- 100-year recurrence interval ground snow load = 24.0 psf
- 48-hour probable maximum winter precipitation = 15.9 inches

From these data, it was found that the corresponding water load of snow and ice loads due to a winter PMP with a 100-year recurrence interval antecedent snow pack is less than the design load (83.2 psf) for the roofs of safety-related structures. The roof drains are designed for a precipitation intensity of 4 in/hr. Conservatively assuming that the roof drains are clogged at the time of the PMP, the maximum accumulation of water on the roofs of safety-related structures is limited by the height of parapet walls, viz. 16 inches. The corresponding water load is therefore 83.2 lb/ft^2. The roofs of safety-related structures at LaSalle can withstand this load. Therefore, snow and ice loads are excluded from further study.

Soil Shrink-Swell, Consolidation

Plant structures are designed for the effects of differential settlement due to consolidation. In addition, such effects occur over a long period and they do not pose a hazard during the plant operation, i.e., the plant can be safely shutdown if needed.

Storm Surge

This event is included under external flooding.

Transportation Accidents

A bounding analysis is performed for this event.

Tsunami

LaSalle site is inland and therefore this event is not applicable to the site.

Toxic Gas

This event is included under transportation accidents, onsite chemical release, and industry and military facilities accidents.

Turbine Generated Missiles

A bounding analysis is performed for this event.

Volcanic Activity

The site is not close to any active volcanoes.

Waves

The LaSalle site is inland and therefore ocean waves can be excluded. Waves in the Illinois River or the cooling lake are included under external flooding.

In summary, the findings of the preliminary screening are as follows:

Aside from seismic, fire and flood which have already been included in the detailed external hazards analysis, the following events were identified for a more detailed study.

1. Aircraft Impact
2. External Flooding
3. Military and Industrial Facilities Accidents
4. Pipeline Accidents
5. Transportation Accidents
6. Turbine Missiles
7. Winds and Tornadoes
8. Release of Chemicals in Onsite Storage

The above events are discussed in Sections 3.3 and 3.4.

Table 3.2-1

Preliminary Screening of External Events
for LaSalle County Station

Event	Applicable* Screening Criteria	Remarks
Aircraft Impact	---	Included in scoping study
Avalanche	3	Topography is such that no avalanche is possible
Biological Events	1	There would be adequate warning for these events
Coastal Erosion	3	LaSalle Site is inland
Drought	1	LaSalle is designed for probable maximum drought. There would be adequate warning so that remedial action can be taken.
External Flooding	---	Included in scoping study
Extreme Winds and Tornadoes	---	Included in scoping study
Fog	1	It effects frequency of occurrence of other hazards, e.g., highway accidents, aircraft landing and take-off
Forest Fire	1	There are no forests in the vicinity of the site; site is cleared
Frost	1	Snow and ice loads govern
Hail	1	Tornado and turbine generated missiles govern
High Tide, High Lake Level or High River Stage	4	Included under external flooding

*See notes

Table 3.2-1

Preliminary Screening of External Events
for LaSalle County Station (Continued)

Event	Applicable* Screening Criteria	Remarks
High Summer Temperature	1	Ultimate heat sink is designed for at least 30 days of operation, taking into account evaporation, drift, seepage, and other water-loss mechanisms; gives adequate warning.
Hurricane	3	LaSalle site is inland and is not affected by hurricanes
Ice Cover	1,4	Plant structures and systems are designed for the ice effects
Industrial or Military Facility Accident	---	Included in scoping study
Internal Flooding	---	Included in external events analysis
Landslide	3	Topography is such that no landslides are possible
Lightning	1	Plant is designed for lightning. All buildings have lightning conductors.
Low Lake or River Water Level	1	The plant is designed for this condition. Also, there will be adequate warning so that remedial action can be taken.
Low Winter Temperature	1	Thermal stresses and embrittlement are insignificant or covered by

*See notes

Table 3.2-1

Preliminary Screening of External Events
for LaSalle County Station (Continued)

Event	Applicable* Screening Criteria	Remarks
		design codes and standards for plant design, generally, there is adequate warning of icing on the ultimate heat sink so that remedial action can be taken.
Meteorite	2	This event has a very low frequency of occurrence for all sites.
Pipeline Accident	---	Included in scoping study
Intense Precipitation	4	Included under internal and external flooding
Release of Chemicals in Onsite Storage	---	Included in scoping study
River Diversion	3	Illinois river is 5 miles away from the plant at a much lower elevation, i.e., river diversion could not become a hazard.
Sandstorm	3	This is not relevant for this region
Seiche	4	Included under external flooding
Seismic Activity	---	Included in external events analysis
Snow	---	Plant is designed for snow load ponding effects and combinations of snow with other loads.

*See notes

Table 3.2-1

Preliminary Screening of External Events
for LaSalle County Station (Concluded)

Event	Applicable* Screening Criteria	Remarks
Soil Shrink-Swell Consolidation	1	Plant structures are all designed for the effects of consolidation.
Storm Surge	4	Included under external flooding
Transportation Accidents	---	Included in scoping study
Tsunami	3	LaSalle site is inland
Toxic Gas	4	Included in transportation accident, onsite chemical release and industry and military facilities accident.
Turbine Generated Missiles	---	Included in scoping study
Volcanic Activity	3	The site is not close to any active volcanoes
Waves	3	LaSalle is inland

*NOTES:

1. The event is of equal or lesser damage potential than the events for which the plant has been designed.

2. The event has a significantly lower mean frequency of occurrence than other events with similar uncertainties and could not result in worse consequences than those events.

3. The event cannot occur close enough to the plant to affect it.

4. The event is included in the definition of another event.

3.3 Screening of External Events Based on FSAR Information

This section describes the external events which could be screened based on the FSAR information supplemented with new data. Section 3.3.1 discusses the military and industrial facilities accidents and Section 3.3.2 describes the pipeline accidents. It is shown that these accidents are unlikely to contribute to the plant risk.

An accident scenario which is usually considered for a BWR plant like LaSalle is an explosion caused by the chlorine which is stored on site. However, the information which was provided by the Commonwealth Edison Company indicated that only a small amount of liquid chlorine is stored on the LaSalle site. Therefore, a chlorine accident is not significant for the LaSalle County Station.

3.3.1 Accidents in Industrial and Military Facilities

According to the LaSalle FSAR, there are no storage facilities, mining and quarry operations, industrial plants, or military facilities within 5 miles of the plant site. The nearest industrial facility which stores hazardous materials is E. I. DuPont de Nemours and Company which is located in Seneca, Illinois, approximately 5.6 miles northwest of the site. There are two other industrial plants within 10 miles of the site which store hazardous materials, namely Beker Industries and Borg-Warner Chemical Corporation. Both of these plants are located in Marseilles, Illinois, which is approximately 6.8 miles north-northwest of the site. Table 3.3-1, which is duplicated from LaSalle FSAR, lists all the hazardous materials, quantities stored, and mode of transportation for the above mentioned industries. In addition to the facilities listed in Table 3.3-1, Tri-State Motor Transit, which is a trucking firm approximately 5 miles northeast of the site, has a holding area for trailers with explosive and/or sensitive loads. Since there has been no activity in this holding area and also there are no plans to increase the use of this area, Tri-State Motor Transit was not included in Table 3.3-1.

There are three possible effects from an industrial accident near the site: 1) incident over-pressure on plant structures due to an explosion, 2) seepage of toxic chemicals into control room which could incapacitate the operators, and (3) flammable vapor clouds leading to heat hazard at the site. Industrial accidents at distances farther than 5 miles to the site are not expected to cause significant overpressure loads on the plant structures. Also, the plant Category I structures are designed for Zone I tornado wind loads, i.e., the Category I structures have a minimum capacity of 3 psi

against blast loads. A detailed description of the Category I structural capacities is given in Section 3.4.4 under Transportation Accidents. Since an industrial accident at a distance of 5 miles or more would result in overpressures on wall panels which are less than 1 psi, an overpressure hazard due to industrial accidents could be screened for the LaSalle site. Flammable vapor clouds at a distance of 5 miles or more would not generate much heat at the site. Also, the probability of a flammable cloud travelling a distance of 5 miles or more to the site is negligible. Thus, flammable vapor clouds due to industrial accidents will not be considered further in the LaSalle external events scoping study.

Release of toxic chemicals near nuclear power plants can potentially result in the control room being uninhabitable. This condition can happen if: (1) large quantities of toxic chemicals are released, (2) there are favorable wind conditions and insufficient dilution of chemicals such that these chemicals reach the control room air intakes, and (3) there are no detection systems and air isolation systems in the control room. According to Regulatory Guide 1.78, chemicals stored or situated at distances greater than 5 miles need not be considered as an external hazard. This is due to the fact that if a release occurs at such a distance, atmospheric dispersion will dilute and disperse the incoming plume to such a degree that there should be sufficient time for the control room operators to take appropriate action. The control room HVAC in LaSalle has redundant equipment and provides chlorine and anhydrous ammonia detectors with appropriate alarms and interlocks.

Provision has been made for the control room air to be recirculated through charcoal filters and also provision has been made to pass outdoor makeup air through impregnated charcoal filters before introduction to the control room system. From the foregoing discussion, the following conclusions are made:

1. The only toxic chemicals which are stored in large quantities near the site are chlorine and anhydrous ammonia. The control room is equipped with detectors for chlorine and anhydrous ammonia and therefore they would not pose a hazard to the plant. The only other hazardous chemical which is stored in large quantities is Butadiene. However, the maximum quantity of Butadiene stored at the Borg-Warner chemical plant (Table 3.3-1) is well within the allowable limit which is calculated based on the Regulatory Guide 1.78 criteria.

2. Even if there is an accident at the DuPont chemical plant in Seneca, Illinois, the hazardous chemicals have to travel a distance of more than 5 miles and an elevation of more than 180 feet before they reach the control room air intakes. Therefore, it is concluded that the probability of core damage due to an industrial accident is negligible.

3. Overpressure and heat load due to industrial accidents at a distance of more than 5 miles would not affect the LaSalle plant.

3.3.2 Pipeline Accidents

The LaSalle FSAR information is used to show that the probability of damage to LaSalle structures due to a pipeline accident is negligibly small. According to the FSAR, there are no gas pipelines or oil pipelines within 5 miles of the site. However, there are two natural gas pipelines between 5 to 7 miles of the site which are operated by Northern Illinois Gas Company. These pipelines are 6" and 8" pipes and operate at 230 psi pressure. Both of the pipelines are buried approximately 30 inches below ground. These two pipelines are not used for storage and are not likely to be used to transport or store any product other than natural gas.

An accident in a gas pipeline would lead to either a fire or an explosion. In any of these events, the distance from existing pipelines to the LaSalle site is such that there would be no damaging effect on the plant structures.

Table 3.3-1

Industries with Hazardous Materials
Within 10 Miles of the Site

Facility (Location)	Maximum Quantities	Mode of Transportation
Baker Industries[1] (Marseilles)		
Anhydrous ammonia	10,000 ton	barge
Sulfuric acid	3,000 ton	truck
Dynamite	100 lb.	-
Wet process phosphoric acid	7,500 ton	rail & truck
Illinois Nitrogen Corp.[2] (Marseilles)		
Anhydrous ammonia	42,000 ton	barge-Illinois River rail-Chicago Rock Island & Pacific Truck-U.S. Hwy. 6
Soil prilled		barge-rail-truck
Liquid blended		barge-rail-
L.P.G., gasoline, #2 fuel oil, chlorine	(small quantities for plant use only)	
E.I. DuPont de Nemours & Co.[3] (Seneca)		
Anhydrous ammonia	150,000 lb.	barge
	30,000,000 lb. at Seneca Port Operating Authority Storage	rail-Chicago Rock Island & Pacific -Penn Central
Monomethlamine	250,000 lb.	rail-Chicago Rock Island & Pacific -Penn Central
Monomethlaminenitrate	7,000 lb.	used in high explosives manufacture-not shipped
Nitric acid 58-80%	3,250,000 lb.	rail-Chicago Rock Island & Pacific truck
Nitric acid 95	360,000 lb.	rail-Chicago Rock Island & Pacific truck

Table 3.3-1

Industries with Hazardous Materials
Within 10 Miles of the Site (Continued)

Facility (Location)	Maximum Quantities	Mode of Transportation
Mixed acid (Nitric)	450,000 lb.	rail-Chicago Rock Island & Pacific truck
Ammonium nitrate prills	7,600,000 lb.	rail-Chicago Rock Island & Pacific truck
Dynamite	80,000 lb.	truck
Initiating explosives (caps)	40,000 (each)	truck
Initiating explosives (primers)	7,500 (each)	truck
Jet tappers (explosives)	3,000 (each)	truck
Nitrocellulose (alcohol wet)	300,000 lb.	truck
Chlorine (H.P. Cylinders) Ammonium nitrate liquor (80 aqueous solution)	7,175 lb. 650,000 lb.	truck rail-Chicago Rock Island & Pacific
Water gel (high explosives)	2,100,000 lb.	truck
Aluminum powder	200,000 lb.	truck
"Gilsonite"	100,000 lb.	truck
Vinyl acetate	480,000 lb.	rail-Chicago Rock Island & Pacific
Liquid ethylene	100,000 lb.	truck-State Highway 47 or U.S. Highway 6
Nitrogen (liquid)	4,000 lb.	truck-State Highway 47 or U.S. Highway 6
Nitrogen (gas)	45,000 ft	truck-State Highway 47 or U.S. Highway 6
Methanol	40,000 lbs. in 55-gal. drums	truck-State Highway 47 or U.S. Highway 6

Table 3.3-1
Industries with Hazardous Materials
Within 10 Miles of the Site (Concluded)

Facility (Location)	Maximum Quantities	Mode of Transportation
Formaldehyde	10,000 lb.	truck-State Highway 47 or U.S. Highway 6
Borg-Warner Chemical, Borg-Warner Corp.[4] (Marseilles)		
Acrylonitrile	500,000 gal	rail
Butadiene	1,066,000 gal	barge, rail
Nitrogen	550,000 ft	truck
Sulfuric acid	30,000 gal, 95 acid	truck
Fuel oil	1,200,000 gal	truck

[1] Source: Mr. W. M. Fraser, Plant Manager, Beker Industries, letter to J. C. Prey, Cultural Resource Analyst, Sargent & Lundy, August 13, 1975.

[2] Source: Mr. R. P. Feser, Manager, Illinois Nitrogen Corporation, letter to J. C. Prey, Cultural Resource Analyst, Sargent & Lundy, July 7, 1975.

[3] Source: Mr. J. D. Graham, E. I. DuPont de Nemours & Company, letter to J. C. Prey, Cultural Resource Analyst, Sargent & Lundy, August 6, 1975

[4] Source: Mr. K. T. Bruns, Project Engineering Manager, Borg-Warner Chemicals, Borg-Watner Corporation, letter to J. C. Prey, Cultural Resource Analyst, Sargent & Lundy, September 9, 1975.

Reproduced from the LaSalle FSAR

3.4 Bounding Analysis

The external events which may be expected to contribute to the plant risk are included in this section. A bounding analysis is performed for each external event to find the annual frequency of core damage due to the event. Section 3.4.1 describes the general methodology of a bounding analysis, and Sections 3.4.2 through 3.4.6 describe the analysis for each individual external event. The events which are included in this section are aircraft impact, winds and tornadoes, transportation accidents, turbine missiles, and external flooding.

3.4.1 Model, Uncertainty, and Acceptance/Rejection Criterion

The probabilistic models used in bounding analyses should integrate the randomness and uncertainty associated with loads, response analysis, and capacities to predict the annual frequency of the plant damage. The aim of the present study is to use conservative models for calculating the annual frequency of core damage. Obviously, if both the median frequency and the high confidence (e.g., 95 percent) value of frequency according to the conservative model are predicted to be low (e.g., $\leq 10^{-7}$/year), the external event may be eliminated from further consideration. The bounding analyses would therefore identify those external events which need to be studied in more detail as part of the PRA external events analysis. Elements of a complete bounding analysis are described in Section 2.4.

For some external events, it is possible to perform a bounding analysis without a structural response analysis. In effect, one could show that the frequency of exceeding design loads is very small. Since the design capacities which are based on the design loads are also conservatively defined, the external event would not contribute significantly to the plant risk. This approach is used in analyses for transportation accidents and external flooding.

In a complete bounding analysis, one needs the probability distribution of load as well as the conditional probability distributions (fragilities) of those components which appear in the plant system and accident sequence analysis. The loads are usually defined in terms of a hazard curve which shows the annual frequency of exceedence for different load levels. The uncertainty in the hazard analysis can be represented by developing a family of hazard curves where each hazard curve is assigned a subjective probability. An example of this plot can be found in the bounding analysis for winds and tornadoes (Section 3.4.3) where the hazard curves are plots of

the probability of exceedence versus maximum tornadic wind speeds. The component fragilities are also developed as a family of fragility curves which represent the median fragility curve and the uncertainty in the median fragility. The probability of core damage (CD) can be expressed as:

$$P[CD] = \int_x P\left[\bigcup_i \bigcap_j \left\{C_{ij} < R_{ij} \mid L = x\right\}\right] f_L(x)\,dx \qquad (3.4\text{-}1)$$

where C_{ij} is the capacity of component i in cut set j, R_{ij} is the resistance of component i in cut set j, and $f_L(x)$ is the probability density function of input load. The first term in the above integral represents the component fragilities appearing in the plant sequence and system analysis and the second term is the slope of the hazard curve.

For the present study, some simplifications to the above equation were introduced. One simplification was to represent each cut set by only one component. As an example, back-face scabbing of the auxiliary building walls in case of an aircraft impact was assumed to lead to core damage even though a sequence of failures is necessary to lead to this damage state.

In addition to calculating a point estimate (median) frequency of core damage, the uncertainties in hazard and component fragilities may be used to find the high confidence (95 percent) frequency of damage. An uncertainty analysis is required only if the external event leads to a best estimate damage frequency which is close to the rejection frequency (10^{-7}/year). For this reason, uncertainty analyses were performed for winds and tornadoes and aircraft impact. An uncertainty analysis was not performed for transportation accidents and external flooding because these events were shown to contribute insignificantly to the plant risk. For turbine missiles, the results include a best estimate frequency as well as confidence bounds based on the FSAR analysis and other recent information.

3.4.2 Aircraft Impact

An assessment of the risk from aircraft crashes into the LaSalle structures is presented in this section. For this purpose, information in the LaSalle FSAR as well as more recent data concerning airports, air corridors, and aircraft activity near the site were used. An attempt was made to correct the data for anticipated changes in aircraft activity near the site. It was concluded that the frequency of plant

damage states initiated by aircraft crashes is on the order of 5×10^{-7}/year. Section 3.4.2.1 describes the information in FSAR and Section 3.4.2.2 describes the present aircraft hazard analysis.

3.4.2.1 FSAR Information

The LaSalle FSAR includes a description of airports and aircraft activity near the site. According to the LaSalle FSAR, there are no commercial airports within 10 miles of the site and there are no private airstrips within 5 miles. Tables 3.4-1 (LaSalle FSAR) and 3.4-2 (LaSalle FSAR) list all commercial airports and private airstrips within 20 miles of the site. As indicated in Table 3.4-1, these commercial airports can handle both single-engine and twin-engine aircraft. The annual number of operations for commercial aircraft is also given in Table 3.4-1. The aircraft using the private airfields are very small single-engine aircraft. The number of operations for private airfields near the site is expected to be low and, in addition, the random path of these aircraft would make the potential risk to the plant negligible.

There are three airway corridors within 10 miles of the site. These airway corridors are approximately 8 miles wide, and most aircraft fly within two miles of their centerline (Figure 3.4-1 (LaSalle FSAR)). All the traffic on these airways are expected to conform to the FAA regulations concerning the minimum low altitudes, i.e., all aircraft must fly at least 1000 feet above the tallest object in the corridor. According to the FSAR, aircraft hazards can be excluded from the external events analysis because of the following reasons:

1. There are no federal airways or airport approaches passing within 2 miles of the station. The closest airway corridor is 3 miles away from the station.

2. There are no commercial airports existing within 10 miles of the site and there are no private airstrips within 5 miles.

3. The projected landing and take-off operations out of those airports located within 10 miles of the site are far less than $500 \cdot d^2$ per year, where d is the distance in miles. The projected operations per year for airports located outside of 10 miles is less than $1000 \cdot d^2$ per year.

4. There are no military installations or any airspace usage for military purposes within 20 miles of the station.

3.4.2.2 Update on FSAR Information

In order to perform a bounding analysis for aircraft impact at the LaSalle site, the information in the FSAR as well as new information on aircraft activity near the site was used. Recent traffic data was provided by the FAA to Sargent and Lundy Engineers in the June 15, 1984 letter to S. Hallaron. Table 3.4-3 summarizes the FAA data which was gathered for June 7, 1984. Among the air corridors in this table, routes V156 and V9 are approximately within 3 miles of the site, whereas routes V116 and V69 are approximately 7 miles away from the plant. Other airway corridors in Table 3.4-3 are far enough from the site such that they would not contribute to the aircraft hazard as discussed in the next paragraphs. According to the FAA letter, aircraft listed as flying at 9000 feet and below (96 percent) are single and twin-engine light aircraft. Also, aircraft listed as flying at 10,000 feet and above (92 percent) are three and four engine heavy jet aircraft. Although the information which is presented in Table 3.4-3 is for one day traffic only, the data was provided for a peak traffic day and it is felt that it could be used to conservatively estimate the annual traffic volumes. In addition, the data in Table 3.4-3 were increased by 50 percent and then used in the bounding analysis to account for future increases in aircraft activity during lifetime of the plant.

3.4.2.3 Aircraft Impact Bounding Analysis

The methodology that is used to calculate the frequency of aircraft impact has been described in the Midland Probabilistic Risk Assessment. The probability of an aircraft impact on the plant structures may be written as:

$$f_k = \sum_i \sum_j N_{ij} \lambda_j d_j \frac{A_{kj}}{A_{pj}} \qquad (3.4\text{-}2)$$

where

N_{ij} = Number of aircraft operations of type j along airway i,

λ_j = Crash rate of aircraft type j,

d_j = Distance traveled by aircraft type j where the site is within striking distance,

A_{kj} = Crash area of the structures,

A_{pj} = Area where the aircraft may crash.

The term A_{kj}/A_{pj} in Equation (3.4-2) represents the probability of an impact given a crash in the vicinity of the site. This probability and also the distance d_j are determined geometrically. The other variables in the above equation are assigned distributions representing our state of knowledge about their values.

Figure 3.4-2 shows the geometry of an aircraft accident. Assuming that the aircraft is disabled at an elevation h, the distance that it would travel before the crash is gh where g is the glide distance per unit of altitude lost. For the present study, it is assumed that there is an equal probability of crash termination anywhere in the sector of radial length gh and angle $\phi = 180°$ in front of the aircraft. Therefore, A_{pj} is the half circle defined by radius gh where g was assumed to be the maximum glide ratio, equal to 17. A_{kj} is the impact area of structures which is minimum when the aircraft crash is vertical and it is maximum when the glide ratio g is maximum. An average value of the two areas was used for A_{kj} in the present study. In addition, a skid distance of 100 feet was assumed for the aircraft which increases the structure impact area (A_{kj}).

The aircraft impact frequency in Equation (3.4-2) was calculated for different types of aircraft. In this study, three types of aircraft were identified for these calculations, i.e., single-engine, twin-engine, and commercial aircraft. Also, a fragility analysis was performed to determine whether these aircraft types are capable of inducing damage to the Category I structures in case of an impact.

Capacities of Category I structures against aircraft impact were determined using the formulas which have been developed for impact of non-deformable missiles on reinforced concrete walls and panels. For an aircraft, it may be assumed that the engine and part of the aircraft body represents the non-deformable missile. Information regarding the characteristics of single-engine and twin-engine aircraft was obtained from Niyogi, et al. (1977). Also, it was conservatively assumed that if an aircraft impacts one of the Category I structures and causes back face scabbing, it would lead to a plant damage state. Another conservatism is that all impacts are assumed to be normal, glancing impacts would have less chance of causing damage. The formulas which have been developed to predict the minimum scabbing thickness all indicate that the concrete wall thickness required to prevent scabbing is independent of the amount of steel reinforcement for low to moderate steel ratios. The formula used in this study was developed by Chang (1981). Chang's formula is based on full-scale and model impact tests. According to Chang, the minimum

wall thickness (inches) which is required to prevent scabbing (t_s) is given as:

$$t_s = 2.47 \frac{w^{0.4} v^{0.67}}{d^{0.2} (f_c')^{0.4}} \qquad (3.4\text{-}3)$$

where

w = weight of missile (lbs),

v = velocity of missile (ft/sec),

d = missile effective diameter (inches) = $\sqrt{\frac{4A_c}{\pi}}$,

f_c' = ultimate strength of concrete (psi),

A_c = contact area of missile (in^2).

The results indicated that a single-engine aircraft must be traveling at speeds faster than 200 mph at the time of impact to cause scabbing of 2'6" reactor building walls. Since this velocity is in the range of the maximum velocity of single-engine aircraft, it was concluded that single-engine aircraft would not damage the reactor building in case of an impact below Elevation 843'. However, a single-engine aircraft could cause damage to the reactor building if it crashes into the building above Elevation 843' (which has metal siding walls) and penetrates the slab at this elevation. It should be noted that there is no safety-related equipment in the reactor building at Elevation 843', so in this analysis only twin engine and commercial aircraft will be considered.

The auxiliary building at LaSalle is surrounded by the turbine building, the diesel generator buildings, and the reactor building. A fragility evaluation of the auxiliary building walls at LaSalle showed that only twin engine and commercial aircraft are capable of scabbing the auxiliary building walls. Because the auxiliary building down to Elevation 786'6" does not contain any non-redundant safety systems, a single-engine aircraft impact at the higher floors of the auxiliary building would not cause damage to critical equipment. Also, the lower elevation walls of the auxiliary building are thick enough to withstand a single-engine aircraft impact.

The diesel generator building for Unit II at LaSalle was excluded from the aircraft impact risk calculations because of the following reasons: 1) the diesel generator building is

much smaller than the other buildings (less impact area), 2) it is shielded on two sides by the reactor building and auxiliary building, and 3) while a crash into this building might fail two diesel generators and also result in loss of offsite power to Unit II only (which enters near the building), the swing diesel is in the Unit I diesel generator building on the opposite side of the plant and AC power would still be available. The conditional probability of getting core damage by crashing into the diesel generator building is, therefore, much smaller than for the other buildings.

The crash rate statistics for different types of aircraft are listed in Table 3.4-4. These statistics were calculated from the 10 years of crash data involving air carriers published in the FAA Statistical Handbook of Aviation (1979) and accident rates for general aviation aircraft published in the Annual Review of Airport Accident Rates by the National Transportation Safety Board (1980). The statistics in Table 3.4-4 were calculated assuming a lognormal distribution for aircraft crash rates.

Table 3.4-5 summarizes the results of LaSalle aircraft hazard bounding analysis. These results were obtained assuming that single-engine aircraft fly at an average altitude of 4000 feet and twin-engine aircraft fly at an average altitude of 5000 feet. For commercial airplanes, data for air corridors near the site was used to estimate average aircraft altitudes. As shown in this table, the point (median) estimate frequency of an aircraft impact on the LaSalle structures leading to a plant damage state is approximately 5×10^{-7}/year. It is noted that most of the contribution to the risk comes from twin-engine aircraft. These aircraft have much higher crash rates than commercial aircraft.

3.4.2.4 Aircraft Impact Uncertainty Analysis

The aircraft impact bounding analysis for LaSalle showed that the median frequency of plant damage due to a crash is 5×10^{-7}/year. In order to evaluate the uncertainty in this frequency, distributions of the random variables in Equation (3.4-2) have to be identified. For this purpose, the probability distribution of crash rate was obtained from the FAA data. In addition, distributions of the other random variables in Equation (3.4-2) were obtained from subjective engineering judgment. It was assumed that for each aircraft type j, the random variable representing uncertainty in crash rate (ε_{fj}) can be modeled as:

$$\varepsilon_{fj} = \varepsilon_N \, \varepsilon_\lambda \, \varepsilon_h \, \varepsilon_g \qquad (3.4\text{-}4)$$

where the ε's are lognormal variables with median equal to unity and logarithmic standard deviation denoted by β. Therefore, for each aircraft type j, the logarithmic standard deviation of crash rate β_{fj} may be written as:

$$\beta_{fj} = \left(\beta_N^2 + \beta_\lambda^2 + \beta_h^2 + \beta_g^2 \right)^{1/2} \quad . \tag{3.4-5}$$

However, since commercial aircraft do not contribute significantly to the risk, they could be excluded from the following uncertainty analysis. From the FAA crash data, β_λ for single-engine and twin-engine aircraft were found to be 0.10 and 0.15, respectively. The logarithmic standard deviation in aircraft altitude (h) was obtained by assuming that the median altitude for single-engine aircraft is 3000 feet and the 95 percent value is 4000 feet. Therefore, β_h can be calculated as

$$\beta_h = \frac{\text{Ln} \frac{4000}{3000}}{1.65} = 0.17 \quad . \tag{3.4-6}$$

This β_h was used for the twin-engine aircraft. As discussed previously, a factor of 1.5 was applied on the number of aircraft operations to estimate the median value of the operation activity accounting for future increases in the aircraft activity near the site. Assuming that a factor of 2.0 represents the 95 percent value, β_N was calculated to be 0.17. For glide ratio (g), it was assumed that the value of 17 which was used in the analysis is the best estimate and a glide angle of 10° represents the 99 percent value. Thus, β_g was determined to be 0.47.

Using Equation (3.4-5), β_{fj} for twin-engine aircraft was calculated to be 0.55. Assuming a lognormal distribution for the annual crash frequency, the 95 percent confidence bound was found to be 10^{-6}. Therefore, based on our model, the high confidence (95 percent) frequency of impact resulting in damage is expected to be in the same order of magnitude as the median frequency of impact.

3.4.3 Winds and Tornadoes

This section describes the bounding analysis of LaSalle structures for the effects of winds and tornadoes. Both seismic Category I structures and non-Category I structures were considered for this task. Seismic Category I structures at LaSalle have been designed for both extreme wind and tornado load effects. Therefore, they are expected to have a high capacity against extreme winds and tornadoes. Non-Category I structures at LaSalle were generally designed against wind loads. However, in the design of the plant, non-Category I structures were shown to not collapse on adjacent seismic Category I structures, if any, in the event of a tornado.

3.4.3.1 Plant Design Criteria

Category I Structures

A design wind velocity of 90 mph based on a 100-year return period was used for Seismic Category I structures (i.e., reactor building, diesel-generator building, and auxiliary building including control room) at LaSalle (LaSalle FSAR). For the purpose of structural analysis, dynamic wind pressures on the structures were converted into equivalent static forces which vary along the height of each structure. In addition, Category I structures at LaSalle were designed to withstand a Design Basis Tornado (DBT) which is defined as follows:

- maximum rotational velocity of 300 mph
- translational velocity of 60 mph
- external pressure drop of 3 psi at the vortex within a 3-second interval
- radius of maximum wind speed of 227 feet

Pressures due to both wind velocity and tornado velocity were assumed to be static in the design of the structures at LaSalle. Since the natural periods of buildings at LaSalle are short compared with the rise in time of applied design pressures, the above assumption is well justified. A comparison of the design wind loads and the design tornado loads along with the corresponding allowable stresses revealed that the tornado loads are more critical. Therefore, it is sufficient to limit the bounding analysis to tornado loads for the Category I structures which were designed for both winds and tornadoes.

The safety related structures at LaSalle were also designed for the effects of postulated tornado missiles. The postulated tornado missiles used in the design of Category I structures are as follows:

- Wood Plank, 4 in. x 12 in. x 12 in. impact velocity = 225 mph
- Automobile weighing 4000 lbs, 20 ft^2 front area, impact velocity = 50 mph

The reactor building superstructure above Elevation 843'6" has metal siding and metal decking roof. The metal siding has been designed to blow off at wind speeds much less than that of the DBT. However, there are no ESF equipment at this elevation in the building.

Non-Category I Structures

The non-Category I structures (i.e., turbine building, radwaste building and service building) at LaSalle have been designed to withstand the effects of 90 mph wind velocity. The turbine building which adjoins the auxiliary building is designed such that it will not collapse on the auxiliary building as a result of a design basis tornado strike. The missiles produced by the tornado induced damage of non-Category I structures (i.e., girts, subgirts and purlins) are generally less damaging than the spectrum of missiles specified in the Standard Review Plan.

The bounding analysis of LaSalle structures for extreme winds, tornado winds and tornado generated missiles are described in the following sections.

3.4.3.2 Seismic Category I Structures

The design of Category I structures was controlled by the tornado loading and tornado missiles. For this reason, the bounding analysis described herein addresses only tornado effects. The probability of straight winds exceeding the capacity of Category I structures is much smaller than the probability of tornadic winds exceeding the same capacity.

3.4.3.2.1 Tornado Loads

The probability of structural failure resulting from tornado strikes on LaSalle Station structures is calculated using the tornado occurrence data and plant design features. It is shown that the probability of tornadoes striking the plant structures with tornadic wind speeds in excess of 300 mph is

of the order of 10^{-7} per year. Even if the plant structures are assumed to fail at this design value (of 300 mph), the contribution of the tornado events to the plant risk is negligibly small.

3.4.3.2.1.1 Characteristics of Tornadoes

Tornadoes are rare events which are usually characterized by their rate of occurrence, direction, maximum intensity, path length and path width. The most important aspect of a tornado is its maximum wind speed. Other characteristics of a tornado such as velocity, pressure, and pressure drop can be estimated from maximum tornado wind speeds. The bounding analysis used in this study is based on the methodology described in Reinhold and Ellingwood (1982). In this approach, the tornado hazard curves at the site are developed in terms of maximum tornado wind speeds, i.e., the hazard curve is a plot of annual frequency of exceedence for a range of maximum tornado wind speeds. It will be shown later in this report that such tornado hazard curves are dependent on the geometry of structures exposed to tornadoes.

Tornadoes are usually classified according to their intensity. The most common classification of tornadoes is the Fujita F-Scale and Pearson length and width scale (FPP) which is a measure of destructiveness of a tornado (Fujita and Pearson, 1973). In this scale, tornadoes are assigned a number from 0 to 6 (F0 - F6) with higher numbers indicating higher intensity tornadoes. Table 3.4-6, reproduced from Fujita with permission, shows the FPP classification of tornadoes along with intensity scale, length scale, and width scale. Also, listed in Table 3.4-6 is an area intensity scale which is based on total damage area. The F-scale intensities are assigned using a qualitative assessment of the worst damage that occurs during a tornado. This is usually accomplished by observing the damage to residential buildings or other structures and calculating the pressure that is needed to cause the observed damage. From calculated tornado wind pressure, one can find the maximum velocity which could generate such pressures. Since classification of tornadoes is based on observation of damage rather than direct measurement of wind speed, two types of errors can be introduced in this process. Direct classification errors are due to inaccuracies in assigning intensity scales to tornadoes whereas random encounter errors are due to lack of damage observation. The uncertainty due to direct classification errors is expected to be unbiased, i.e., it is equally likely that a tornado is underscaled as it is overscaled. On the other hand, random encounter errors are due to the lack of damage medium in a tornado path which could subsequently be used for the tornado classification. Therefore, random

encounter errors are always associated with underestimating the tornado characteristics. Another source of random encounter errors is that small tornadoes are often undetected in unpopulated areas. As an example, increased public awareness has led to a trend toward increased reporting of weaker tornadoes in recent years whereas the average number of strong tornadoes reported is basically unchanged (Twisdale and Dunn, 1983). This error would tend to underestimate the rate of occurrence of all tornado intensities but it would overestimate the occurrence rates of higher intensity tornadoes. An attempt was made in the study by Twisdale and Dunn (1983) to correct the reported tornado data for the above errors.

The tornado hazard model in this study includes the following elements:

- variation of tornado intensity with occurrence frequency; the frequency of tornado occurrences decrease rapidly with increased intensity
- correlation of width and length of damage area; longer tornadoes are usually wider
- correlation of area and intensity; stronger tornadoes are usually larger than weaker tornadoes
- variation in tornado intensity along the damage path length; tornado intensity varies throughout its life cycle
- variation of tornado intensity across the tornado path width

3.4.3.2.1.2 Tornado Occurrence Rate

As a first step in the bounding analysis, the frequency of occurrence of all tornadoes (irrespective of their intensities) at the site was calculated. Based on historical data, the frequency of occurrence of all tornadoes at LaSalle County has been reported to be 1.7 tornadoes per year for a 1° x 1° square (LaSalle FSAR). Assuming a Poisson process for the occurrence of tornadoes, mean arrival rate of tornadoes at the site is found to be 4.8×10^{-4} tornadoes/year-square mile. The calculated occurrence rate for the LaSalle site is compared to two other tornado risk regionalizations. Figure 3.4-3 shows the tornado risk regionalization scheme which was reported by WASH-1300 (Markee et al., 1974) and Figure 3.4-4 shows the regionalization scheme which was proposed by Twisdale and Dunn (1981). Regulatory Guide 1.76 (USNRC) describes the design basis tornado for nuclear power plants and has adopted the

scheme in WASH-1300. The occurrence rates for each region is shown in Table 3.4-7, reproduced from Reinhold and Ellingwood. These occurrence rates have been corrected for possible unreported tornadoes in sparsely populated areas. It is noted that using either regionalization scheme, the occurrence rates of 4.12×10^{-4}/year-mi^2 for Region I or 5.18×10^{-4}/year-mi^2 for Region A compare favorably with the calculated occurrence rate of 4.8×10^{-4}/year-mi^2 for the LaSalle site.

3.4.3.2.1.3 Tornado Hazard Model

Using a Poisson process for occurrence of tornadoes, the probability of a tornado striking the structures during time T with a velocity exceeding V* may be written as:

$$P[\text{strike by tornado with } V > V^*] = \nu T \bullet E[V(A_I) > V^*(A_I)] \quad (3.4\text{-}7)$$

where ν is the mean arrival rate per unit area per year for the site, $V(A_I)$ is the velocity in an area A_I which will be defined below, and E(.) is the expectation operator taken over all tornado parameters.

Figure 3.4-5, (reproduced from Garson, et al, 1974 with permission) shows a rectangular structure with dimensions A and B. Assume that this structure is approached by a tornado that travels at an angle α measured from the side B. Also, let us assume that this tornado travels a distance equal to L and the damage is limited to width W during lifetime of the tornado. Knowing the above information, one can define an area A_I where any tornado initiated in this area would strike the structure. Here, the point of initiation for the tornado is assumed to be the mid-point of width W, but in general the following results are not dependent on this assumption. The area A_I is shown in the lower part of Figure 3.4-5. Using simple geometry, it is observed that A_I is made up of four distinct regions (Garson et al., 1974).

1. The sum of the areas denoted by T_1 and T_2 is equal to the total tornado damage area WL.

2. The area denoted by P is equal to HL where H is the projection of the structure on a line which is perpendicular to the tornado path.

3. The areas denoted by BA_1 and BA_2 sum to the structure area AB.

4. The areas denoted by E_1, E_2, E_3 and E_4 sum to WG where G is the projection of the structure on the tornado path.

Therefore, it is observed that the tornado will strike the structure if it is initiated within an area A_I given by

$$A_I = WL + HL + WG + AB \qquad (3.4\text{-}8)$$

The first term in Equation (3.4-8) is the tornado damage area whereas the next two terms indicate an interaction between the tornado and the structure. Finally, the last term in Equation (3.4-8) is the structure's area. Thus, the tornado hazard curves for a site are expected to depend on the structure's size. For typical structures struck by tornadoes, the last two terms in Equation (3.4-8) may be neglected and A_I may be written as

$$A_I = WL + HL \qquad (3.4\text{-}9)$$

where WL is the area for a point structure and HL is the lifeline term which also contributes to the probability of a tornado strike. Normally, one would integrate the results over the probability distribution of angle α for all possible tornado strikes. For this study, angle α was conservatively chosen such that it would maximize the second term in Equation (3.4-9), i.e., H was chosen as the maximum projection length of the structure. In the following paragraphs, a matrix formulation for calculating the annual frequency of tornado strikes with $V > V^*$ is presented which accounts for both terms in Equation (3.4-9).

The probabilistic model for calculating tornado hazard curves at the site may be briefly described as follows. The occurrence of tornadoes in this model is assumed to have a Poisson distribution (Equation (3.4-7)), i.e., the probability distribution of tornado inter-arrival times is assumed to be exponential. Given that a tornado has occurred at the site, the conditional probability of the tornado intensity scale (FPP) is then based on historical data. Next, for each tornado intensity scale, one has to determine the average or the expected value of tornado area (WL) and tornado path length (L) which is to be used in Equation (3.4-9). Thus, one can calculate the expected value of area A_I for each tornado intensity scale (FPP). Assuming that the maximum tornado wind velocity for each FPP intensity scale is the mid-point of the velocity scale as reported in Table 3.4-6, the probability of a tornado strike with maximum wind speeds exceeding a given velocity V^* is equivalent to the probability of that tornado

being initiated in the area A_I. As an example, an F3 tornado in Table 3.4-6 would correspond to a maximum wind velocity of 182 mph. Also, one can calculate a corresponding A_I area for F3 tornadoes. Therefore, the probability of exceeding 182 mph winds at the site is equivalent to the probability of an F3 tornado occurring in the corresponding A_I at the site. However, the problem is complicated by the fact that an F3 tornado does not exhibit a uniform level of damage along its path. A detailed description of the probabilistic model is given in the next paragraphs.

Table 3.4-7 shows the variation of tornado intensity with occurrence for the regions which are identified in Figures 3.4-3 and 3.4-4. The occurrence-intensity (OI) relationships in this table are based on historical data and they have been corrected for direct classification errors and random encounter errors. Each row of Table 3.4-7 is a vector {OI} which shows the conditional probability of each F-scale intensity tornado given that a tornado has occurred.

As stated previously, each tornado FPP scale is also associated with an area scale, a length scale, and a width scale as shown in Table 3.4-6. For example, an F4 tornado is expected to have a damage area of 1.0 mi^2 to 9.999 mi^2. On the other hand, it is possible for an F4 tornado to have a smaller or a larger damage area. The same statement may be made about the length scale and width scale of tornadoes which are listed in Table 3.4-6. For the present study, one is interested in the expected value of tornado damage area (WL) for each FPP intensity scale. These average areas may be calculated from historical measured damage areas of observed tornadoes, i.e., one has to obtain an area-intensity relationship for tornadoes. Table 3.4-8 (reproduced from Reinhold and Ellingwood, 1983) shows a matrix of area-intensity relationship for all tornadoes. This area-intensity relationship is based on the area and intensity of 10,240 observed tornadoes (Schaefer et al., 1980). Each row of this table shows the percentages of each F-scale intensity tornado which were classified according to area classifications in Table 3.4-6. Since F6 tornadoes have not been observed in the past, the last row in Table 3.4-8 represents engineering judgment in assigning area classifications. This matrix shows that the calculated area and wind scales are slightly skewed and that no tornados are expected to have areas in the A6 range. Representing the average of area scales in Table 3.4-6 by a vector {AA} and the matrix in Table 3.4-8 by {AIM}, the vector of expected values of areas for each F-scale intensity {AI} may be written as

$$\{AI\} = \{AIM\} \bullet \{AA\} \qquad (3.4\text{-}10)$$

Thus, mean tornado area (mi^2) for each F-scale intensity were obtained as $\{AI\}^T = \{0.30, 0.72, 1.8, 4.3, 8.5, 15.7, 18.9\}$.

Another characteristic of a tornado is that its intensity does not stay constant along its path. As noted previously, an FPP intensity scale is assigned to a tornado based on the most severe observed damage. However, a tornado is usually at its highest intensity only for a fraction of the time that it is active. Figure 3.4-6, reproduced from Reinhold and Ellingwood, shows a hypothetical F4 tornado with variation of intensity along its path. Table 3.4-9, reproduced from Reinhold and Ellingwood, shows a matrix {VWL} for combined variation of tornado intensity along its path length and across its path width. Each column of matrix {VWL} in Table 3.4-9 shows the percentage of each F-scale damage in the area (WL) for a tornado which has been assigned an intensity scale based on the most severe observed damage. As an example, F3 tornadoes are expected to inflict F3 damage on only 2.7 percent of the total damage area. In fact, 61.5 percent of the damage that is indicated by an F3 tornado is expected to be very light (F0). This matrix was obtained from the analysis of the damage from 149 tornadoes that occurred on April 3 and 4, 1974.

For a point structure where A_I = WL (see Equation (3.4-9)), the probability of wind speeds exceeding {V*} at the site may be written as:

$$P[\{V(A_{I,WL})\} > \{V^*\}] = \{VWL\} \bullet \{AI \bullet OI\} \qquad (3.4\text{-}11)$$

where {V*} is taken to be the mid-point of tornado velocity scales as shown in Table 3.4-6, i.e., the left-hand side of Equation (3.4-11), which is the probability of exceedence for F-scale intensities, is also equivalent to the probability of exceedence of the mid-point velocities for F-scale intensities from Table 3.4-6. The matrix {VWL} was described in the above paragraph and {AI • OI} is a vector where its elements are the expected values of tornado areas times the occurrence-intensity rates for the same F-scale intensity. As an example, for F6 tornadoes, the above equation for Region A may be written as

$$P_A[F \geq F_6] = P_A[V(A_{I,WL}) > 349 \text{ mph}] = 0.001 \times 18.9 \times 0.0013$$

$$= 2.46 \times 10^{-5} \qquad (3.4\text{-}12)$$

As described previously, there is a second contribution to the probability of the tornado wind speeds exceeding a certain value which arises from the lifeline term in Equation (3.4-9). As shown in Equation (3.4-9), the lifeline term (HL) depends on the tornado length and it is independent of tornado width. In fact, the effect of tornado width variations on the probability of exceedence was ignored by neglecting the term WG in Equation (3.4-8).

Table 3.4-10, reproduced from Reinhold and Ellingwood, shows a matrix of intensity-length relationship {LIM} where each row of the matrix is the fraction of tornadoes with a given F-scale intensity which were observed to have length scales according to Table 3.4-6. This matrix was based on an analysis of 7953 tornadoes between 1971-1979 (Reinhold and Ellingwood, 1982). The expected value of tornado length for each F-scale intensity tornado {LI} may then be computed from

$$\{LI\} = \{LIM\} \bullet \{LL\} \qquad (3.4\text{-}13)$$

where {LL} is the vector of mid-point length scales from Table 3.4-6. Thus a length-intensity vector $\{LI\}^T$ = {1.53, 3.01, 4.76, 9.15, 18.8, 26.9, 30.1} was obtained (miles).

Since a tornado's intensity varies along its length, one needs to establish a relationship between the total length for a given F-scale tornado and the percentages of total length which were observed to have different F-scale intensities. Such a relationship is shown in terms of the matrix of variation of intensity along length {VL} in Table 3.4-11, reproduced from Reinhold and Ellingwood, where each column of the matrix lists the percentages of total tornado length with different F-scale intensities. This matrix was based on 149 tornadoes which occurred on April 3 and 4, 1974.

Thus, the contribution of the lifeline term to the probability of exceedence of a wind speed {V*} at the site may be written as

$$P[\{V(A_{I,WH})\} > \{V^*\}] = \{VL\} \bullet \{LI \bullet OI\} \bullet H \qquad (3.4\text{-}14)$$

Again, {V*} is taken to be the mid-point of velocity scales for each F-scale tornado as shown in Table 3.4-6. The vector

{LI • OI} is obtained by multiplying each term of the length-intensity vector {LI} by the occurrence-intensity vector {OI}. As an example, the contribution of a structure with a characteristic length of H = 1 ft. to the probability of exceedence of F6 tornadoes for Region A is

$$P_A[F \geq F6] = P_A[V(A_{I,WH}) > 349 \text{ mph}] = 0.160 \times 30.1 \times 0.0013 \times \frac{1 \text{ ft}}{5280 \text{ ft/mile}}$$

$$= 1.19 \times 10^{-6} \qquad (3.4\text{-}15)$$

Combining the point structure strike probability and the lifeline strike probability and using the Poisson arrivals for tornadoes (Equation (3.4-7)), the annual probability of exceedence for each F-scale velocity may be written as

$$\{P[F \geq F_i]\} = \{P[V > V_i^*]\} = \nu[\{c_1\} + \{c_2\}H] \qquad (3.4\text{-}16)$$

where vectors $\{c_1\}$ and $\{c_2\}$ are obtained from Equations (3.4-11) and (3.4-14). For the LaSalle site located in Region A, vectors $\{c_1\}$ and $\{c_2\}$ are obtained as

$$\{c_1\}^T = \{1.28,\ 4.76(E\text{-}1),\ 1.52(E\text{-}1),\ 3.08(E\text{-}2),\ 4.39(E\text{-}3),\ 3.66(E\text{-}4),\ 2.46(E\text{-}5)\} \qquad (3.4\text{-}17)$$

$$\{c_2\}^T = \{2.15(E\text{-}4),\ 2.79(E\text{-}4),\ 2.69(E\text{-}4),\ 1.31(E\text{-}4),\ 4.84(E\text{-}5),\ 9.31(E\text{-}5),\ 1.19(E\text{-}5)\} \qquad (3.4\text{-}18)$$

Figure 3.4-7 shows the tornado hazard curves for the LaSalle site which were calculated for lifeline lengths of 100, 300 and 500 feet. The Category I structures at Lasalle are built adjacent to each other. For Unit 2, the dimensions of a rectangle which would enclose all Category I structures are approximately 180′ x 215′. Assuming that a tornado approaches the plant at 45° angle to one of the sides, the maximum lifeline length of the structure is calculated to be H = 280′. From Figure 3.4-7, the annual probability of exceedence of 300

mph winds for a characteristic length of 280' is approximately 1×10^{-6}. The Category I structures are designed for rotational tornado wind speeds of 300 mph and translational tornado velocity of 60 mph, i.e., a total wind speed of 360 mph was used in design and therefore 300 mph may be assumed to be a lower limit on the wind load capacity of the Category I structures. Thus, it is concluded that structural failures due to tornado wind pressures are not significant contributors to the overall plant risk.

3.4.3.2.2 Tornado-Generated Missiles

Missiles generated by tornadoes may lead to a plant damage state if they impact the Category I structural walls or roof slabs with critical velocities. The tornado missile hazard is a low probability event because a sequence of events must occur in order for the missile to cause any damage. This sequence includes the missile injection and transport, missile impact and barrier damage of Category I structures, and an accident sequence. A description of tornado missile bounding analysis for LaSalle Category I structures follows.

The tornado missiles used in the present study are representative of construction site debris and they are the set of missiles which have been listed in the Standard Review Plan. Table 3.4-12 (from the Standard Review Plan, USNRC, 1975) gives a description of these missiles and their respective maximum horizontal velocities for tornado Zone I as defined in Figure 3.4-3. Missiles A, D and F in Table 3.4-12 may be classified as deformable missiles whereas missiles B and C are nondeformable missiles. Except for missile C, these missiles have vertical velocities of 70 percent of postulated horizontal velocities. Missile C which is used to test barrier openings is assumed to have the same velocity in all directions. Missiles A, B, C and E are considered at all elevations and missiles D and F are considered at elevations up to 30 feet above grade.

Based on test data, several formulas have been suggested for nondeformable missile impact on reinforced concrete walls. In all of the studies on missile impact which have been performed to date, it has been concluded that the amount of reinforcement is not an important factor in calculating the scabbing thickness or perforation thickness of a reinforced concrete wall. The most widely used formulas for determination of minimum wall thicknesses required to prevent scabbing are Chang's formula and the modified National Defense Research Committee (NDRC) formula (Chang, 1981). According to Chang, the scabbing thickness (t_s) of a wall or slab may be calculated by (Equation (3.4-3)).

$$t_s = 2.47 \frac{w^{0.4} v^{0.67}}{d^{0.2} (f_c')^{0.4}}$$

where

w = weight of missile (lbs),

v = velocity of missile (ft/sec),

d = missile effective diameter (inches) $= \sqrt{\frac{4A_c}{\pi}}$,

f_c' = ultimate strength of concrete (psi),

A_c = contact area of missiles (in^2).

The modified NDRC formula gives the penetration depth x of a solid missile as

$$x = \sqrt{4KNWd \left(\frac{v}{1000d}\right)^{1.8}} \qquad \text{for } \frac{x}{d} \leq 2.0$$

$$x = \left[KNW\left(\frac{v}{1000d}\right)^{1.8}\right] + d \qquad \text{for } \frac{x}{d} > 2.0 \qquad (3.4\text{-}19)$$

where

$$K = \frac{180}{\sqrt{f_c'}}$$

N is an empirical constant equal to 0.72 for flat-nosed missiles, 0.84 for blunt-nosed missiles, 1.0 for average bullet nosed missiles, and 1.14 for very sharp missiles. Scabbing thickness is then related to penetration depth as follows:

$$\frac{t_s}{d} = 7.91\left(\frac{x}{d}\right) - 5.06\left(\frac{x}{d}\right)^2 \qquad \text{for } \frac{x}{d} \leq 0.65$$

$$\frac{t_s}{d} = 2.12 + 1.36\left(\frac{x}{d}\right) \qquad \text{for } 0.65 < \frac{x}{d} \leq 11.75 \qquad (3.4\text{-}20)$$

For the NDRC formula, best results are obtained for pipe missiles when d is the actual outside diameter of the pipe in calculating penetration depth and equal to an effective diameter in calculating scabbing thickness.

Using the above formulas for the missiles in Table 3.4-12, wall and slab thicknesses which are required to prevent horizontal and vertical missiles from scabbing were calculated (Table 3.4-13). The NRC recommended minimum thicknesses of 16" for roof and 20" for walls compare favorably with the results obtained by the Chang's formula. These calculated thicknesses are higher than some of the wall and roof slab thicknesses of the LaSalle Category I structures. For example, the diesel generator structures at LaSalle have 12" walls and 12" roof slabs. Although the auxiliary building roof and the reactor building roof have 6" slabs on top of a metal deck, they are not considered in this study because the floors which are immediately below the roof slabs in these structures do not contain any ESF equipment. Also, as mentioned in the FSAR, the spent fuel pool which is located at Elevation 843'6" on the operating floor of the reactor building has been analyzed for postulated tornado missiles. All other Category I buildings at LaSalle are protected by walls or slabs which are at least 18" thick. Therefore, it is concluded that the only critical structure at LaSalle that needs to be analyzed further for tornado missile impact is the diesel generator building which has 12" thick walls and 12" thick roof slab.

In performing a bounding analysis for the diesel generator building tornado missile impact, the following factors should be taken into consideration:

1. Given that there is a tornado at the site, the probability of a missile injection and transport resulting in the missile impact of the diesel generator building is very low.

2. Even if a tornado missile impacts the diesel generator building, it may not have enough energy to cause scabbing of the walls or the roof slab.

Twisdale and Dunn (1981) have performed a simulation study for a typical nuclear power plant to obtain tornado missile impact probabilities and probability distributions of missile velocities. They used a total of 65,550 potential missiles which could be injected from different zones near the plant. Since most of these missiles represent objects which would be available during construction of a plant, the total number of missiles is expected to be conservative for the LaSalle station where both units are operating. In fact, the site visit

by SMA personnel verified that the potential missile population at LaSalle is about one-fifth to one-tenth of the number used by Twisdale and Dunn (1981). In Twisdale and Dunn (1981), a flat terrain similar to the LaSalle site was used. Also, a comparison of the plant layout and geometry of the buildings between LaSalle and the example plant in Twisdale and Dunn (1981) showed that the diesel generator building at LaSalle is protected on two sides whereas the diesel generator building for the example plant is protected on one side only. Therefore, using the results of the simulation study by Twisdale and Dunn (1981) for the diesel generator building at LaSalle is expected to be conservative.

Results of the simulation study by Twisdale and Dunn (1981) indicates that given a tornado at the site, the probability of a tornado missile impacting the diesel generator building is approximately 10^{-2}. Since the total number of potential missiles for LaSalle site was estimated to be approximately 12,000, which is lower than 65,500, the conditional probability of missile impact for LaSalle was estimated to be 2×10^{-3}. Also, distributions of the missile velocities show that given a nondeformable missile (6" pipe or 12" pipe) impact with the diesel generator building, the probability of scabbing is high, e.g., roughly 0.6 for the 6" pipe and 0.98 for the 12" pipe. The probability of scabbing due to a nondeformable tornado missile impact may be written as

$$P[S] = P[TS] \cdot P[MI|TS] \cdot P[S|MI] \qquad (3.4\text{-}21)$$

where

S = scabbing

TS = tornado strike

MI = missile impact

Assuming that tornadoes with intensities greater than F1 can transport missiles and cause damage to the diesel generator building, the probability of a tornado strike was estimated to be 1.0×10^{-4}/year (see Figure 3.4-7). Since the nondeformable 6" and 12" pipe missiles represent only 25 percent of the total potential missile population, the last term in Equation (3.4-21), $P[S|MI]$, is estimated to be 0.25. Therefore, using $P[MI|TS] = 2 \times 10^{-3}$ the probability of scabbing was conservatively estimated to be 5.0×10^{-8}. This probability is comparable to a probability of scabbing of 2.8×10^{-7}/year for Region A reported by Twisdale and Dunn (1981).

The deformable tornado missiles, namely wood plank and automobile impact, were included in the design of Category I structures. The velocity used for wood plank in the design was 225 mph which is higher than the suggested velocity by the Standard Review Plan (Table 3.4-12). On the other hand, the automobile velocity used in the design was 50 mph which is lower than the value listed in Table 3.4-12. Results of the simulation study by Twisdale and Dunn (1981) show that given a tornado, the probability of an automobile impacting any of the structures in the plant with a velocity greater than 57 mph is less than 10^{-3}. Due to the inherent conservatisms in design, it may be concluded that the capacity of diesel generator walls for an automobile impact is at least 57 mph. Therefore, the automobile impact's contribution to the plant risk would be less than 10^{-8}/year. The only deformable tornado missile which was not specifically considered in the plant design is the utility pole. However, based on the full-scale tornado missile impact tests conducted by EPRI (Stephenson, 1976), utility poles are not expected to cause any damage to the 12"-thick reinforced concrete walls.

Based on the conservative bounding analysis performed in this study, it is concluded that nondeformable tornado missiles as well as deformable missiles are not significant contributors to the plant risk. It is noted that the HVAC air intakes and exhausts are protected from tornado missiles using adequate concrete barriers. The barriers are placed such that the tornado missiles cannot reach the fan-openings. Also, the auxiliary building roof ventilation stack which is the tallest structure in the plant is designed to withstand the effects of the design basis tornado and therefore will not collapse on the auxiliary building.

3.4.3.3 Non-seismic Category I Structures

3.4.3.3.1 Design Capacity

The non-seismic Category I structures at LaSalle are designed to withstand the effects of 80 miles per hour straight winds and the approaching tornado. The siding enclosures for the following structures are designed to blow-in and blow-out under predetermined tornado wind pressure:

Reactor buildings

Turbine building (above Elevation 767'0")

The metal roof decking for the following structures is designed to blow off under tornado conditions:

Reactor buildings

Turbine building

Auxiliary building

A review of the metal siding specifications used for LaSalle indicated that the siding is designed to blow-in (or out) at tornadic wind pressures between 52 psf and 84 psf, i.e., the siding will start blowing in at 52 psf, and all the siding will have blown in at 84 psf leaving the bare structural frame. Therefore, the structural frame is designed to withstand the 84 psf wind pressure acting on the building with the entire siding intact. The structure is also analyzed for the design basis tornado of 300 mph maximum tangential velocity acting on the bare frame to ensure that it will not collapse on adjacent seismic Category I structures.

The lowest wind speed at which the siding will start blowing in (or out) is estimated as $(52/C_p \times 0.002558)^{1/2} = 136$ mph for $C_p = 1.1$ from Figure 4 in ANSI A58.1 (1982).

3.4.3.3.2 Exceedence Probability

Structural failure of the siding or roof decking could occur when the wind speed exceeds 136 mph. This could happen in either a tornado or a strong wind storm. Therefore, the exceedence probability is estimated considering both tornadoes and straight winds.

Tornado Loads

The probability of exceedence of the lowest capacity of siding by tornadic winds is obtained from Figure 3.4-7 as 1×10^{-4} per year.

Straight Extreme Winds

The probability of extreme wind speeds at LaSalle exceeding 136 mph is estimated by reviewing the wind speed data for the pertinent weather stations.

Figure 3.4-8 from the report by Changery (1982) shows the weather stations in the vicinity of the site. The LaSalle weather station had only 9 years of wind speed data. Therefore, data from the neighboring stations (Chicago, Moline and Peoria, Illinois) were utilized in estimating the wind speed probabilities at LaSalle. It was found that Moline, Illinois, station had the highest annual wind speed exceedence probabilities among these stations. Thus, for the purpose of bounding analysis, Moline, Illinois, data was used. The probability of exceeding 136 mph wind speed was calculated by

fitting an extreme value Type I distribution to the annual maximum wind speed data as recommended in ANSI A58.1 (1982). This probability of exceedence value was obtained as 3.8×10^{-6} per year.

The probability of wind speeds exceeding 136 mph as a result of tornado strikes or extreme wind storms was estimated as $1 \times 10^{-4} + 3.8 \times 10^{-6} = 1 \times 10^{-4}$ per year. It is assumed that the failure of non-seismic Category I structures will not lead to core damage. However, if any components housed in these structures are included in the fault trees, the failure rates used in calculating their unavailabilities should be assumed not less than 1×10^{-4} per year (lower rates might be used if the components are protected somehow from the structural failure). Similarly, the exposed tanks (e.g., condensate storage tank) which are typically designed to withstand the effects of earthquake and straight wind loads using the Uniform Building code (1973) requirements should be assumed to have failure rates not less than 1×10^{-4} per year.

3.4.3.4 Uncertainty Analysis for Winds and Tornadoes

A probabilistic bounding analysis for wind and tornado hazard and tornado missile hazard at the LaSalle site was performed in Sections 3.4.3.1 through 3.4.3.3. Based on the results presented in these sections, it was concluded that the probability of potential core damage due to winds and tornadoes is negligible. The bounding analysis was based on conservative assumptions regarding tornado hazard and structural fragility models; however, it did not address the question of uncertainties in models and modeling parameters. In this section, estimates of these uncertainties are presented. Also, these uncertainties are propagated in the bounding analysis to obtain an estimate of the uncertainty in the probability of severe core damage. Since wind loads were shown to be of lesser importance in comparison with tornado loads for LaSalle structures, attention will be focused on uncertainty in tornado loads and tornado generated missiles.

Uncertainty in the calculated probability of core damage due to tornado loads arises from the following:

1. Uncertainty in tornado hazard calculations

2. Uncertainty in wind pressure calculations given a tornado wind speed

3. Uncertainty in structural response and fragility calculations.

The hazard model utilized in this study has been previously discussed in detail (Section 3.4.3.1). The model is based on historical data as well as subjective classification of tornadoes based on their maximum observed damage. Also, the data base for the model is not uniform, e.g., the area-intensity relationship is based on a sample of 10,240 observed tornadoes whereas variation of tornado intensity with path is based on an analysis of 149 tornadoes which occurred in a tornado outbreak during a two-day period. The tornado model developed by Reinhold and Ellingwood (1982) has corrections for tornado classification errors and random encounter errors.

Recently, McDonald (1983) completed a tornado hazard probability assessment which accounts for uncertainty in area-intensity and occurrence-intensity relationships. The model used by McDonald (1983) is very similar to the model used in the present study. Hazard uncertainty reported in McDonald (1983) is due to dispersion in data, i.e., regression models were fitted to historical tornado data to represent area-intensity and wind speed occurrence relationships. Confidence bounds on the best estimate tornado hazard curve were established from uncertainties in regression models. Figure 3.4-9 shows the median tornado hazard curve for the LaSalle site with 95 percent confidence bounds as estimated based on the study by McDonald (1983).

The uncertainty in tornado pressure coefficient was estimated using the reported uncertainty for straight wind pressure coefficient (Ellingwood, 1978). The pressure coefficient relates the induced pressure on wall panels to maximum wind velocity. Induced pressure on a wall panel is a function of structural shape as well as the location on a wall panel. Therefore, there is some uncertainty associated with the pressure coefficient. Ellingwood (1978) reports a coefficient of variation equal to 0.15 for uncertainty in the straight wind pressure coefficient and a coefficient of variation equal to 0.05 representing the uncertainty in wind modeling. Due to lack of data for tornado wind pressures, the uncertainty in straight wind pressure coefficient was used in the present study. Since the physical phenomenon of induced pressure due to straight winds is the same for tornadoes, this assumption is judged to be realistic.

As discussed in Section 3.4.3.1, the seismic Category I structures at LaSalle have an effective design capacity of 360 mph against tornado wind loads. There are two sources of conservatism in design: (1) there is an inherent conservatism in the nominal steel yield stresses and the nominal concrete strengths specified by the designer, and (2) the code allowable stresses are lower than ultimate or yield stresses. The conservatism factors in nominal yield and design code

allowable stresses were estimated to be 1.2 and 1.1, respectively, for screening purposes due to assumed variations in material behavior. Since the induced wind pressure on a wall panel is proportional to the square of applied wind velocity, the median wind capacity of LaSalle Category I structures (V) is calculated as:

$$V = [1.1 \times 1.2 \ (360)^2]^{1/2} = 414 \text{ mph} \qquad (3.4\text{-}22)$$

Uncertainty in the median wind capacity of the LaSalle buildings is due to uncertainties in the material behavior used in the structural model. The coefficient of variation in material yield stress was estimated to be 0.15 (Galambos and Ravindra, 1978; Mirza and MacGregor, 1979; Mirza, Hatzinikolas and MacGregor, 1979). Also, a coefficient of variation equal to 0.15 was used for modeling uncertainty.

Next, it is assumed that the variability in wind pressure (ε_p) can be modeled as the product of random variables representing variabilities in pressure coefficient (ε_{pc}), wind modeling (ε_{wm}), material yield (ε_{my}) and structural modeling (ε_{sm}).

$$\varepsilon_p = \varepsilon_{pc} \ \varepsilon_{wm} \ \varepsilon_{my} \ \varepsilon_{sm} \qquad (3.4\text{-}23)$$

Assuming that the ε's are lognormally distributed, the logarithmic standard deviation for wind pressure (β_p) was calculated to be 0.26. Since the calculated wind pressure is proportional to the square of wind velocity, logarithmic standard deviation of wind velocity is 1/2(0.26) = 0.13. Thus, the wind fragilities of reinforced concrete structures at LaSalle are defined in terms of their median capacity (v = 414 mph) and a composite logarithmic standard deviation (β_v = 0.13). Figure 3.4-10 shows the tornado fragility curves for LaSalle Category I structures. In order to develop the fragility curves, it was assumed that the composite variability β_v can be split into two terms $\beta_{v,r}$ = 0.08 and $\beta_{v,u}$ = 0.11 representing the randomness and uncertainty in the tornado wind capacity calculations.

Figure 3.4-11 shows the distribution of annual frequency of severe core damage calculated from the family of tornado hazard and structural wind fragilities. From this distribution, the median frequency of severe core damage was found to be 3×10^{-8}/year whereas the 95 percent confidence bound was calculated to be 3×10^{-7}/year. Since the bounding analysis has been conservative and the 95 percent confidence bound probability is extremely low, it is concluded that

tornadoes do not contribute significantly to the probability of core damage.

3.4.3.5 Conclusions

The bounding analysis described in this section has shown that the high confidence probability of failure under wind and tornado loading for Seismic Category I structures housing critical equipment is on the order of 10^{-7} per year. Even if these structural failures are conservatively assumed to lead to core damage, their contribution to the plant risk is negligible small when compared to other events.

The non-seismic Category I structures and exposed tanks have frequencies of failure under wind and tornado loading on the order of 10^{-4} per year. Their failures may not lead to core damage; if components in the structures should appear in the fault trees, the failure rates used to calculate their unavailabilities should not be less than 10^{-4} per year unless the components have additional protection.

3.4.4 Transportation Accidents

This section describes the bounding analysis for transportation accidents near the LaSalle site which could contribute to the plant core damage frequency. A transportation accident near the plant may lead to core damage in one of the following ways: (1) a chemical explosion due to a transportation accident may cause damage to Category I structures and safety-related equipment, and (2) toxic chemicals which are released in a transportation accident may drift into the control room and cause incapacitation of the operators. A bounding analysis was performed taking into consideration the frequency of occurrence of transportation accidents as well as fragility of the plant structures against accident effects. The bounding analysis for chemical explosions is described in Section 3.4.4.1 and the analysis for toxic chemical release is described in Section 3.4.4.2.

There are three modes of transportation near the site, i.e., highway, railroad, and river. Major highways near the site (Interstate 80 and U.S. Highway 6) are farther than 5 miles from the plant and therefore will not be considered in this study. LaSalle County Road 6 is the only paved road near the site and passes approximately 2000 feet south of the plant structures. The Chicago Rock Island and Pacific railroad is farther than 3.5 miles north of the plant structures. The Illinois River is approximately 3.5 miles north of the plant at its closest point. The transportation routes near LaSalle County Station are shown in Figure 3.4-12 (LaSalle FSAR).

3.4.4.1 Chemical Explosions

A chemical explosion near the plant structures may cause overpressure, dynamic pressures, blast-induced ground motion, or blast generated missiles. However from previous research in this topic, it has been determined that overpressures would be the controlling consideration for explosions resulting from transportation accidents (Regulatory Guide 1.91, USNRC). An accident overpressure at the site can also occur because of vapor cloud explosions drifting towards the structures. This type of explosion involves complex phenomena which depend on the material involved, combustion process, and topographical and meteorological conditions. According to a study by Eichler and Napadensky (1978), present theoretical and empirical knowledge is too limited to quantitatively evaluate realistic accidental vapor cloud explosion scenarios. However, vapor cloud explosions are implicitly included in the TNT equivalents which are used to represent transportation accidents. According to the Regulatory Guide 1.91 (USNRC), chemical explosions which would result in free-field overpressures of less than 1 psi at the site do not need to be considered in the plant design. Based on experimental data on hemispherical charges of TNT, a 1 psi pressure would be translated into a safe distance R (feet) which is defined as:

$$R \geq KW^{1/3} \qquad (3.4\text{-}24)$$

where K = 45 and W is an equivalent weight of TNT charges. The maximum probable equivalent TNT charge is 50,000 lbs for a highway truck, 132,00 lbs for a single railroad box car, and 1×10^7 lbs for a river barge. A recent study be Eichler, Napadensky and Mavec (1978) shows that accidents in an empty barge due to vaporization of liquid left in the tank would lead to a maximum TNT equivalent explosive load of 1000 lbs. Since this type of accident does not produce a more severe condition, it will not be considered further in this analysis. Figure 3.4-13, which is reproduced from Regulatory Guide 1.91 (USNRC), shows the safe distances for a highway truck, a railroad box car, and a river barge. Based on this analysis, it may be concluded that explosions outside of LaSalle County Station in any of the transportation routes will not pose an overpressure hazard to the plant structures.

In the study by Eichler, Napadensky, and Mavec (1978), the hazard from vapor cloud drifts which could be generated in

barge accidents were examined. According to this study, although a vapor cloud may theoretically drift towards the site and produce higher incident overpressures at the site, the following reasons minimize the threat due to drifting vapor clouds.

1. Probability of vapor cloud explosion rapidly decreases due to the decrease in concentration as it travels away from the accident site.

2. Range of unfavorable wind directions (i.e., wind directions that can impact the plant) rapidly decreases as spill to site distance increases.

Based on this study, it was concluded that the equivalent TNT explosive weights which are specified by the NRC are very conservative.

Vapor cloud explosions were also considered in the Limerick Severe Accident Risk Assessment. In the Limerick study, vapor cloud drifts from a railroad accident which is approximately 600 feet away from the nearest Category I structure were considered. The equivalent TNT in the Limerick study was calculated according to:

$$W_i = \left[F \frac{S_i Q \rho}{A} \Delta H_c E \right] 500 \text{ Kcal/lb of TNT} \qquad (3.4\text{-}25)$$

where:

F = fraction of spill quantity involved in vapor cloud,

$\frac{S_i Q \rho}{A}$ = gm-mole of combustible chemicals spilled,

S_i = spill fraction,

Q = quantity of shipment,

ρ = density of liquid,

A = molecular weight,

ΔH_c = heat of combustion (Kcal/gm-mole),

E = yield of explosion.

Also, based on historical data, the cumulative density function of distance from the accident site to ignition was obtained. This is shown in Figure 3.4-14, reproduced from Eicher 1978, where the curve may be represented by a line as:

$$P_I = \frac{1}{2}\left[1 + \text{erf}\left(\frac{\log_{10}A - 1.38}{2.45}\right)\right] \qquad (3.4\text{-}26)$$

$$A = 0.175\ r^2$$

where r is the distance from the spill site in meters. As mentioned before, the railroad in the LaSalle area is approximately 4 miles from the site. Therefore, if the plume travels a distance of 1 mile, the probability of not having an ignition before that distance is reached reduces to approximately 10^{-3}. If the same CDF is assumed for a barge accident, it is observed that vapor clouds do not pose a hazard to the plant structures, i.e., assuming that the vapor cloud can travel a maximum distance of 1 mile, an explosion will result in a small incident overpressure on the buildings.

Although the NRC Regulatory Guide is conservative in defining the equivalent TNT explosive loads, it is unconservative with respect to structural capacities because of the following reason. The free-field pressure wave which results from a TNT explosion is reproduced from Kennedy et al. (1983) in Figure 3.4-15. This pressure consists of an instantaneous rise and a decay to zero followed by a slight negative pressure. The values of peak incident overpressure (P_{so}), positive phase impulse (I), and positive duration (t_d) which were based on experiments are shown in Figure 3.4-16, also reproduced from Kennedy. Note from Figure 3.4-15 that the overpressure acting on the wall panels of a structure also includes a reflected pressure.

Therefore, the overpressure on the wall panels is approximately twice the incident overpressure. In addition, the dynamic effect of peak overpressure for a wall panel may be significant. Figure 3.4-17 shows dynamic load factors for a single-degree-of-freedom system as a function of the ratio of pulse duration (t_d) to period of structure (T) for a triangular pulse and a rectangular pulse (reproduced from Biggs, 1964 with permission). It can be observed that the dynamic load factor for a pulse can reach a maximum value of 2.0 for higher t_d/T ratios. As a result of pressure reflection and dynamic effects, a free-field overpressure of 1 psi at the site could result in an effective static overpressure of up to 4 psi on the wall panels. Therefore, a

more detailed study of overpressure due to transportation explosions was deemed necessary.

An examination of the transportation accidents in the vicinity of the LaSalle site showed that the controlling accident is a truck explosion on County Road 6 south of the plant. Assuming Regulatory Guide maximum explosive load of 50,000 lbs, a peak free-field incident overpressure P_{so} of 0.66 psi was calculated from Figure 3.4-16. Therefore, maximum static overpressure on the wall panels could be as high as 2.64 psi. Since the LaSalle Category I structures have been designed for Zone I tornado effects, their minimum static lateral design load capacity is at least 3.0 psi. Based on this conservative comparison, it may be concluded that the Category I structures have a higher capacity than the maximum postulated overpressure due to an explosion.

The above analysis for calculating overpressure capacity of the wall panels neglected the ability of structural walls to absorb energy under inelastic behavior. In fact, Kennedy et al. (1983) suggest that a conservative ductility value equal to 3.0 should be used as the limit of inelastic behavior for structural wall panels. Ductility is defined as the ratio of peak inelastic displacement to the yield displacement for an elastic-plastic structure. The maximum ductility which was assumed by Kennedy et al. is conservative because of the following reason. When a reinforced concrete panel is subjected to blast loads, it develops extensive cracking which means that the tension in cracked sections is resisted by the steel reinforcement. In fact, ultimate capacity of a reinforced concrete panel may be calculated using the yield line theory (Ferguson, 1973, Park and Paulay, 1975). According to the yield line theory, ultimate capacity of a reinforced concrete panel which is subjected to a uniform pressure is dependent on its geometry and ultimate moment capacity of the cracked sections. Since ultimate moment capacity of a cracked section is dominated by the steel ultimate strength, well designed reinforced concrete panels are expected to exhibit fairly high ductilities under blast loads.

Using the results from Kennedy, et al. (1983), free-field incident overpressure capacity of wall panels in LSCS structures was calculated to be a minimum of 1.95 psi. There are two differences between the calculations for wall panel capacities in Kennedy, et al. (1983) and the present study.

The first difference is that blast capacities in Kennedy et al. (1983) were calculated for a barge explosion. This is a conservative assumption because barge explosions correspond to largest pulse durations and therefore result in higher dynamic load factors (see Figure 3.4-17). The second difference is that the wall panel thicknesses used in Kennedy, et al. were 18 and 24 inches. This is an unconservative factor because the diesel generator walls are 12 inches thick. However, it is shown in Kennedy et al. (1983) that the wall thickness does not have a significant effect on the wall capacity, i.e. a maximum difference of 15 percent was observed between capacities of 18" walls and 24" walls. Considering all other conservative assumptions used in Kennedy et al., (1983), 1.95 psi may be accepted as a lower bound capacity of structural wall panels in LaSalle. A comparison of minimum wall capacity of 1.95 psi (incident overpressure) with a free-field incident overpressure of 0.66 psi reveals that there is at least a factor of 3 against an overpressure failure of structures due to the worst truck explosion. Therefore, it is concluded that chemical explosions do not contribute to the plant risk.

3.4.4.2 Toxic Chemicals

A toxic chemical spill near the LaSalle site would pose a danger to the plant if toxic chemicals penetrate into the control room through air intakes and cause the operators to be incapacitated. As discussed in Section 3.3.1, this condition can happen if (1) large quantities of toxic chemicals are released, (2) there are favorable wind conditions which would cause a drift of chemicals towards the control room air intakes at excessive concentrations, and (3) there are no detection systems and air isolation systems in the control room.

Among the three transportation modes near the site, a barge accident in the Illinois River could result in the largest amount of chemical spill. As reported previously, the Illinois River is 3.5 miles away from the plant structures at its closest distance. Also, the river elevation is approximately 180 feet below the plant grade. Considering the fact that many of the toxic vapors are denser than air, the atmospheric dispersion of these chemicals towards the plant under favorable wind conditions is unlikely because of the difference in plant and river elevations. Also, for more turbulent wind conditions, it is highly unlikely that a toxic vapor would reach the control room air intakes at excessive concentrations. An examination of Table 3.3-1 shows that among the hazardous chemicals transported on barge to the nearby industrial facilities, chlorine, anhydrous ammonia, and

butadiene are shipped at large quantities. Since the control room HVAC at LaSalle is equipped with detectors for chlorine and anhydrous ammonia, these two chemicals are excluded from further consideration. According to the Regulatory Guide 1.78 (USNRC), butadiene has a low toxicity limit. Therefore, even if the maximum quantity of butadiene required at the Borg-Warner chemical facility was shipped on one barge it would still meet the requirements of Regulatory Guide 1.78 (USNRC) as to the proximity of toxic chemicals to a nuclear power plant. From the foregoing discussion, it was concluded that chemical spills resulting from barge accidents do not contribute significantly to the plant risk. Using the same logic, railroad accidents are also excluded from external events analysis because the Chicago Rock Island and Pacific Railroad is further from the plant than the Illinois River and a railroad accident would result in a much lower quantity of spill than a barge accident.

As shown in Figure 3.4-12, the major U.S. highways in the vicinity of LaSalle site are more than 5 miles away from the plant structures. Also, state highway 170 is more than 3 miles from the plant structures. The nearest paved road to the plant is LaSalle County Road 6 which is 2000 feet south of the plant structures. Therefore, the only possible hazard to the site would come from the County Road 6. Since this road is not a major highway, there is no reason to believe that it is used for transportation of chemicals other than those shipped to the plant or to the nearby industrial facilities. On this basis, a chemical spill near the site would be either detected, i.e., chlorine or anhydrous ammonia spill, or it would be of no consequence to the plant operators, i.e., butadiene spill. Thus, it was concluded that transportation accidents leading to toxic chemical spills are not significant contributors to the plant risk.

3.4.5 Turbine Missiles

This section describes the bounding analysis of the LaSalle plant for the risks from turbine missiles. A review of the historical background, FSAR analysis and recent issues in regards to turbine missiles is given.

3.4.5.1 Historical Background

Failures of large steam turbines in both nuclear and fossil-fueled power plants, although rare, have occurred occasionally in the past. These failures have occurred because of one or more of the following broad classes of reasons: (1) metallurgical and/or design inadequacies, (2) environmental

effects, (3) out-of-phase or generator field failures, and (4) failures of overspeed protection systems. The failures have resulted in loss of blades, disk cracking, rotor and disk rupture, and even missiles. Turbine missiles are highly energetic and have the potential to damage safety-related structures housing critical components. Therefore, protection of nuclear power plants from turbine missiles is an important safety consideration. Also, rupture of the turbine casing in a boiling water reactor plant (e.g., LaSalle) may lead to release of primary coolant steam and radioactivity to the environment. Hence, the plant owners aim to minimize the frequency of turbine failures resulting in casing rupture even if there are no significant turbine missile strikes on safety-related components.

In a total of 2,500 years of turbine operation in nuclear power plants in the free world, only four failures have occurred: Calder Hall (1958), Hinkley Point (1969), Shippingport (1974), and Yankee Rowe (1980). External missiles were produced in the Hinkley Point and Calder Hall failures. Although the causative mechanisms of these failures have been identified and are generally corrected in the modern nuclear turbines, there is no assurance that other types of turbine failures will not occur in the future. Recent discovery of widespread stress corrosion cracking in the disks and rotors of operating nuclear turbines has revived the industry's interest in the issue of turbine failures.

Nuclear plant turbines rotate at 1800 rpm with the low-pressure (LP) and high-pressure (HP) sections on a contiguous shaft. The LP sections have blade hubs (called "wheels" or "disks") shrunk onto the rotor. Depending on the manufacturer and rated capacity of the turbine, there could be 10 to 14 disks on each LP section. The disks are massive components each weighing between 4 and 8 tons. These disks, because of their relatively large radius, are the most highly stressed spinning components in the turbine. With the turbine unit running at less than 120 percent of the rated speed, the disks are stressed well below the yield strength of material so that failures can be caused only by undetected material flaws that may be aggravated by stress corrosion and fatigue. At 180 percent of the rated speed, the disks are stressed at or above their ultimate strength so that they burst into fragments. At intermediate speeds (i.e., 120 to 180 percent), rupture of disks may be caused by a combination of flaws and weaker material in the disks.

Turbine missiles are spinning, irregular fragments with weights in the range of 100 to 8,000 pounds, and velocities in the range of 30 ft/sec to 800 ft/sec. It is conventional to discuss two types of turbine missile trajectories: low trajectory missiles (LTM) and high trajectory missiles (HTM). The low trajectory missiles are those which are ejected from the turbine casing at a low angle toward a barrier protecting an essential system. High trajectory missiles are ejected vertically (almost) upward through the turbine casing and may strike critical targets by falling on them. The customary ballistic distinction between LTM and HTM is the initial elevation angle (ϕ) of the missile (LTM is for $\phi < 45°$ and HTM is for $\phi \geq 45°$). Turbine manufacturers have specified that the maximum deflection angle for the missiles produced in the burst of the last disk on the rotor is 25°. Based on this, the NRC has defined a low trajectory missile strike zone in the Regulatory Guide 1.115 (USNRC) and recommends that the essential systems be located outside this LTM strike zone. If a turbine missile impacts a barrier enclosing a safety-related component, interest lies in knowing if the missile perforates or scabs the barrier to cause sufficient damage to the component. Using empirical formulas for scabbing derived on the basis of the full scale and model tests, it is estimated that concrete barriers should be at least 4 feet thick to prevent scabbing. The need for providing such barriers depends on the probability of turbine failure and the arrangement of safety-related components with respect to turbine missile trajectories. In the design of a nuclear power plant, the designers have many alternative approaches for treating the potential effects of turbine failures (Sliter, Chu, and Ravindra, 1983). These approaches can be grouped as: (1) prevention of turbine failure, (2) prevention of missiles, (3) prevention of strike on critical components, and (4) performance of probabilistic analysis to demonstrate that the probability of turbine missile damage is acceptably low. In the LaSalle FSAR, it is shown that the probability of turbine missile damage is acceptably low. The following subsections review the FSAR Analysis from a PRA standpoint and utilize and update the results for the bounding analysis.

3.4.5.2 Probabilistic Methodology

The probability of serious damage from turbine missiles to a specific system in the plant is calculated as (Bush, 1973):

$$P_4 = P_1 \; P_2 \; P_3 \qquad (3.4\text{-}27)$$

where:

P_1 = probability of turbine failure leading to missile generation,

P_2 = probability of missiles striking a barrier which encloses the safety system given that the missile(s) have been generated,

P_3 = probability of unacceptable damage to the system given that one or more missiles strike the barrier.

In practice, the evaluation of P_4 should include consideration of different speed conditions, distribution of missiles, and all the safety-related components and systems in the plant.

3.4.5.2.1 Probability of Turbine Failure P_1

LaSalle County Station has 38" last stage bucket 1800 rpm turbine generators manufactured by the General Electric Company (GE). Typically, turbine failures under three speed conditions are considered. Failures at or near the rated speed of the turbine could occur primarily due to brittle fracture of disk material. Overspeed failures could occur because of turbine overspeeding and subsequent disk rupture due to brittle fracture or ultimate tensile failure of material. Design overspeed is defined as follows. The calculated speed attained following the loss of full load and the malfunctioning of the turbine speed governing system along with a successful tripping of the turbine overspeed trip mechanism will not exceed overspeed which is 120 to 130 percent of the rated speed. The turbine disks may rupture at this overspeed from brittle fracture propagating from an undetected flaw. Destructive overspeed is the lowest calculated speed at which any LP rotor disk (or wheel) will burst based on the average tangential tensile stress being equal to the maximum ultimate tensile strength of the disk material, assuming no flaws or cracks in the disk. The destructive overspeed is typically between 180 and 190 percent of the rated speed of the turbine.

Probability of failure at an overspeed (e.g., design overspeed and destructive overspeed) is calculated as the product of the probability P_{11} of attaining the specified overspeed condition when the turbine generator unit at full load is unexpectedly separated from the system and the probability P_{12} that a turbine disk(s) ruptures and disk fragments exit the turbine casing when the overspeed condition is reached. The probability of attaining an overspeed, P_{11}, is calculated by modeling the overspeed event as a sequence of simple events

and performing a fault tree analysis. The analysis utilizes the failure rates for electronic components, control valves, stop valves, overspeed trips, etc., and incorporates the effects of in-service inspection (GE, 1973).

General Electric (1973a) has established that the probability of missile generation at the rated speed or at the design overspeed conditions (called "the low speed burst") is statistically insignificant and as such no missiles are postulated at these speeds. The probability of disk failure leading to the ejection of a missile at the destructive overspeed (called the "high speed burst") is calculated by GE as 5×10^{-9} per year.

Bush (1973) has analyzed nuclear and relevant fossil turbine failure data with the objective of making a realistic estimate of the probability of turbine failure leading to missile generation. Operating history of nuclear turbines is too short to make a reliable estimate of the failure probability based on only nuclear data. Hence, fossil turbine failures that are judged to be relevant to this analysis are also included. The most comprehensive study to date on the historical failure data is that performed by Patton et al., (1983) for the Electric Power Research Institute. They estimate the probabilities of turbine missile generation at operating speed and overspeed as 1.20×10^{-4} per year and 0.44×10^{-4} per year, respectively. These estimates are several orders of magnitude higher than those reported by GE (1973a). Recent discovery of stress corrosion incidents in the operating GE turbine-generators (Southwest Research Institute, 1982) suggest that P values are not as low as what the manufacturers have estimated.

Following the approach taken in the Seabrook PRA (Pickard, Lowe and Garrick, Inc., 1983), the estimates made by GE (1973a) were taken to be the lower bounds (i.e., 5 percentile) on P_1 for the two speed conditions. Similarly, the estimates made by Patton et al. (1983) were assumed to be the upper bounds (i.e., 95 percentile). The uncertainty in the P_1 values was modeled as lognormally distributed with the percentiles given above. Table 3.4-14 shows the estimates of annual probability of turbine missile generation. Since the mean value of P_1 is estimated to be about three orders of magnitude higher than 10^{-7}/year, turbine missiles cannot be excluded in the scoping quantification solely on the basis of the probability of missile generation.

3.4.5.2.2 Probability of Missile Strike P_2

When the fragments produced in a disk rupture escape the turbine casing, their paths have to be determined in order to

know if they intersect barriers protecting essential systems of the nuclear power plant. For this purpose, a description of the parameters of these missiles is needed. Major turbine manufacturers have developed their own - generally proprietory - techniques for assessing whether or not disk fragments exit the turbine casing and the parameters of resulting missiles. By making a set of conservative assumptions regarding the disk breakup mechanism and the impact between the disk fragments and casing structure, they estimate the missile exit conditions. These conditions include weight, cross-sectional areas, shape, size, number of fragments, and exit velocities at different speed conditions. Table 3.4-15, reproduced from the LaSalle FSAR, shows the properties of missiles postulated in a wheel burst of GE 38" last stage bucket 1800 rpm low pressure turbine generators installed at LaSalle County Station.

The probability of missile striking a barrier is calculated as follows: low trajectory missiles are considered to travel in straight line paths. Their direction is defined in terms of two angles i.e., the ejection angle, θ_1, from the horizontal plane and the deflection angle θ_2 from the plane of rotation of the ruptured disk (Figure 3.4-18). The angle θ_1 could vary from 0° to 90°. The limits on θ_2 are specified by the turbine manufacturer (e.g., GE specifies -5° to +5° for interior disks and 0° to 25° for end disks). It is customary to assume that the angles θ_1 and θ_2 are distributed uniformly within the specified limits. The probability of a low trajectory missile strike on a structural barrier protecting an essential system is calculated as the ratio of the solid angle the barrier subtends at the missile origin to the total solid angle within which the missile can be ejected out of the turbine casing (GE, 1973a).

High trajectory missile strikes are analyzed using ballistic theory (Bush, 1973; General Electric 1973a; Semanderes, 1972; Filstein and Ravindra, 1979). The missile is modeled as a point mass experiencing no drag forces. Since the initial velocity of a missile and the ejection and deflection angles are random variables, there is a finite probability that any essential system will be struck by high trajectory missiles. The strike probability density, P_A per unit horizontal strike area, located at a radial distance r from the missile origin is expressed as (Filstein and Ravindra, 1979).

$$P_A = \frac{x_{max}^3 - x_{min}^3}{48\, r^3 g \sin\Delta (V_2 - V_1)} \qquad (3.4\text{-}28)$$

where $x_{min} = \frac{rg}{V_2}$

$$x_{max} = \begin{cases} \frac{rg}{V_1} & \text{if} \quad r \leq \frac{2V_1^2 \sin\Delta}{g \cos\theta_3} \\ \sqrt{rg \sin^2\left[\cos^{-1}\left(\frac{\sin\Delta}{\cos\theta_3}\right)\right]} & \text{otherwise.} \end{cases} \qquad (3.4\text{-}29)$$

In the above equations, the missile velocity is assumed to vary between V_1 and V_2; the coordinates of the point along the missile trajectory are (x,y,z) where $x = r \cdot \sin\theta_3$ and $y = r \cdot \cos\theta_3$. θ_3 is given in terms of θ_1 and θ_2 by

$$\text{Cot } \theta_3 = \text{Cot } \theta_2 \cdot \text{Cot } \theta_1 \qquad (3.4\text{-}30)$$

and g is the acceleration due to gravity.

Twisdale et al. (1983) have developed a Monte Carlo simulation methodology for tracking the turbine missiles. A six-degree-of-freedom (6D) model for predicting the free-flight motion of rigid bodies has been formulated. It considers drag, lift, and side forces and simulates missile tumbling by periodic reorientation. A computer code called TURMIS has been developed to integrate the coupled nonlinear ordinary differential equations of motion. Sensitivity studies performed using this sophisticated 6D model clearly support the use of no-drag ballistic model for low-trajectory turbine missile calculations. For high trajectory missiles, the ballistic model introduces prediction errors for individual trajectories, but these errors may not be significant (due to compensating effects of reduced speed and increased impact probability) when statistically averaged for plant risk analysis.

3.4.5.2.3 Probability of Barrier Damage P_3

When a missile impacts a structural barrier (i.e., wall or roof) protecting an essential system, one or more of the following events could take place: penetration, front-face spalling, perforation or back-face scabbing of the barrier, overall response of the barrier, and ricochet of the missile. All of these events may be important in evaluating the damage

potential of turbine missiles. However, local effects of turbine missiles on concrete and steel barriers normally provided in nuclear power plants are particularly important and include penetration, perforation, and scabbing. Penetration into a reinforced concrete barrier that does not produce back-face scabbing may not constitute a safety-related damage event unless front-face spalling is of concern. Perforation is the event in which the missile completely penetrates the barrier and continues its flight with a residual velocity less than the initial impact velocity. Scabbing is the failure mode of most interest because the scabbed concrete fragments may damage the enclosed safety-related component or the piping, electrical cable, or instrumentation attached to it.

The probability of barrier damage P_3 is calculated using the random properties of the missile (i.e., weight, velocity, impact area, obliquity, and noncollinearity) and the empirical impact formulas (Chang, 1981; Berriaud et al., 1978; Twisdale et al., 1983). The dispersion in the impact test data about the empirical formulas is used to develop probability density functions of perforation or scabbing thickness. For any given missile impacting a structural barrier of known material and thickness, the probability of perforation or scabbing is calculated using these probability density functions.

Evaluation of P_2 and P_3 can be done numerically if the missile initial conditions are described by a limited set of parameters and if the plant is assumed to be damaged when the external barrier of a safety-related structure is breached (i.e., perforated or scabbed). In general, turbine missiles are described by a number of random parameters and several barriers separate the safety-related components from the missile sources. A Monte Carlo simulation procedure such as the TURMIS computer code developed by Twisdale et al. (1983) would be needed to handle the multitude of missile trajectories and possible impact conditions encountered in a nuclear power plant. The nuclear power plant is modeled for this analysis as follows. A component may be damaged by a missile physically impacting it, or by the missile damaging the electrical cables or piping that are needed for the component to function. Since it is impractical to model all piping, electrical cables, and HVAC ducts for the turbine missile analysis, the components may be modeled as being enclosed in fire zones. Each fire zone's boundaries are delineated such that the component and all its lifelines (piping, electrical cables, etc.) are within this zone. Therefore, the fire zones are independent of each other. By this technique, the safety-related structures of a plant are divided into a small number of fire zones (at each elevation

in the structures and/or through different elevations). The sequences of fire zones which if damaged by missiles in a single turbine failure may lead to core damage or serious release (i.e., "cut sets") are obtained by fault tree analysis.

3.4.5.3 FSAR Analysis

An analysis was performed during the FSAR preparation to evaluate the probability of damage from turbine missiles to LaSalle County station. The turbine placement and orientation at LaSalle are such that there are some safety-related components located within the low trajectory missile zone. However, the main control room is outside this zone. Both low and high trajectory missiles were considered in the FSAR analysis. General Electric Company (1973a) provided the P_1 values and missile data as input to this analysis (Table 3.4-15). GE has established that the probability of missile generation at or near the operating speed (i.e., low speed burst) is statistically insignificant; therefore, no missiles were postulated for this speed condition. The probability of disk failure leading to ejection of missiles at the destructive overspeed (i.e., high speed burst) was calculated by GE as 5×10^{-9} per year.

The FSAR analysis considered the redundancy of equipment and systems and the multiple barriers that must be breached by the missiles before they could affect the equipment and systems. It concluded that the portion of auxiliary building housing the turbine-driven feedwater pump and 480V Switchgear (between column rows R and N and between column lines 19 and 21 at Elevations 768'0" and 786'6") is the only area exposed to LTM strikes. Similarly, the reactor building was assessed to be the only area exposed to high trajectory missile strikes and that has equipment that does not have redundant items in other areas of the plant. The probability of missile damage to concrete barriers was calculated using modified Petry formula and by treating the impact velocity and impact area as random variables. The probability of turbine missile damage conditional on the missile generation was calculated as 6.86×10^{-4} for two reactor units.

Using the estimates of the probability of turbine missile generation given in Table 3.4-14, the probability of turbine missile damage to the plant is calculated as:

P_4 (5 percentile) $= 3.42 \times 10^{-12}$/year
P_4 (mean) $= 9.50 \times 10^{-8}$/year
P_4 (95 percentile) $= 1.12 \times 10^{-7}$/year

Based on these low probability values of unacceptable turbine missile damage, it was concluded that turbine missiles were not a significant contributor to the plant risk.

3.4.5.4 Recent Turbine Missile Issues

Subsequent to the preparation of the FSAR, there have been some significant activities in the area of turbine missile analysis. These may be grouped into two categories: stress corrosion cracking issues and refinements in the analytical techniques.

3.4.5.4.1 Stress Corrosion Cracking Issues

Following the discovery of widespread stress-corrosion cracking in disks and rotors of operating turbines, turbine manufacturers have proposed several "hardware" fixes and changes in the operating procedures. Until the proposed hardware fixes are accepted, the manufacturers suggest that the turbine disks, and turbine control and overspeed protection systems be periodically inspected. Two approaches have been proposed for deriving the frequency of volumetric inspection of the turbine disks. In the deterministic approach, several conservative assumptions are made in the initiation and growth rate of stress-corrosion cracking and in the critical crack size. The disks are inspected periodically such that any existing crack is detected before it reaches the critical crack size. In the probabilistic approach, a program for inspection of turbine disk, valve, and control systems is chosen such that the probability of unacceptable damage to the nuclear power plant systems due to turbine missiles is maintained at some acceptable level. The uncertainties in the crack initiation, crack growth rate, critical crack size, and in the success of overspeed protection systems are explicitly modeled in the evaluation of turbine failure probability. The probabilistic analysis would also consider the particular features of the turbine (i.e., missile parameters), the arrangement of safety systems within the specific plant, and the effect of barriers in the path of turbine missiles.

The NRC staff has established the maximum value of P_1, i.e., probability of turbine missile generation using an acceptable limit of 10^{-7} per year for P_4. For unfavorably oriented turbine generators (i.e., for plants having some safety-related systems within the LTM zone), the NRC staff has concluded that P_2P_3 would lie in the range of 10^{-3} to 10^{-2}. Therefore, the staff recommends that P_1 should not be larger than 10^{-5} per year (NUREG-0887, USNRC, 1983). The value of P_1 calculated using historical failure data (Patton et al., 1983) may not be appropriate in calculating the turbine missile risks; since, it is our judgment that the stress corrosion

cracking issue would be resolved in the near future and that the probability of turbine failure leading to missile generation at LaSalle would be less than 10^{-5} per year.

3.4.5.4.2 Refinements in Turbine Missile Risk Analysis

The FSAR analysis was utilized as a screening evaluation to show that the probability of unacceptable damage from turbine missiles to any of the ESF systems is acceptably small. The conservatisms and uncertainties in these analyses have to be assessed in light of the recent developments in the techniques for turbine missile analysis. The range of P_2P_3 calculated in the FSAR has many conservatisms:

- o the missile data provided by the turbine manufacturers tend to overpredict the missile sizes and velocities
- o damage was assumed when scabbing of concrete barrier occurred; scabbing could lead to equipment damage only if there are sensitive instrumentation lines, valves, and cables in the path of scabbed pieces of concrete
- o damage to any ESF equipment was deemed unacceptable; typically, a sequence of equipment failures ("cut sets") has to take place in order to have core damage.

The FSAR analysis used the modified Petry formula for calculating the value of P_3. Recent full-scale missile impact tests have shown that this formula is not a good predictor of scabbing or perforation thickness.

As described in Section 3.4.5.1, a comprehensive probabilistic analysis of turbine missile damage would consider both the probabilistic characteristics of missile generation events, missile transportation, and missile impact with barriers, and the nuclear plant system characteristics wherein a sequence of components have to fail for the undesired event. If such an analysis is done for LaSalle, it is judged that the probability of turbine missile induced core damage would be estimated as less than 1×10^{-7} per year using the value of P_1 of 10^{-5} per year.

3.4.5.5 Conclusion

Based on the bounding analysis, it is concluded that the turbine missiles are not a significant contributor to the plant risk. Therefore, no further detailed analysis of this event is considered necessary.

3.4.6 External Flooding

The LaSalle County Station is located approximately 5 miles south of the Illinois River. The man-made cooling lake adjacent to the plant has a surface area of 2058 acres at its normal pool elevation of 700′ MSL. Make-up water for the cooling lake is pumped from the Illinois River, and part of the water in the lake is blown down to the Illinois River to prevent dissolved solids in the lake from building up to excessive levels. The ultimate heat sink for LSCS is an excavated pond which is constructed within the lake and has a surface area of 83 acres at the design level of 690′ MSL.

Three modes of flooding were considered in the design of LaSalle County Station, i.e., (1) a postulated probable maximum flood (PMF) in the Illinois River, (2) a probable maximum precipitation (PMP) with antecedent standard project storm (SPS) on the cooling lake and its drainage area, and (3) a local PMP at the plant site. For the present bounding analysis, modes of flooding for the site were also judged to be either from the river or from the lake or due an intense precipitation at the site. The plant design criteria as well as meteorological data for the site were used to perform a bounding frequency analysis for external flooding. As shown below, the contribution of flooding to the overall plant risk is negligible.

3.4.6.1 Illinois River

The structures in LaSalle Station have a floor elevation of 710.5′ MSL and the plant grade is at Elevation 710′ MSL. In comparison, the Illinois River is normally at elevations under 500 MSL in the vicinity of the site. The terrain at the site is gently rolling with ground surface elevations which vary from 700′ to 724′ MSL, i.e., the site elevation is much higher than the Illinois River at all locations. For the plant design, probable maximum flood elevation at the Illinois River including coincident wave effect was calculated to be 522.5′ MSL (FSAR). This is 188′ below the plant floor elevation. Although the probable maximum flood level is not calculated on the basis of a given annual probability of exceedence, it is thought to be associated with a very low exceedence probability. In fact, the observed maximum flood water elevation in the Illinois River has been 504.7′ MSL recorded in 1831. The river screen house and the out-fall structure which are not safety-related structures are the only plant facilities which could be damaged by floods in the Illinois River. There are some low navigation dams in the Illinois River upstream from the plant. However, failure of these dams due to floods or other events would not affect the site.

Therefore, it may be concluded that floods at the Illinois River would not either directly or indirectly affect the plant safety.

3.4.6.2 Cooling Lake

The cooling lake at LaSalle site is at a lower elevation than the plant grade elevation, i.e., 700' MSL vs 710' MSL. There are three baffle dikes within the lake which channel the flow of water and increase the flow path for efficient heat dissipation. In case of an overflow due to an intense precipitation, runoff from the lake would flow away from the plant towards existing creeks and gullies. Also, in case of breaching of the peripheral dikes of the cooling lake, the impounded water would discharge directly into local creeks that meet the Illinois River. Thus, it is concluded that the plant safety-related structures would not be affected by the probable maximum water level in the lake with coincident wind waves.

3.4.6.3 Local Precipitation

In the LaSalle FSAR, it was concluded that the critical mode of flooding at the site is due to an intense local precipitation. The assumptions which were used in the design were as follows: a standard project storm followed by three rainless days and next followed by the probable maximum precipitation for a period of 48 hours. A hydrological analysis of the site was carried out which included the site topographic data, the cooling lake, and data for both the main spillway and the auxiliary spillway. It was shown that the water surface elevation near the plant buildings could reach an elevation of 710.34' MSL which is slightly lower than the floor elevation of 710.5' MSL. However, it is shown in the following paragraphs that the analysis was conservative and the calculated flood level corresponds to a very low annual probability of exceedence.

An examination of the hydrologic analysis of LaSalle site showed that conservatism in the analysis is mostly due to the definition of probable maximum precipitation. In the plant design, the 24 hour local probable maximum precipitation for the site was calculated to be 32.1". Data from the meteorological tower at the site and other weather stations near the site which were considered in the FSAR indicated maximum 24-hour and 48-hour precipitations of 4.45" and 8.62", respectively for record periods of up to 15 years. In the present study, meteorological data for weather stations near the site were obtained from the National Oceanic and Atmospheric Agency in Ashville, North Carolina. The most

complete set of precipitation records near the site is for the city of Chicago which covers a 100 year period starting in 1871. These data show a maximum 24 hour precipitation of 6.19" which occurred in 1885. An examination of other weather station data in northern and central Illinois revealed a maximum recorded 24 hour precipitation of 7.56" which occurred in Cairo, Illinois in 1952. Therefore, the probable maximum precipitation which was calculated for LaSalle is expected to have a low negligible probability of exceedence.

Table 3.4-16 shows the 100 year maximum 24 hour precipitation data for Chicago. Figure 3.4-19 shows the histogram of maximum 24 hour rainfall for the 100 year period 1871 to 1970. Also, shown in Figure 3.4-19 is a normal distribution fit to the rainfall data. In addition to the normal distribution, four other probability distributions were also fit to the data, i.e., lognormal distribution, gamma distribution, extreme value type I distribution, and Log-Pearson type III distribution. Figures 3.4-20 through 3.4-24 show plots of probability of exceedence of daily rainfall for frequencies of 10^{-10} to 10^{-4} based on these distributions. Also, depicted in these figures are 90 percent confidence bounds on the probability of exceedence. From Figures 3.4-20 through 3.4-24, it may be concluded that the 24 hour PMP has a very low probability of occurrence, i.e., the 95 percent confidence value of 24 hour PMP has a probability of occurrence of less than 10^{-8} per year. Other conservative assumptions which were made in the site hydrological analysis are as follows:

1. It was conservatively assumed that all drains are clogged during the PMP.

2. No leakage or permeation of water into ground was assumed to occur during the storm.

3. The maximum precipitation is expected to occur for a very short period of time. However, the analysis assumed a 48 hour PMP for the site.

4. An inspection of the plant during the site visit by SMA personnel revealed that the doors are leak-tight, i.e., even if water elevation rises above the plant grade, the buildings will not be flooded. In addition, the structures have adequate drainage at ground elevation and they have been designed for possible flooding.

In view of these conservatisms and the conservatism in definition of PMP, it was concluded that external flooding does not contribute significantly to the risk of core damage in LaSalle.

Table 3.4-1

Commercial Airports Within 20 Miles of the Site

Airport	Runways: Orientation/ Length (/ft)	Type	Type of Aircraft	Number of Operations Per Year By Type	Distance & Direction From Site
Dwight	90-27/2340 18-36/2000	asphalt turf	a) single-engine b) twin-engine	a) 9,850 b) 1,100	16 miles SE
Morris Municipal	18-36/3000 9-27/2500	asphalt turf	a) single-engine b) twin-engine	a) 6,570 b) 730	17 miles ENE
Ottawa	5-23/2300 18-36/2600 9-27/1900	paved turf turf	a) single-engine b) twin-engine	a) 2,500 b) 2,500	16 miles NW
Starved Rock	10-28/3200	turf			17 miles WNW
Streator (B&S Aviation)	9-27/2500 18-36/1700	asphalt turf	a) single-engine b) twin-engine	a) 9,000 b) 1,000	12 miles SW

Reproduced from the LaSalle FSAR.

Table 3.4-2

Private Airstrips Within 20 Miles of the Site

Airstrip	Distance & Direction From Site
Cody Port	11 miles NW
Cwain	18 miles N
Fillman	14 miles ESE
Gillespie	5 miles N
Holverson	6 miles N
Kenzie	16 miles NW
Lentman	17 miles SW
Matteson	15 miles ESE
Mitchell	5 miles N
Prairie Lake	7 miles N
Reicheing	18 miles NNW
Skinner	12 miles WSW
Testoni	16 miles S

Reproduced from the LaSalle FSAR.

Table 3.4-3

Aircraft Traffic Statistics Near the LaSalle Site for June 7, 1984

		9,000 Feet and Below	10,000 Feet and Above
1.	Peoria, IL direct Joliet, IL, V116	3	1
*2.	Pontiac, IL direct Joliet, IL, V69	22	36
3.	Airway J64 or direct routes which overly the airway (24,000 and above)	0	61
4.	Airway V156 or direct routes which overly the airway (23,000 and above)	5	14
5.	Airway V38 or direct routes which overly the airway	11	4
6.	Pontiac, IL direct Joliet, IL Joliet 360 Radial	0	13
*7. **	Pontiac, IL V9 Plano, IL	24	92
8.	Random routes over your facility	0	4
	Totals	65	225

* Preferential Arrival Routes.

** 20,000 feet descending to 10,000 feet.

Summarized from June 15, 1984 Ltr. to S. Halloran.

Table 3.4-4

Annual In-Flight Crash Rates (1 Mile)

Aircraft Type	5th Percentile	50th Percentile	95th Percentile
Single-Engine	1.91×10^{-7}	2.27×10^{-7}	2.70×10^{-7}
Twin-Engine	5.54×10^{-8}	7.14×10^{-8}	9.20×10^{-8}
Commercial	6.95×10^{-10}	1.39×10^{-9}	2.76×10^{-9}

Table 3.4-5

Annual Frequencies of Aircraft Impact For LaSalle Structures

Building	Aircraft Type	Impact Area (mi^2)	Airway	Impact Frequency (/yr)
Reactor Building	Twin-Engine	0.0115	V9,V156	2.1×10^{-7}
			V69,V116	1.7×10^{-7}
				3.8×10^{-7}
	Commercial	0.0115	V9,V156	1.2×10^{-8}
			Random	7.5×10^{-10}
				1.3×10^{-8}
Aux Building	Twin-Engine	0.0026	V9,V156	4.8×10^{-8}
			V69,V116	4.0×10^{-8}
				8.8×10^{-8}
	Commercial	0.0026	V9,V156	2.6×10^{-9}
			Random	1.7×10^{-10}
				2.7×10^{-9}
			Total	5.0×10^{-7}

Table 3.4-6

Intensity, Length, Width and Area Scales

Scale No.	Fujita - F Intensity Scale (mph)	Pearson - P Length Scale (mi)	Pearson - P Width Scale (mi)	Area Scale (mi2)
0	72	1.00	0.010	0.001
1	73-112	1.00-3.15	0.010-0.31	0.001-0.009
2	113-157	3.16-9.99	0.032-0.099	0.010-0.099
3	158-206	10.0-31.5	0.100-0.315	0.100-0.999
4	207-260	31.6-99.9	0.316-0.999	1.000-9.999
5	261-318	100-315	1.00-3.15	10.00-99.99
6	319-380	316-999	3.16-9.99	100.0-999.9

Table 3.4-7

Regional Tornado Occurrence - Intensity Relationships Corrected for Direct Classification Errors and Random Encounter Errors (Each Row in the Table is the Vector 0I)

Region	F Scale	Corrected Probability of Occurrence at Each F-Scale Intensity						
		F0	F1	F2	F3	F4	F5	F6
Fig. 3.4.3-1	I	.2227	.3785	.2576	.1016	.0324	.0066	.0009
	II	.3610	.3116	.2198	.0912	.0147	.0015	.0002
	III	.3044	.4421	.1730	.0681	.0112	.0012	.0001
Fig. 3.4.3-2	A	.1658	.3379	.3122	.1322	.0413	.0093	.0013
	B	.2263	.3527	.2785	.1040	.0312	.0063	.0008
	C	.2830	.3611	.2426	.0856	.0225	.0047	.0006
	D	.3034	.3799	.2436	.0622	.0096	.0011	.0001

Region		Regional Occurrence Rates Corrected for Unreported Tornadoes (occurrences per square mile per year)
Fig. 3.4.3-1	I	4.12×10^{-4}
	II	2.67×10^{-5}
	III	1.35×10^{-5}
Fig. 3.4.3-2	A	5.18×10^{-4}
	B	6.98×10^{-4}
	C	3.37×10^{-4}
	D	3.53×10^{-5}

Reproduced from Reinhold and Ellingwood 1983.

Table 3.4-8

Intensity-Area Relationship Including Corrections
for Direct Observation and Random Encounter Errors (AIM Matrix)

	Percentage of Tornadoes With Indicated Area Classification					
Actual Maximum Tornado State	A0	A1	A2	A3	A4	A5
F0"	.155	.421	.269	.125	.029	.0016
F1"	.057	.255	.355	.259	.071	.003
F2"	.022	.139	.303	.368	.155	.013
F3"	.009	.070	.210	.376	.289	.046
F4"	.003	.033	.123	.299	.435	.107
F5"	.001	.017	.068	.216	.461	.237
F6"	.001	.012	.049	.185	.458	.295

Reproduced from Reinhold and Ellingwood 1983.

Table 3.4-9

Variation of Tornado Intensity Along Path Length and Across Path Width (VWL Matrix)

	True Maximum Tornado State						
Local Tornado State	F0"	F1"	F2"	F3"	F4"	F5"	F6"
F0*	1.000	.743	.658	.615	.637	.632	.625
F1*	0	.257	.248	.267	.234	.236	.238
F2*	0	0	.094	.091	.093	.088	.089
F3*	0	0	0	.027	.028	.033	.033
F4*	0	0	0	0	.008	.009	.011
F5*	0	0	0	0	0	.002	.003
F6*	0	0	0	0	0	0	.001

Reproduced from Reinhold and Ellingwood 1983.

Table 3.4-10

Intensity-Length Relationship Including Corrections for Direct Observation and Random Encounter Errors (LIM Matrix)

Actual Maximum Tornado State	Percentage of Tornadoes With Indicated Length Classification					
	PLO	PL1	PL2	PL3	PL4	PL5
F0"	.801	.115	.069	.014	.001	0
F1"	.590	.219	.140	.046	.005	0
F2"	.436	.249	.212	.093	.010	0
F3"	.272	.226	.268	.195	.038	.001
F4"	.141	.152	.272	.326	.090	.019
F5"	.079	.113	.197	.444	.131	.036
F6"	.058	.101	.155	.496	.147	.043

Reproduced from Reinhold and Ellingwood 1983.

Table 3.4-11

Variation of Intensity Along Length
Based on Percentage of Length Per Tornado (VL Matrix)

	Recorded Tornado State						
Local Tornado State	F0	F1	F2	F3	F4	F5	F6
F0	1.000	.383	.180	.077	.130	.118	.100
F1	0	.617	.279	.245	.131	.125	.110
F2	0	0	.541	.310	.248	.162	.120
F3	0	0	0	.368	.234	.236	.160
F4	0	0	0	0	.257	.187	.200
F5	0	0	0	0	0	.172	.150
F6	0	0	0	0	0	0	.160

Reproduced from Reinhold and Ellingwood 1983.

Table 3.4-12

NRC SRP Tornado Missiles (Standard Review Plan)

Missile	Weight (Lbs)	Dimensions	V (Ft/Sec) Region I
A. Wood Plank	120	3.6" x 11.4" x 144"	270
B. 6" Sch. 40 Pipe	300	6.6" D x 180"	170
C. 1" Steel Rod	9	1" D x 36"	167
D. Utility Pole	1100	13.5" D x 420"	180
E. 12" Sch. 40 Pipe	750	12.6" D x 180"	154
F. Automobile	4000	16.4′ x 6.6′ x 4.3′	194

Table 3.4-13

Minimum Reinforced Concrete Thicknesses (Inches)
Required to Prevent Scabbing (NDRC and Chang's Formulas)

Missile	t_s (NDRC) In	t_s (Chang) In
Horizontal		
B. 6" Sch. 40 Pipe	8.2	18.8
C. 1" Steel Rod	4.5	6.6
E. 12" Sch. 40 Pipe	10.3	22.3
Vertical		
B. 6" Sch. 40 Pipe	7.3	14.8
C. 1" Steel Rod	4.5	6.6
E. 12" Sch. 40 Pipe	8.3	17.5

Table 3.4-14

Estimates of Annual Probability of
Turbine Missile Generation

Source	Failure Mode		Total
	Operating Speed P	Overspeed P′	
General Electric	0	5.00×10^{-9}	5.00×10^{-9}
Patton et al.	1.20×10^{-4}	0.44×10^{-4}	1.64×10^{-4}
This Report	$1.17\text{-}\times 10^{-4}$	2.10×10^{-5}	1.38×10^{-4}

Table 3.4-15

38-Inch Last Stage Bucket, 1800 RPM Low-Pressure Turbine -
Hypothetical Missile Data (1) (2)

STAGE GROUP	I				II				III			
Stage Members in Group; Number of Representative Stage	1 - 4;2				4 - 6;5				(Last);7			
MISSILE DIMENSIONS												
Fragment Group	a	b	c	d	a	b	c	d	a	b	c	d
Number of Fragments in Group	2	1	3	10	2	1	3	10	2	1	3	10
Sector Angle, degrees	120	60			120	60			120	60		
Fragment Weight, lbs	2000	1000	300	100	3000	1500	500	150	6500	3200	1000	200
Radius, in., R_1 Bore	18	18			17	17			16	16		
R_2 Hub	24	24			25	25			25	25		
R_3 Vane Root	45	45			45	45			45	45		
Thickness, in., T_1 Hub	10	10			12	12			21	21		
T_2 Web	3	3			5	5			10	10		
Approximate Rectangular Dimensions, in.			19x19x3	11x11x3			19x19x5	19x10x5			19x19x10	8x8x10
LOW SPEED BURST												
Postulated Speed: 2160 RPM (120)												
Lifetime Probability: Not Statistically Significant												

Table 3.4-15 (cont'd)

38-Inch Last Stage Bucket, 1800 RPM Low-Pressure Turbine -
Hypothetical Missile Data (1) (2)

HIGH SPEED BURST(3)

Postulated Speed: 3240 RPM (180%)
Lifetime Probability: 1.5 E-7(4)

	STAGE GROUP I	STAGE GROUP II	STAGE GROUP III
Conditional Probability of Occurrence in Stage Group	3/7	3/7	1/7
Probability of Occurrence in Stage Group	6.4 E-8	6.4 E-8	2.1 E-8

Fragment	a		b		a		b		a		b	
	Energy	Velocity	Energy	Velocity	Energy	Velocity	Energy	Velocity	Energy	Velocity	Energy	Velocity
Minimum	0	0	0	0	0	0	0	0	16	400	0	0
Maximum	7	470	6	620	14	550	13	750	38	610	30	780
Midpoint	3.5	340	3	440	7	390	6.5	530	27	520	15	550

Fragment Group	c		d		c		d		c		d	
	Energy	Velocity	Energy	Velocity	Energy	Velocity	Energy	Velocity	Energy	Velocity	Energy	Velocity
Minimum	0	0	0	0	0	0	0	0	0	0	0	0
Maximum	4	930	2	1130	6	880	2	930	13	910	3	980
Midpoint	2	660	1	800	3	620	1	660	6.5	650	1.5	690

Notes: (1) Energy of ejected missiles is given in million foot-pounds; velocity in feet/second.
(2) Energies are postulated to be uniformly distributed over stated ranges.
(3) Sixteen missiles in four size classes are postulated to occur per boost.
(4) 1.5 E-7 means 1.5×10^{-7}.

Reproduced from the LaSalle FSAR.

Table 3.4-16
Maximum 24 Hour Precipitation for Chicago

Year	Inches	Year	Inches	Year	Inches
1871	2.57	1906	2.91	1941	1.71
1872	2.70	1907	1.80	1942	1.98
1873	2.82	1908	4.34	1943	3.93
1874	2.19	1909	3.52	1944	1.64
1875	3.44	1910	1.81	1945	1.96
1876	1.94	1911	1.51	1946	2.46
1877	2.65	1912	1.87	1947	4.08
1878	4.14	1913	1.83	1948	2.50
1879	3.25	1914	1.65	1949	2.73
1880	1.91	1915	2.48	1950	3.52
1881	3.35	1916	2.61	1951	2.93
1882	1.92	1917	1.51	1952	1.60
1883	3.39	1918	1.92	1953	2.42
1884	3.26	1919	2.28	1954	2.20
1885	6.19	1920	2.28	1955	3.11
1886	2.11	1921	2.60	1956	1.57
1887	1.39	1922	2.64	1957	6.24
1888	2.43	1923	3.70	1958	2.25
1889	4.02	1924	3.75	1959	4.58
1890	2.60	1925	1.85	1960	2.86
1891	1.92	1926	3.02	1961	2.63
1892	3.11	1927	2.92	1962	1.82
1893	1.46	1928	2.71	1963	2.67
1894	3.35	1929	3.12	1964	2.09
1895	3.65	1930	1.48	1965	2.78
1896	2.42	1931	3.84	1966	5.39
1897	2.01	1932	2.03	1967	2.95
1898	2.50	1933	2.81	1968	3.83
1899	2.17	1934	1.86	1969	3.29
1900	1.48	1935	3.00	1970	2.97
1901	1.96	1936	2.69		
1902	2.02	1937	1.85		
1903	1.54	1938	1.63		
1904	1.83	1939	2.09		
1905	2.78	1940	1.91		

*1957, 6.24 was 100 year maximum

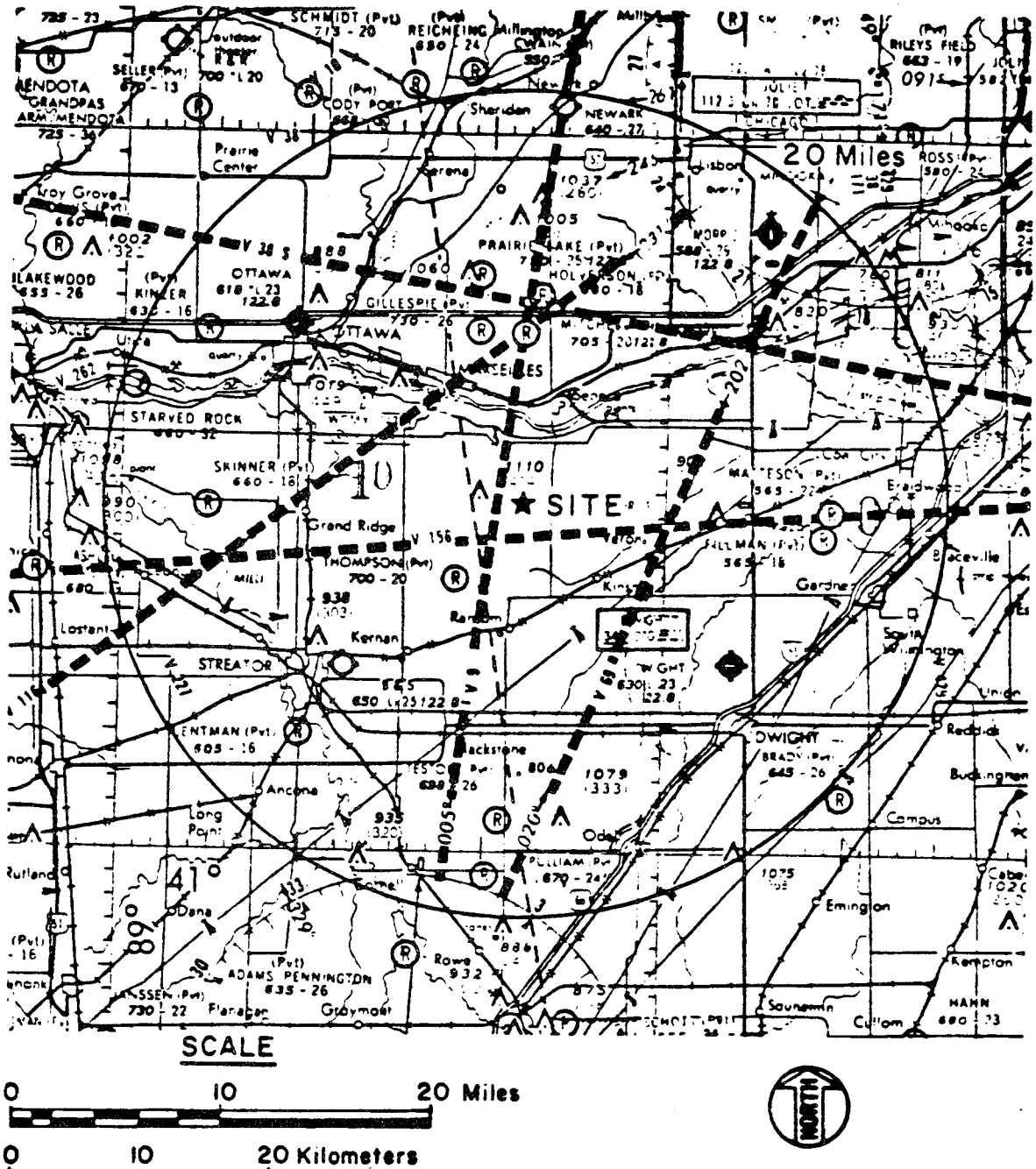

LEGEND

Airports

○ No paved runway

Ⓡ No paved runway (Restricted use)

◆ Hard surface runway

Figure 3.4-1. Airports and Flight Patterns Within 20 Miles of the Site

Reproduced from the LaSalle FSAR.

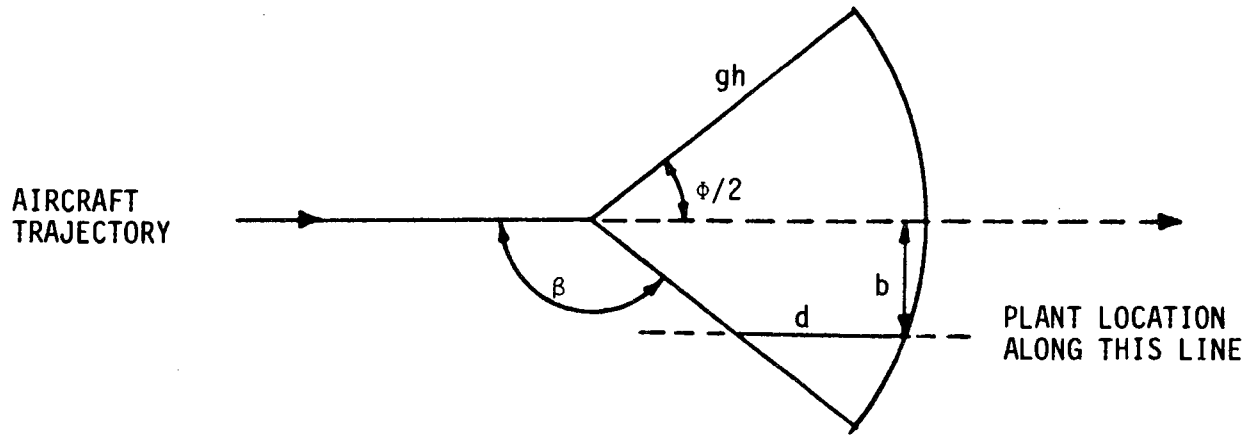

Figure 3.4-2. Geometry for Aircraft Impact Probabilistic Model

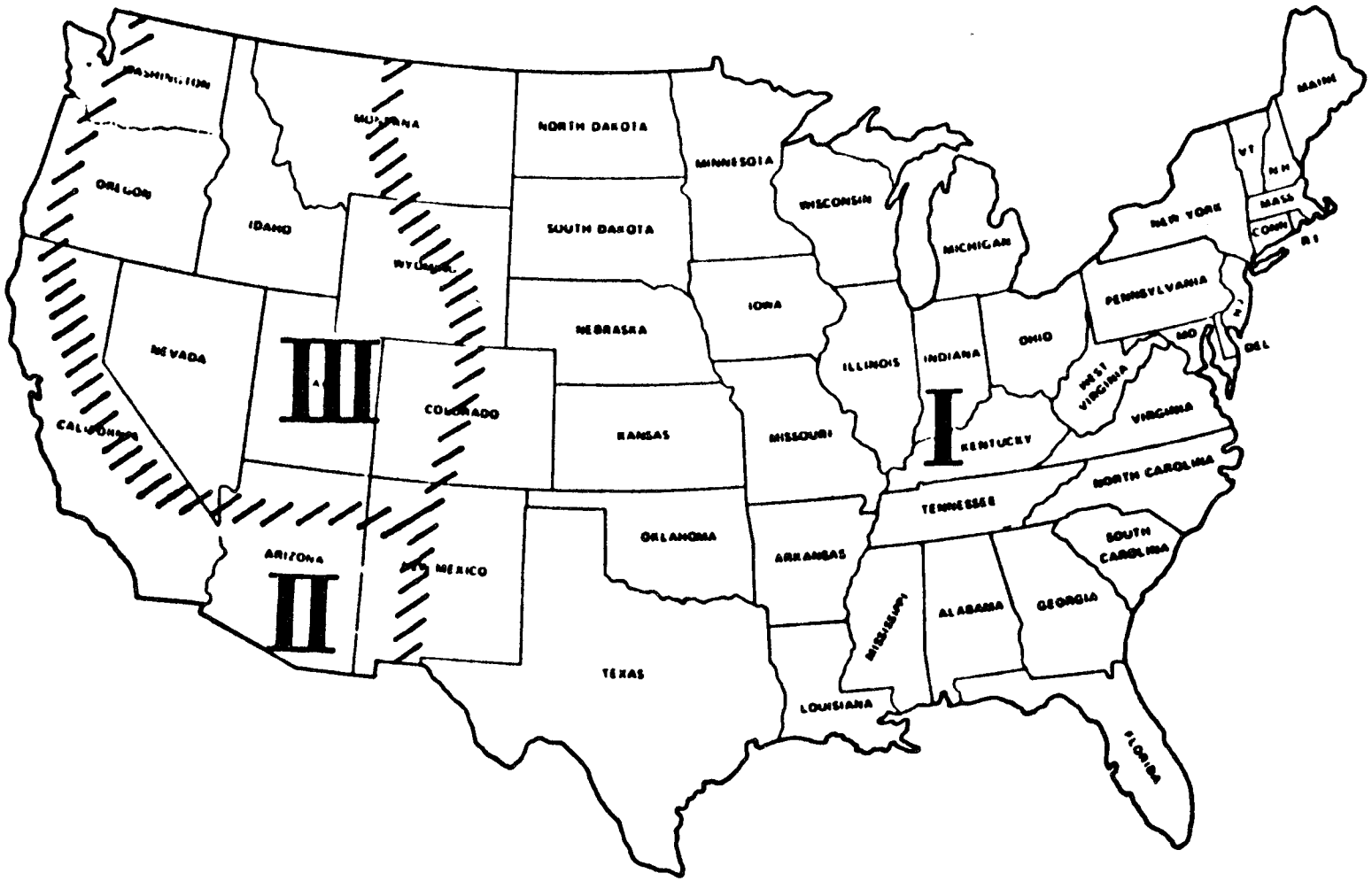

Figure 3.4-3. Tornado Risk Regionalization Scheme Proposed by Wash-1300, Markee et al. (1975)

Reproduced from Reinhold and Ellingwood 1983.

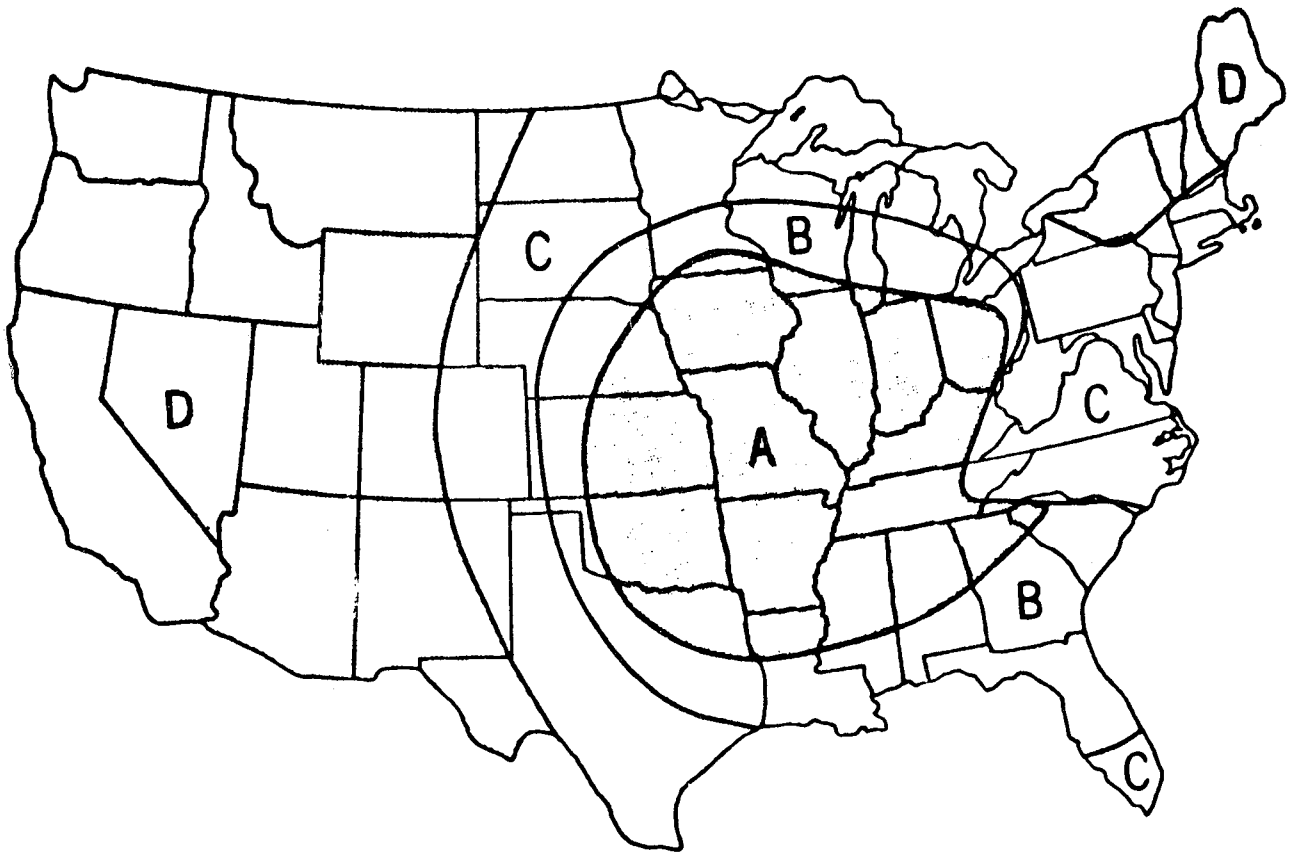

Figure 3.4-4. Tornado Risk Regionalization Scheme Proposed by Twisdale and Dunn (1983).

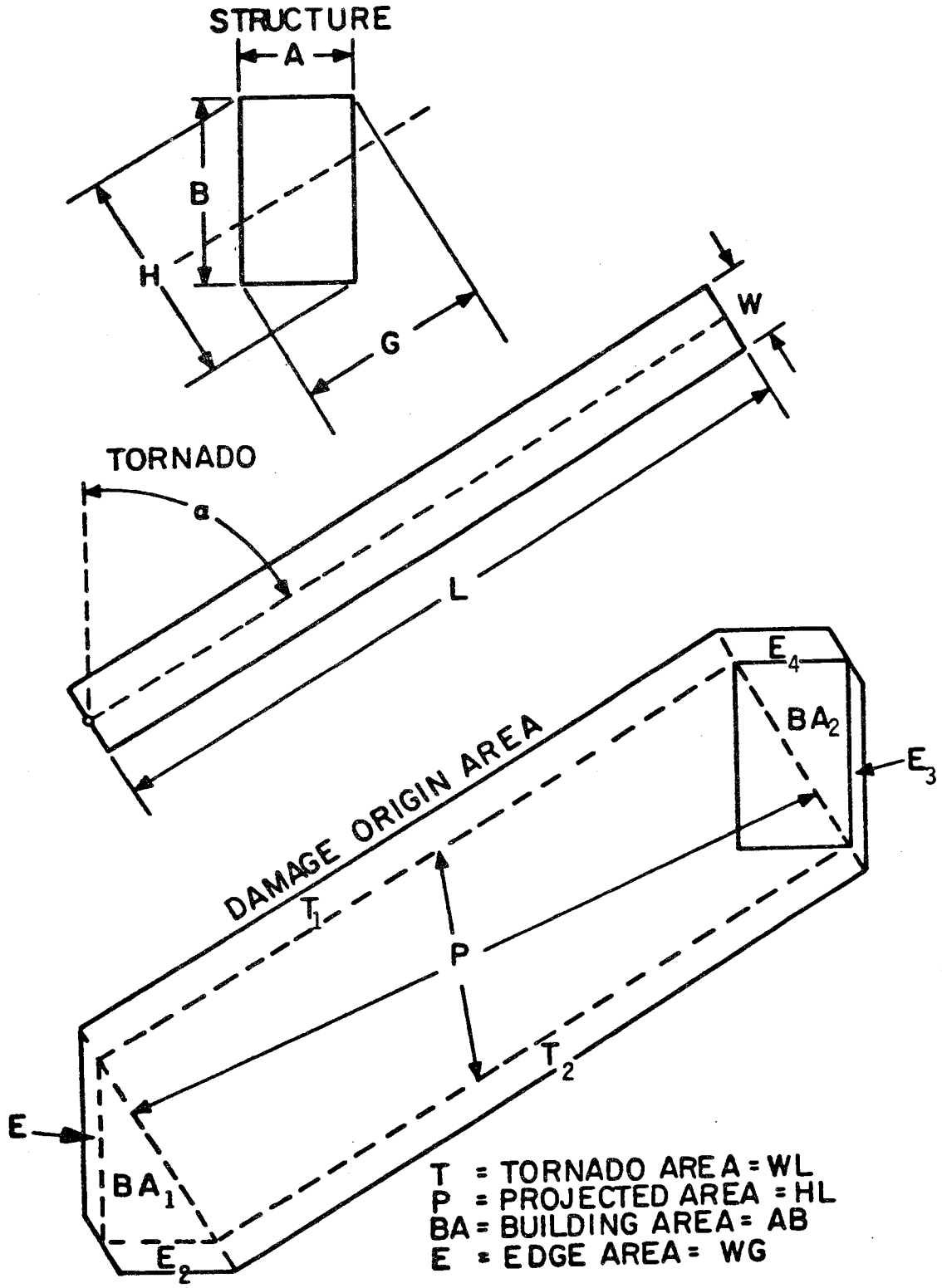

Figure 3.4-5. Tornado Parameters and Damage Origin Area Definition

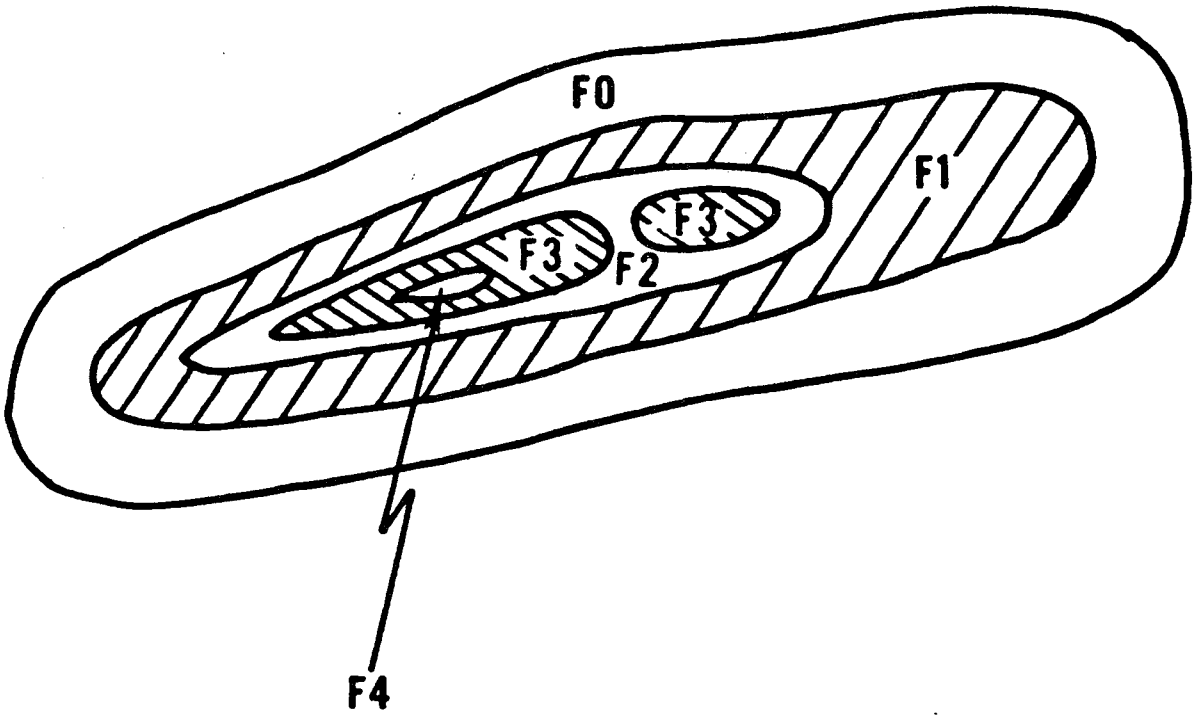

Figure 3.4-6. Sketch of Hypothetical F4 Tornado Illustrating Variation of Intensity

Reproduced from Reinhold and Ellingwood 1983.

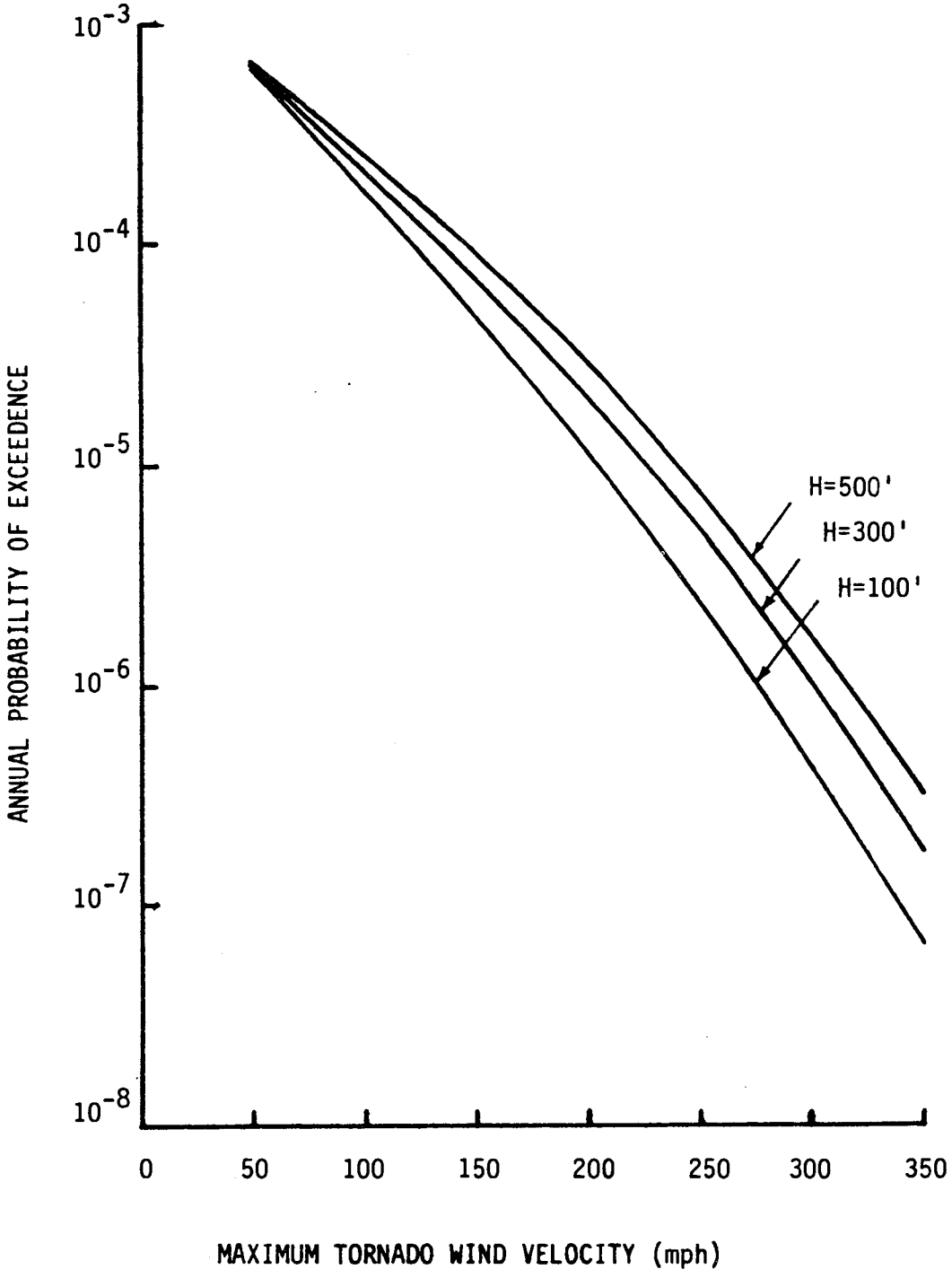

Figure 3.4-7. Tornado Hazard Curves for LaSalle Site

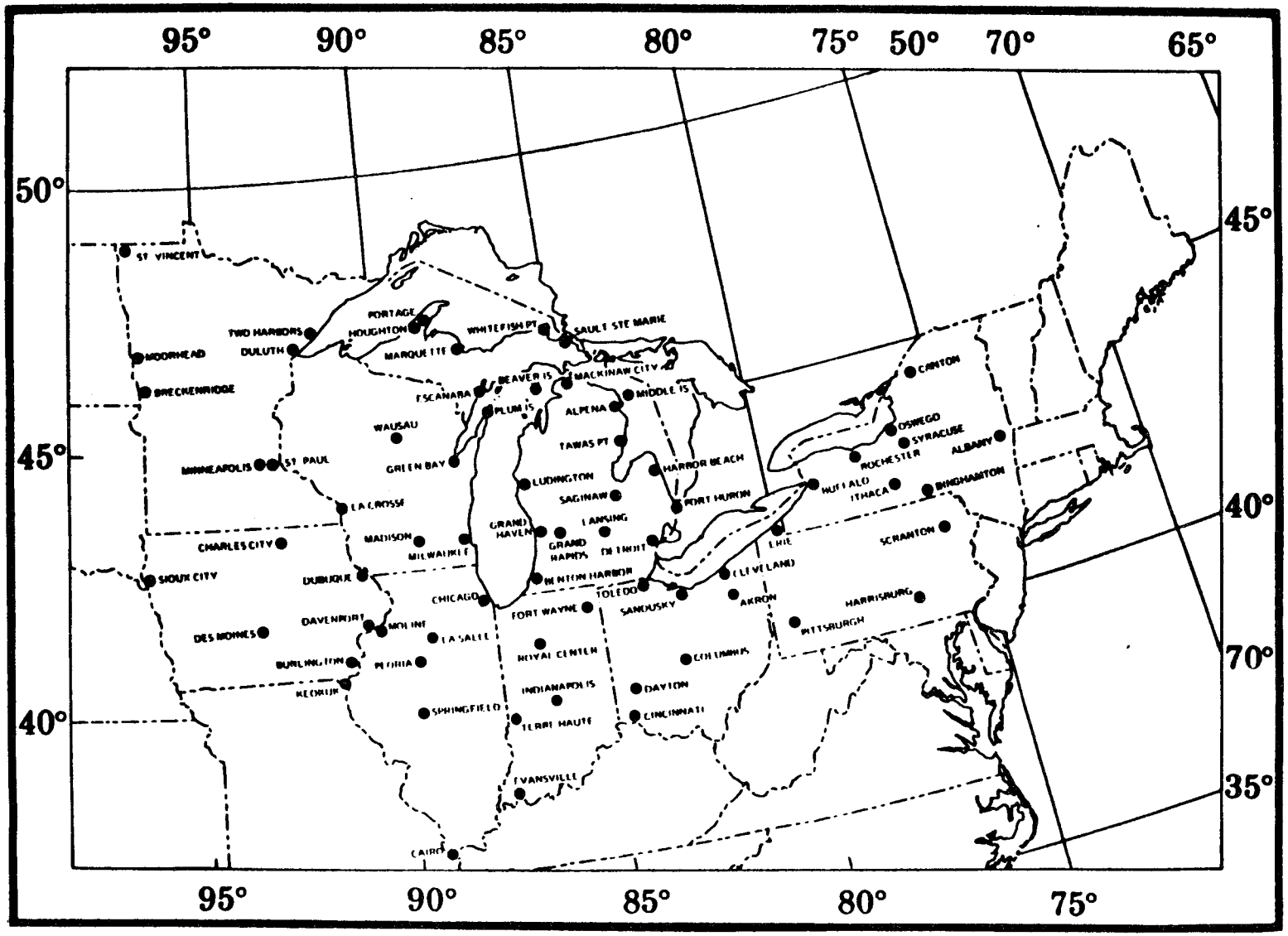

Figure 3.4-8. Station Locations

Reproduced from Changery 1982.

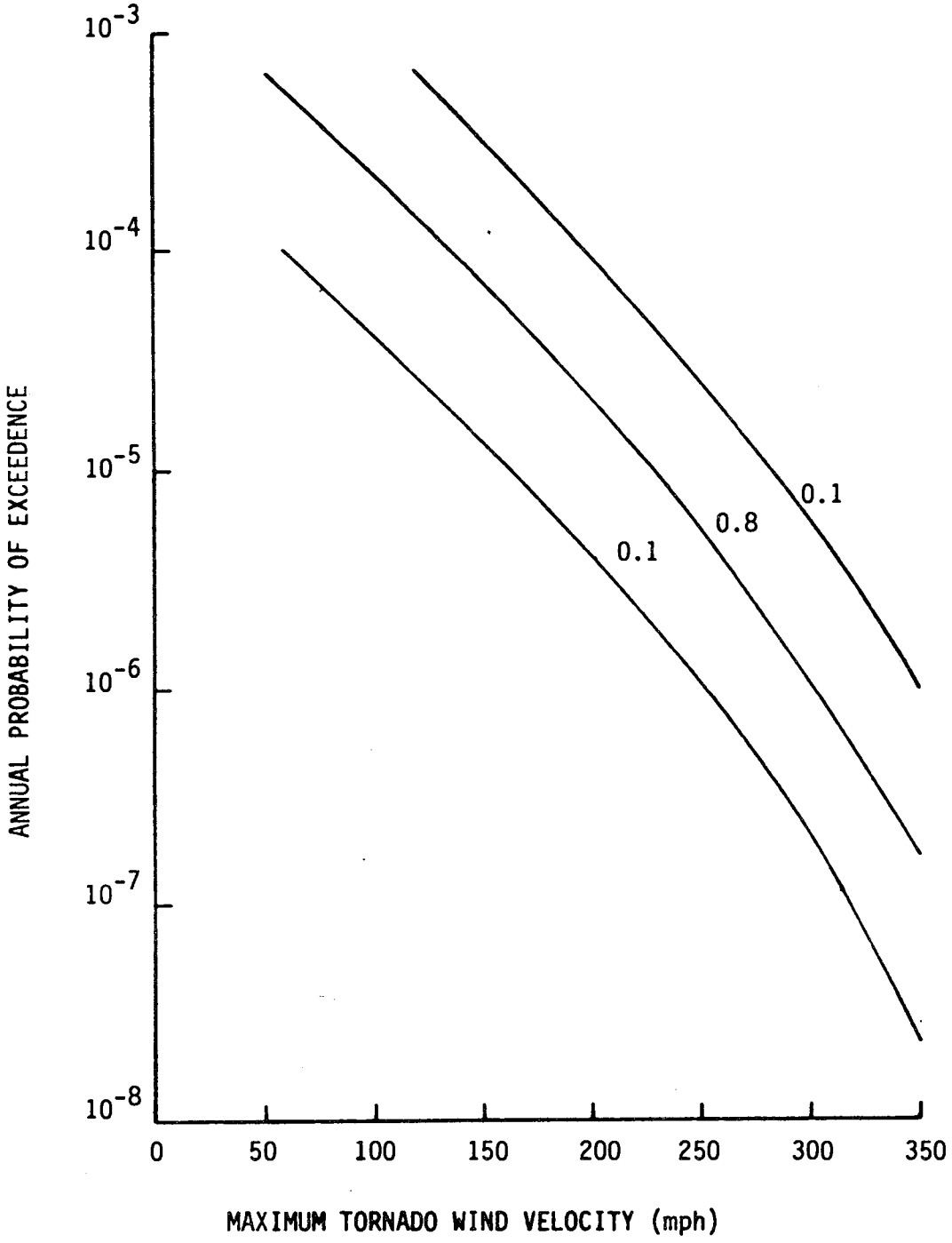

Figure 3.4-9. Family of Tornado Hazard Curves for the LaSalle Site With Corresponding Subjective Probabilities

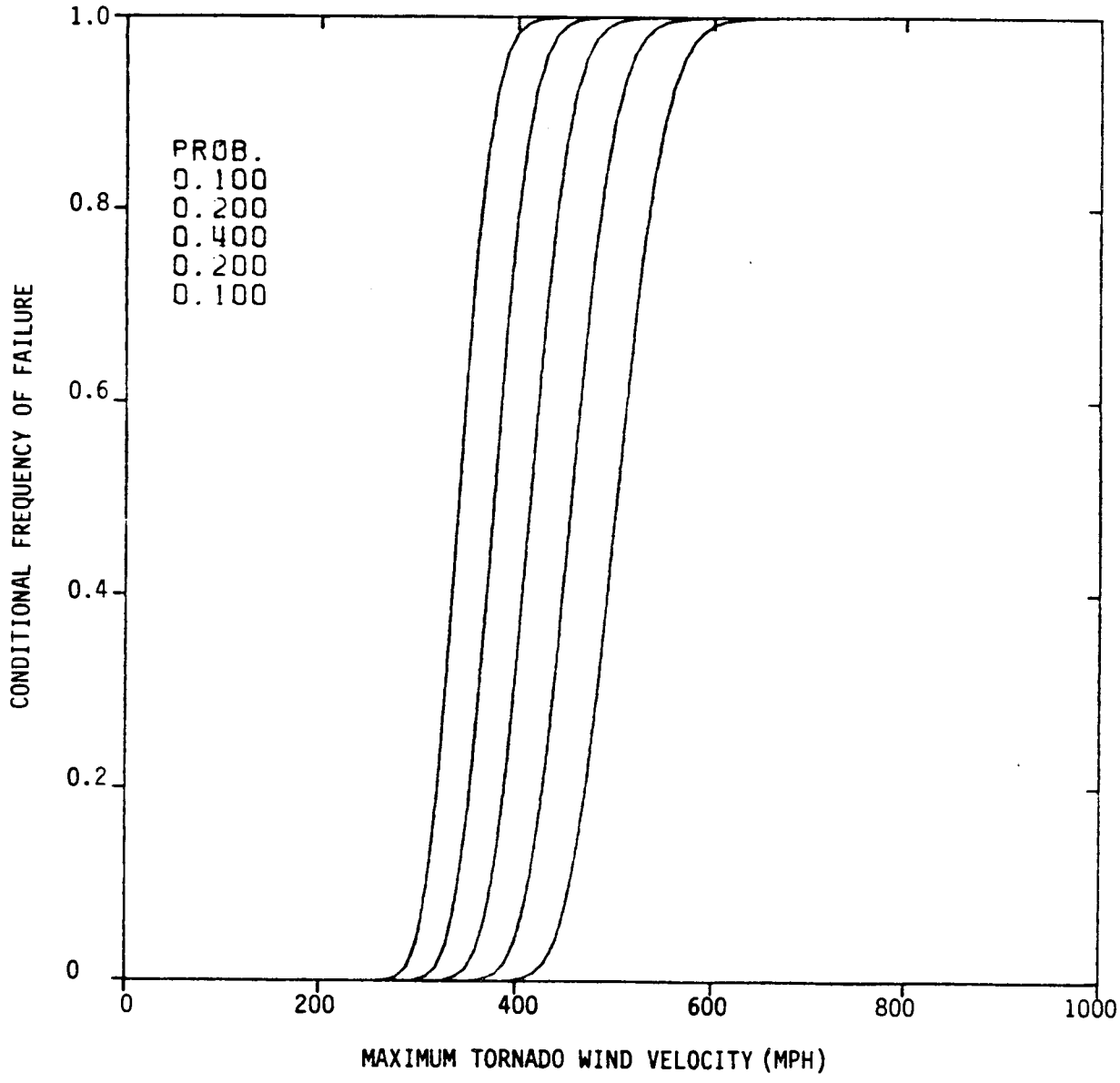

Figure 3.4-10. Tornado Fragility Curves for LaSalle Including Uncertainty in Median Capacity

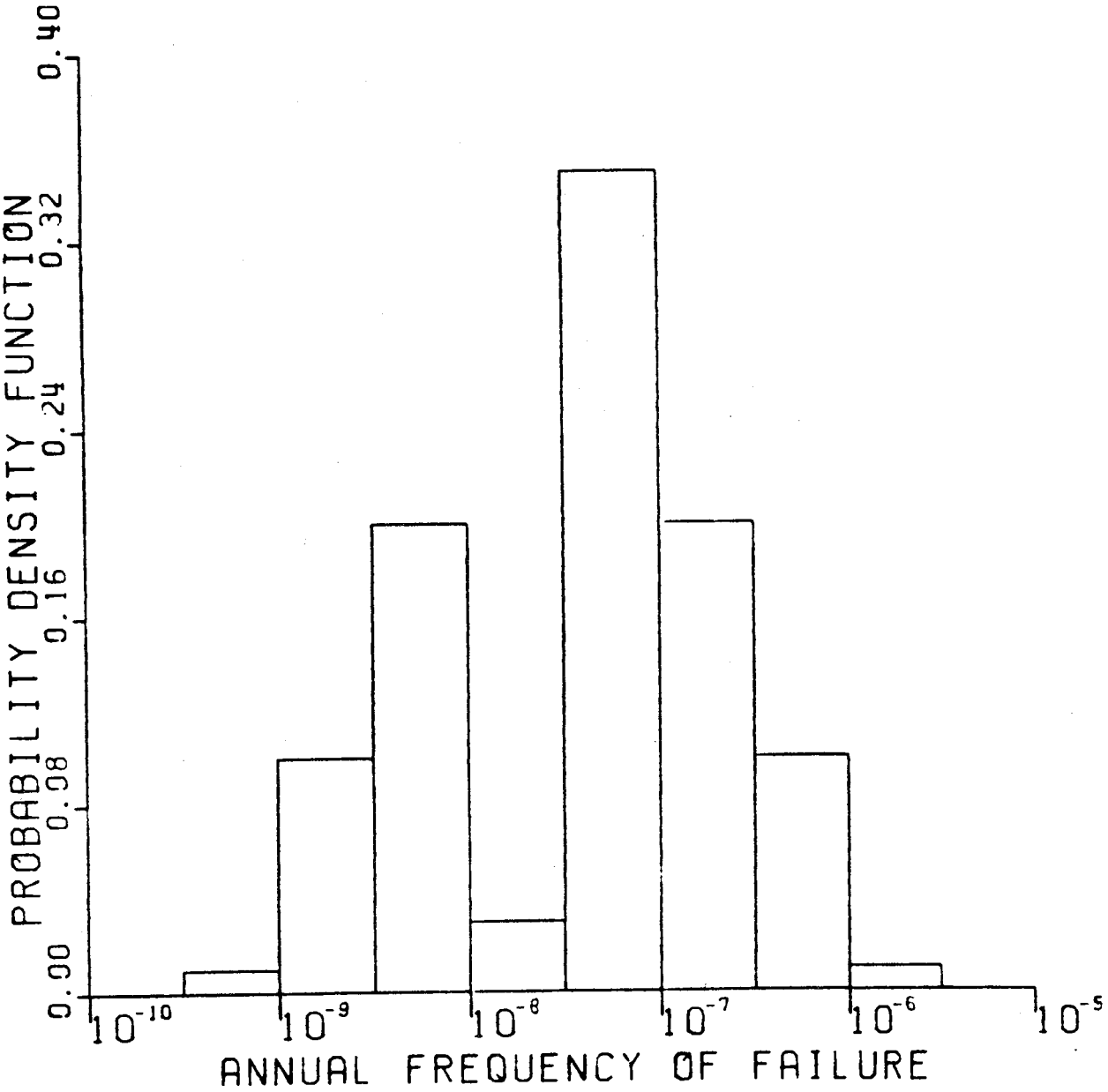

Figure 3.4-11. Distribution of Annual Frequency of Core Melt in LaSalle Due to Tornadoes

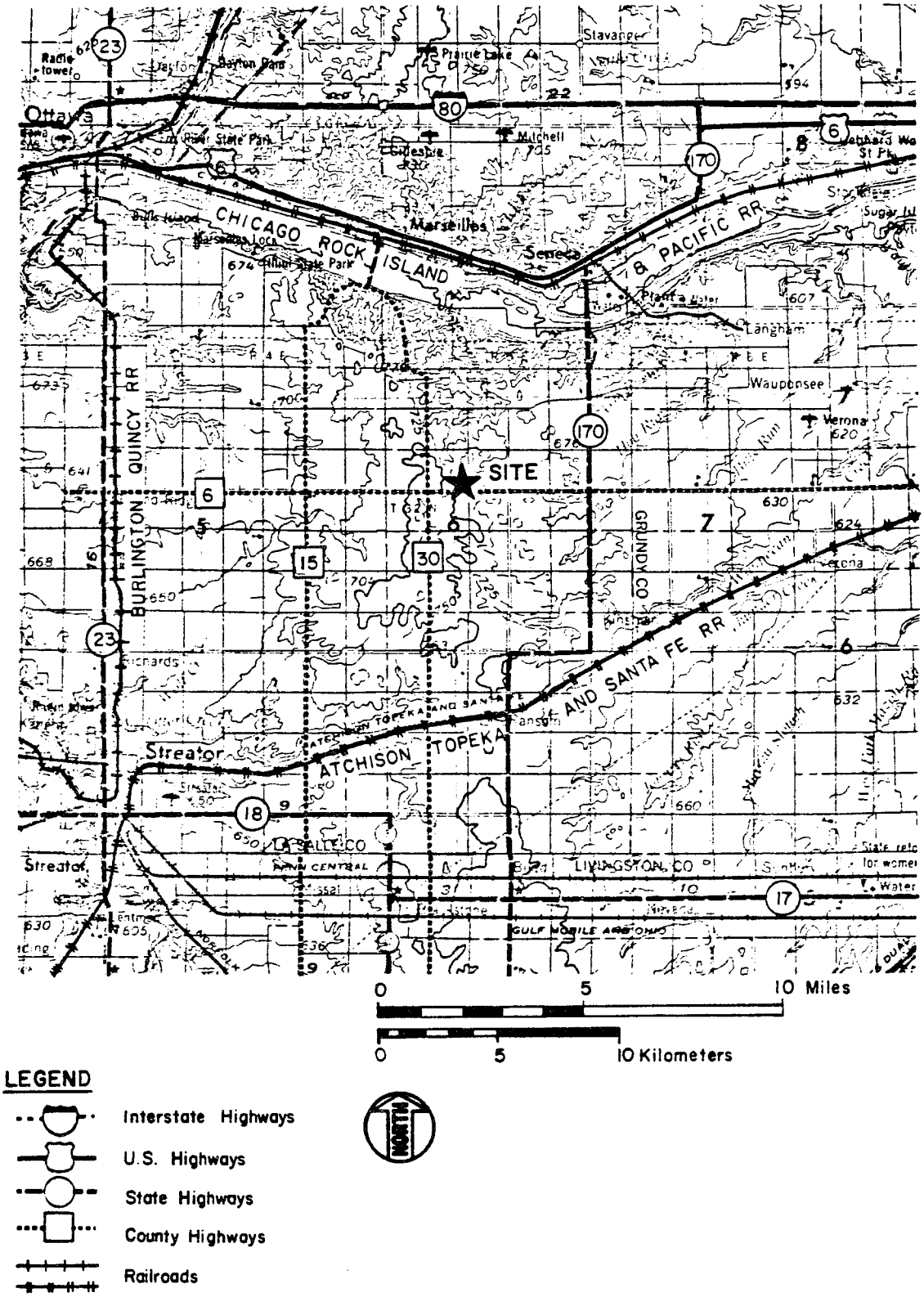

Figure 3.4-12. Transportation Routes Near LaSalle County Station

Reproduced from the LaSalle FSAR.

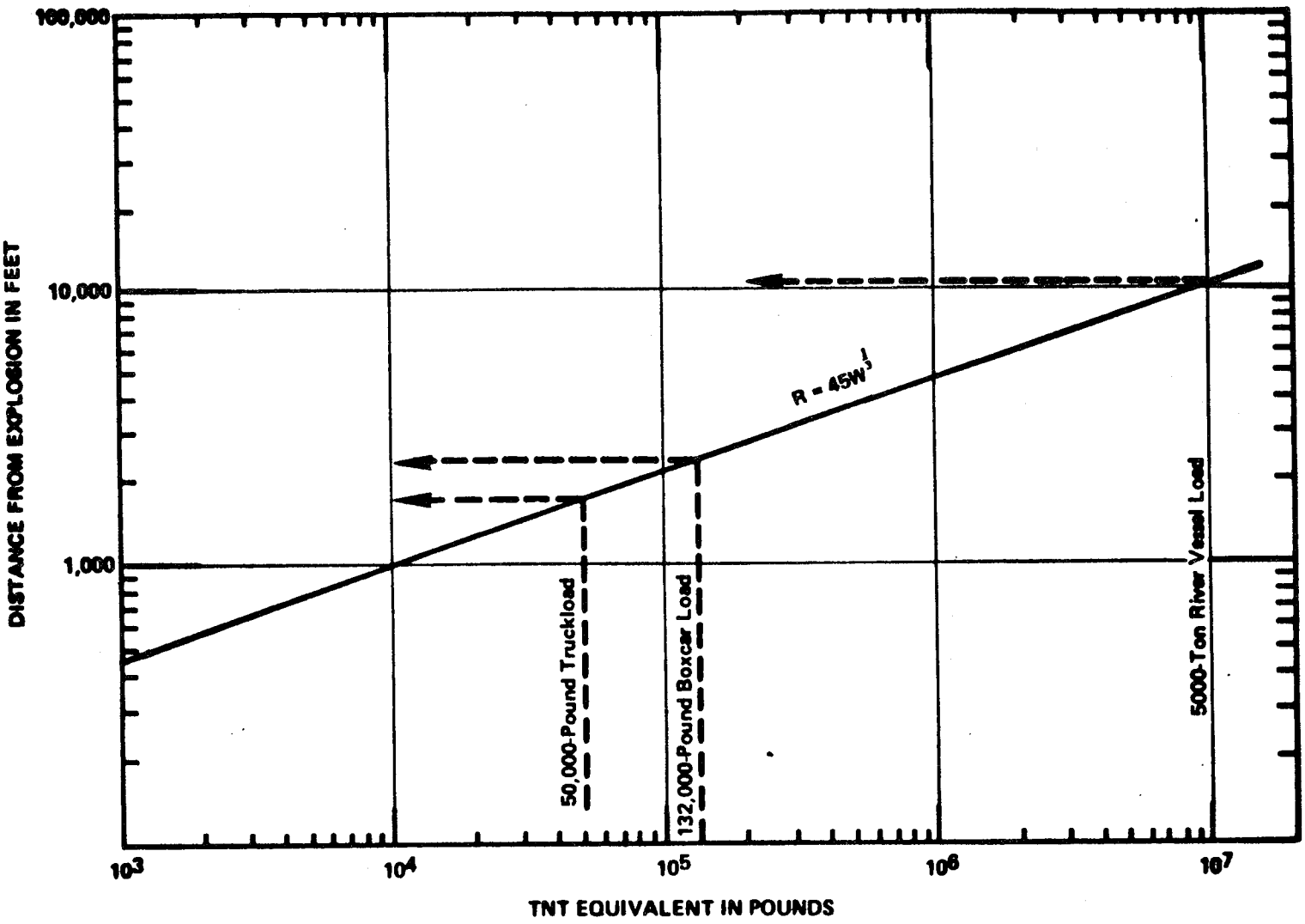

Figure 3.4-13. Radius to Peak Incident Pressure of 1 psi

Reproduced from Regulatory Guide 1.91.

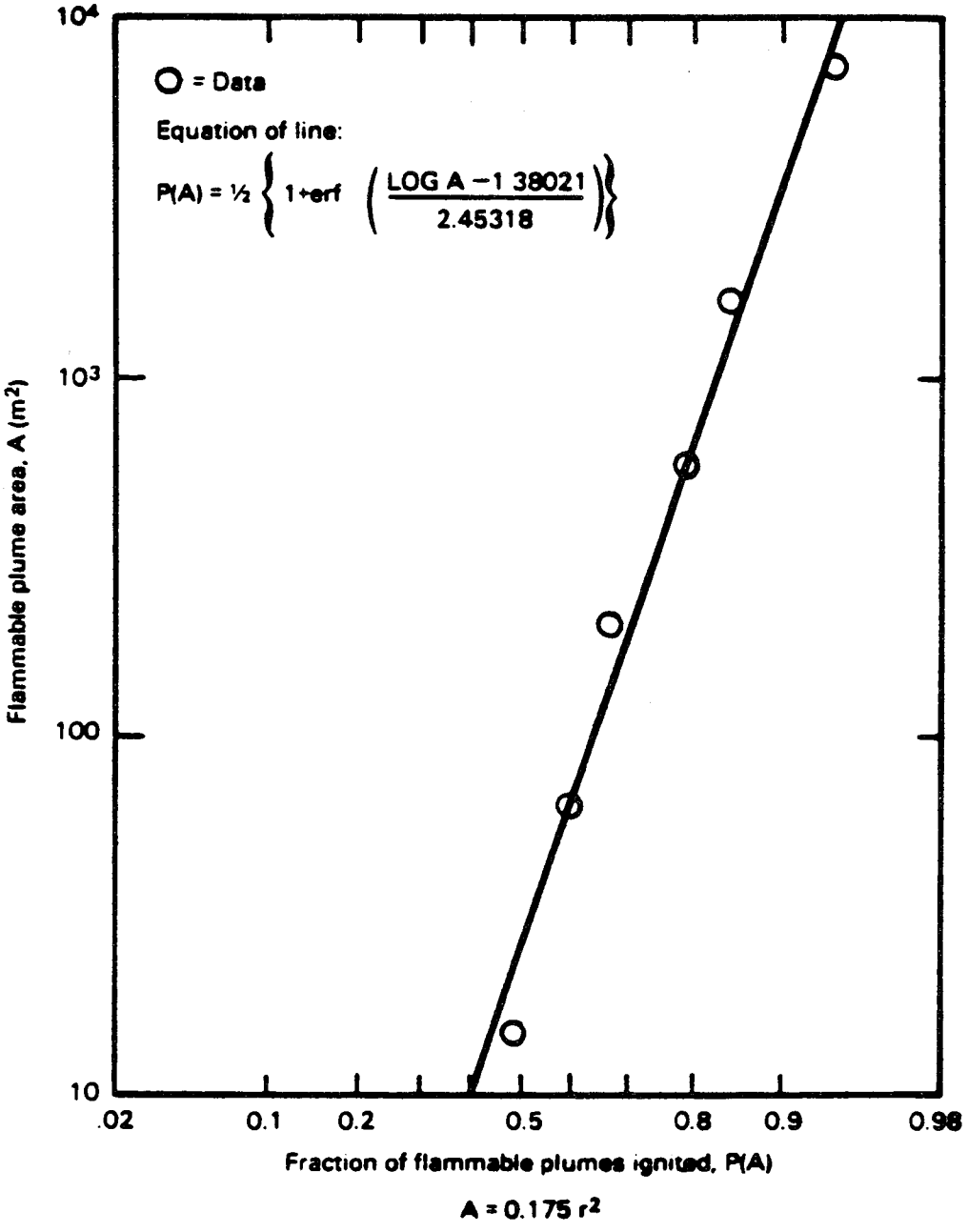

Figure 3.4-14. Probability of Flammable-Plume Ignition Versus Plume Area at Time of Ignition

Reproduced from Eichler 1978.

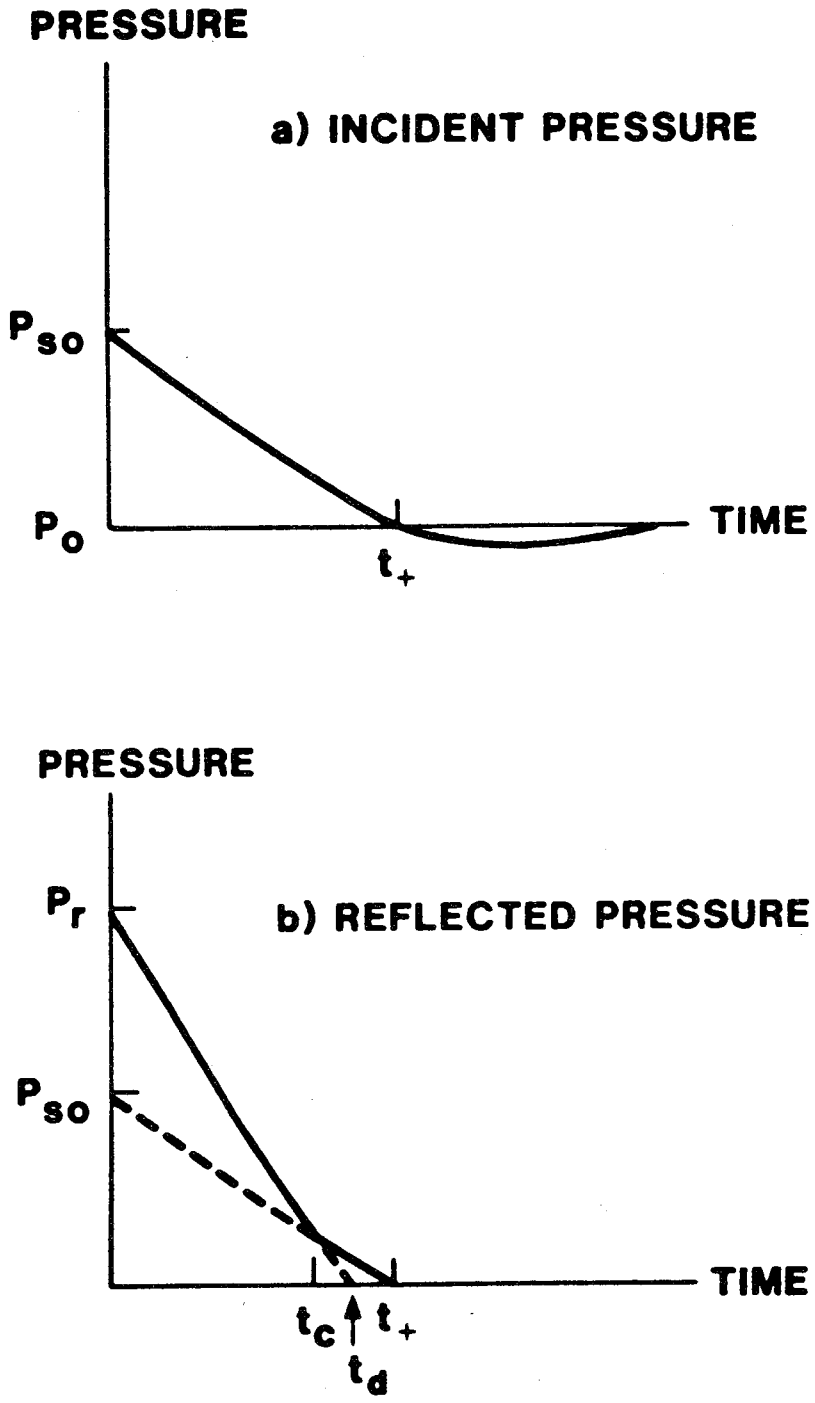

Figure 3.4-15. Pressure Pulses From TNT

Reproduced from Kennedy 1983.

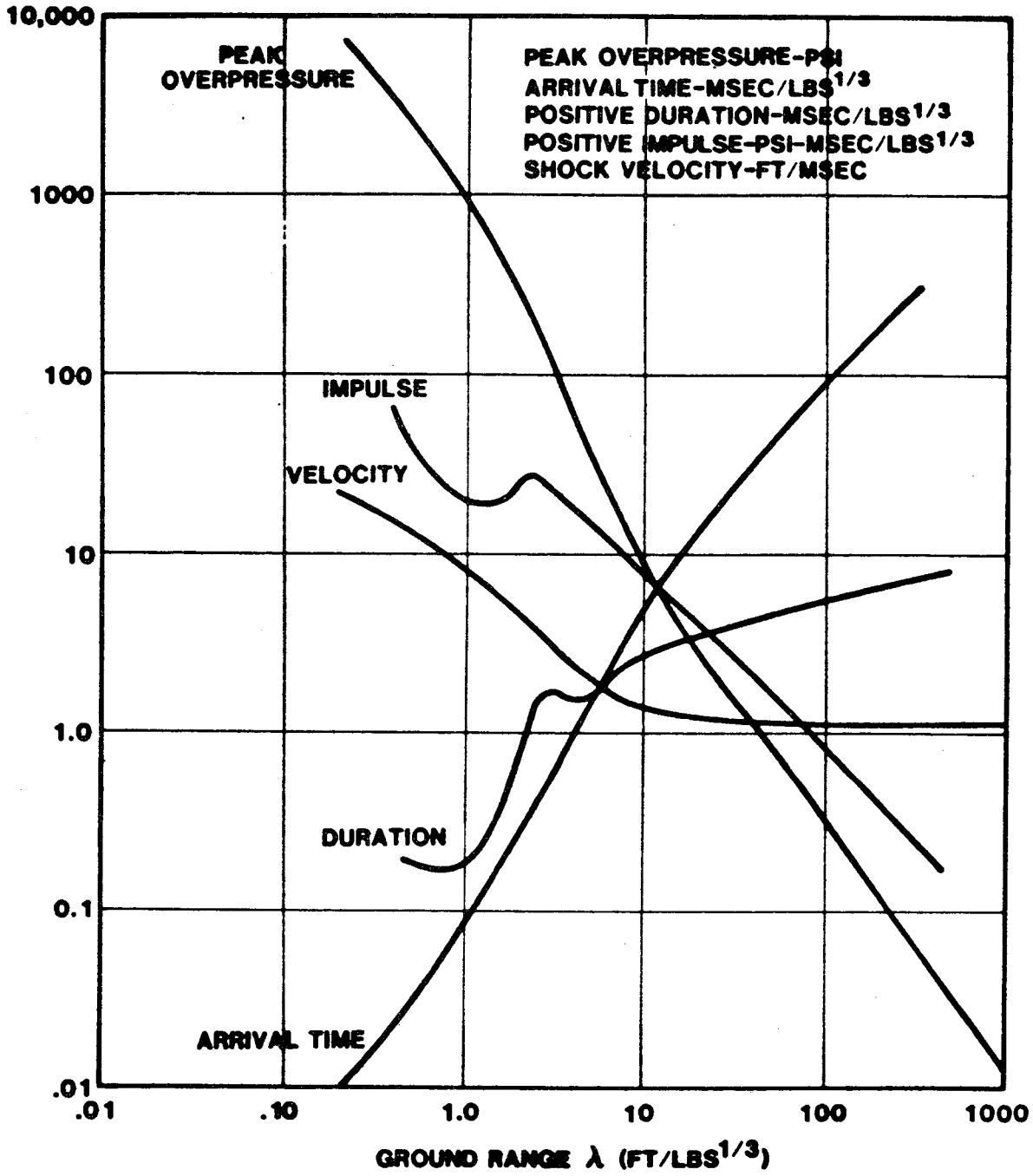

Figure 3.4-16. Free-Field Blast Wave Parameters Versus Scaled Distance for TNT Surface Bursts (Hemispherical Charges)

Reproduced from Kennedy 1983.

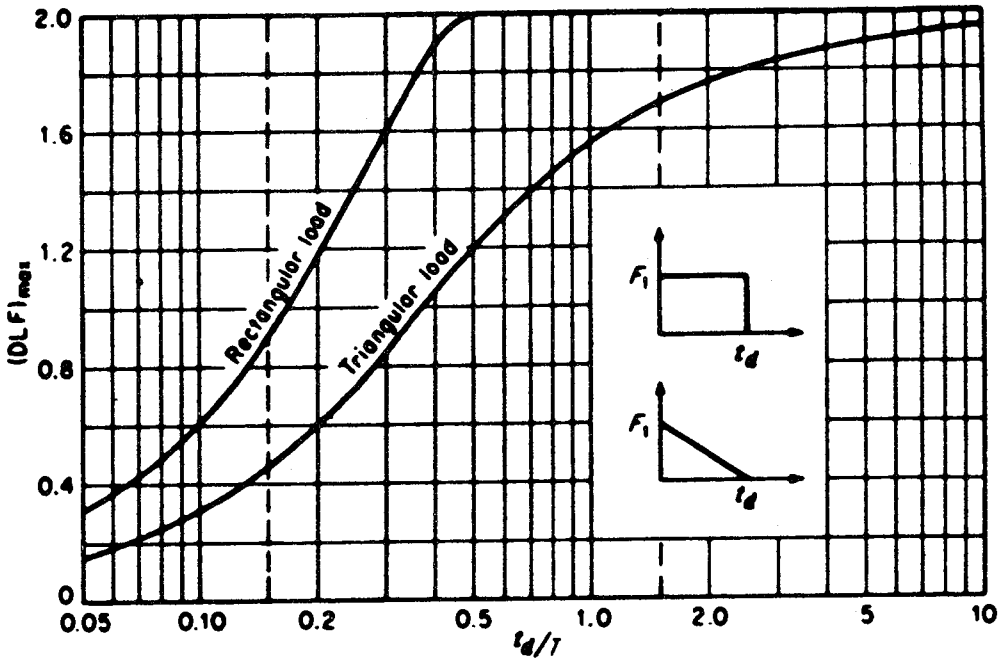

Figure 3.4-17. Dynamic Load Factors. Maximum response of one-degree elastic systems (undamped) subjected to rectangular and triangular load pulses having zero rise time.

Reproduced from Biggs 1964 with permission.

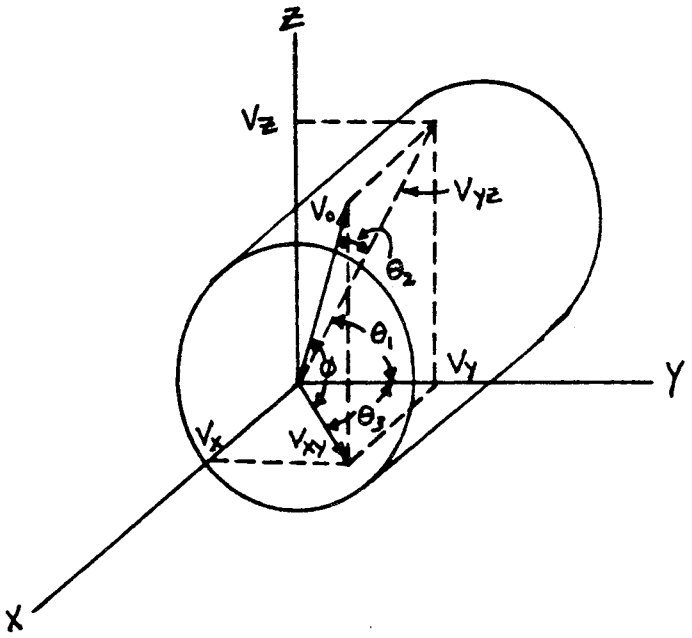

V_O Initial Velocity

θ_1 Angle from Y Axis to V_{yz}, $0 \leq \theta, \leq 90°$

θ_2 Angle from YZ Plant To V_0, $-\Delta \leq \theta_2 \leq \Delta$, $\Delta < 5$ (Inner Disk); $0 \leq \theta_2 \leq \Delta$, $\Delta \leq 25°$ (Outer Disk)

θ_3 Angle on the Ground, $\_90° \leq \theta_3 \leq 90°$

Φ Angle from Ground to V_0, $\theta_2 \rightarrow 0$, Then $\Phi \rightarrow \theta_1$

Figure 3.4-18. Variables and Terminology Used in Calculating Missile Strike Probabilities

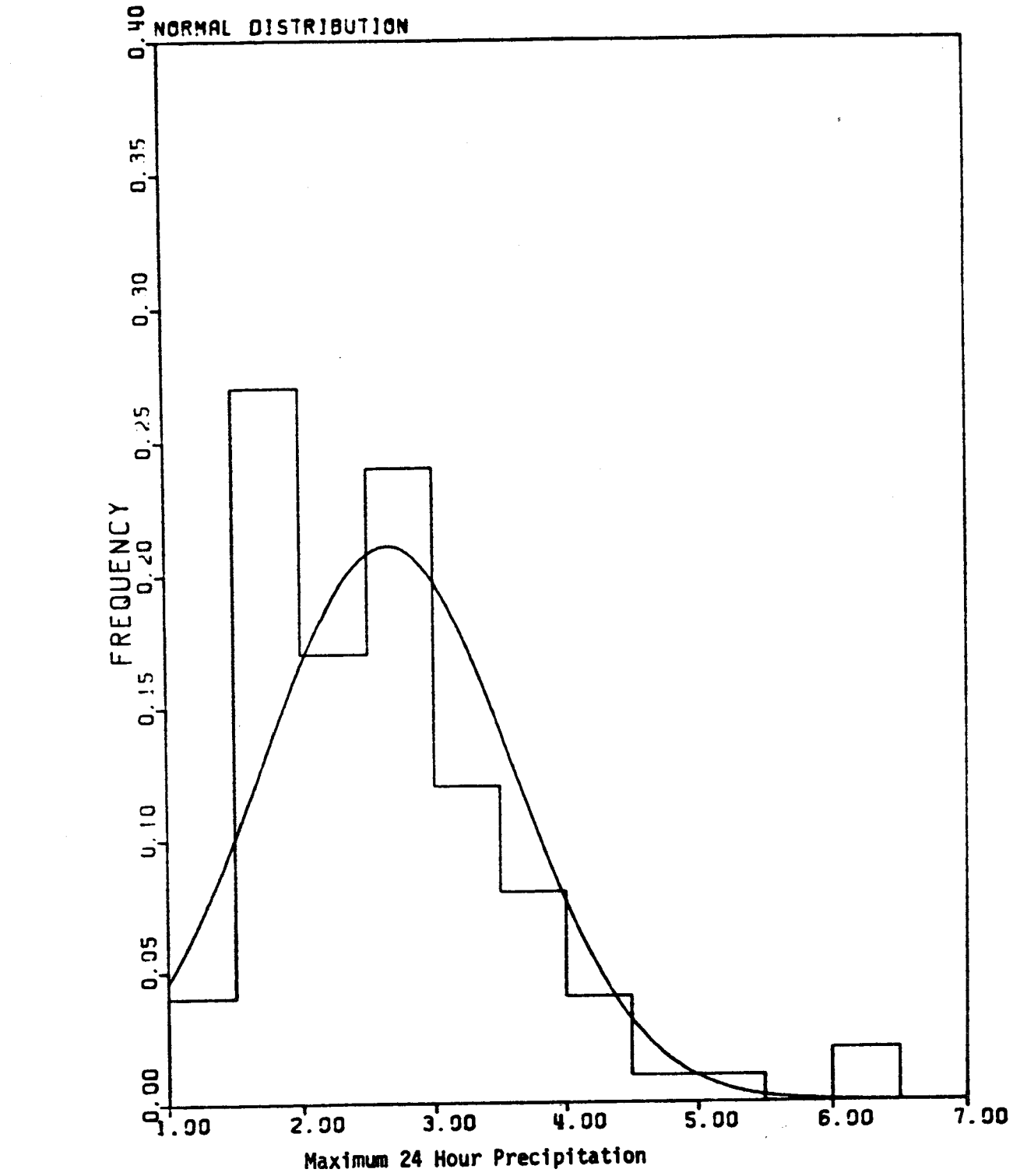

Figure 3.4-19. Histogram of Maximum Daily Precipitation for Chicago

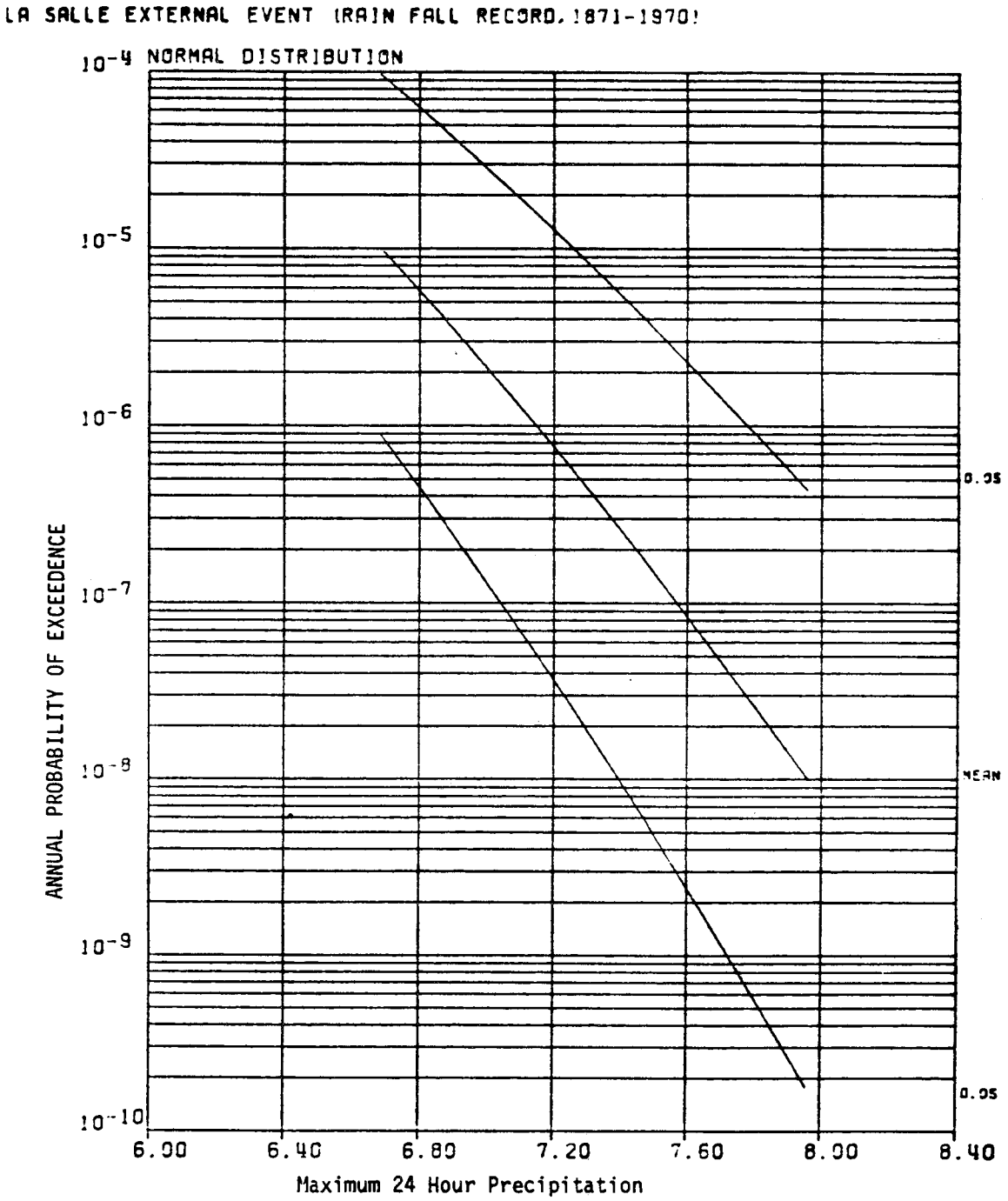

Figure 3.4-20. Normal Distribution Fit for Maximum Daily Precipitation

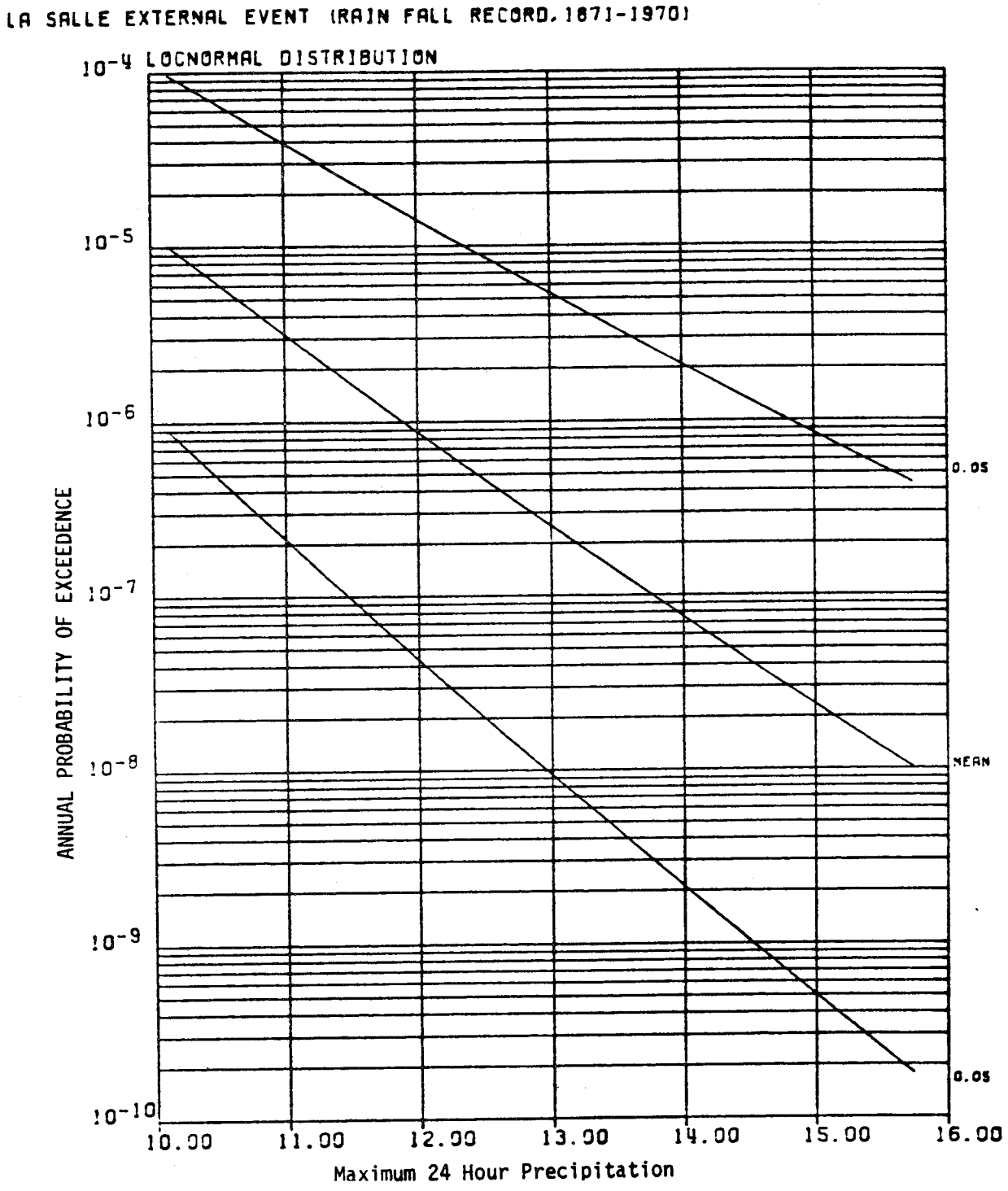

Figure 3.4-21. Lognormal Distribution Fit For Maximum Daily Precipitation

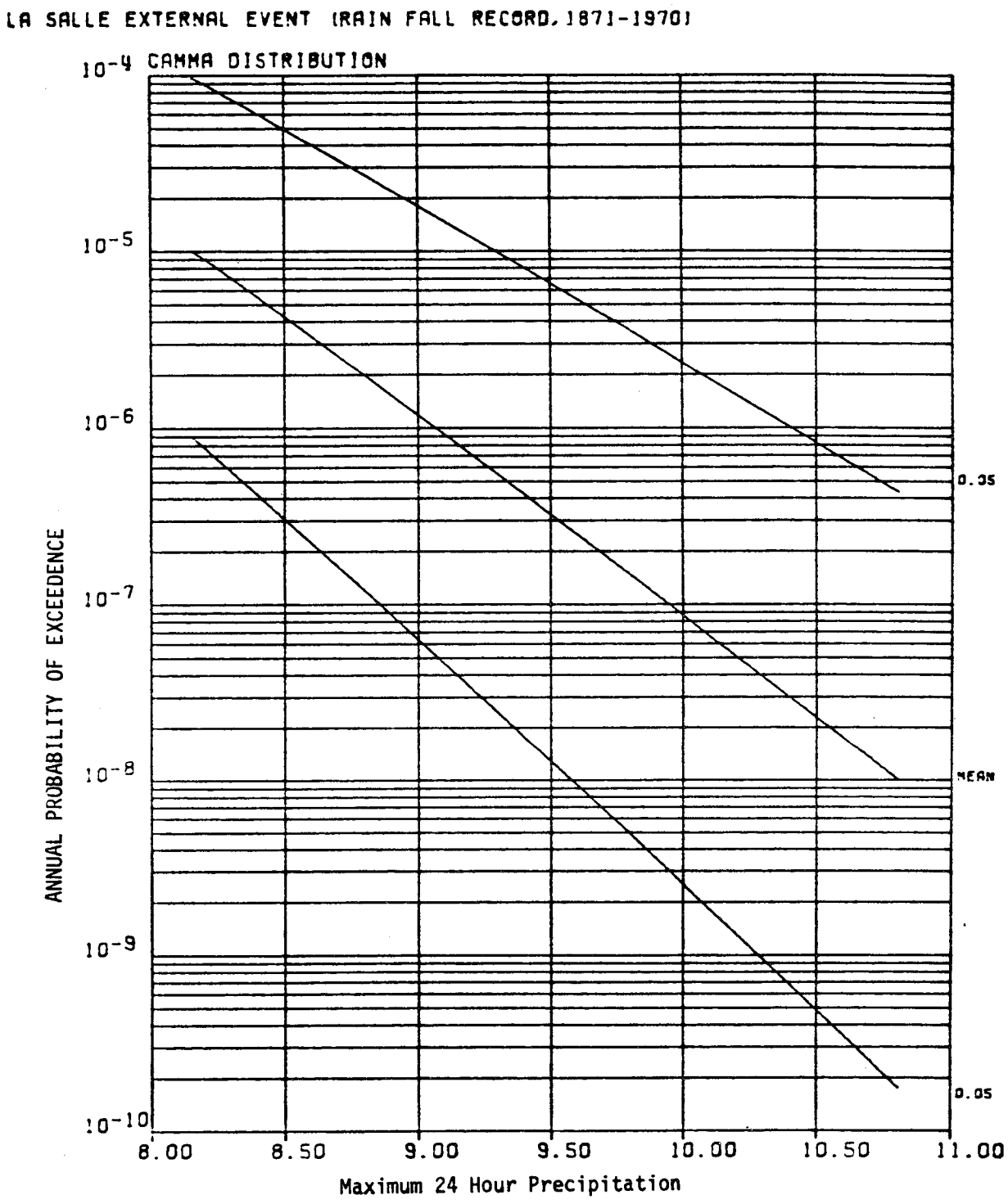

Figure 3.4-22. Gamma Distribution Fit for Maximum Daily Precipitation

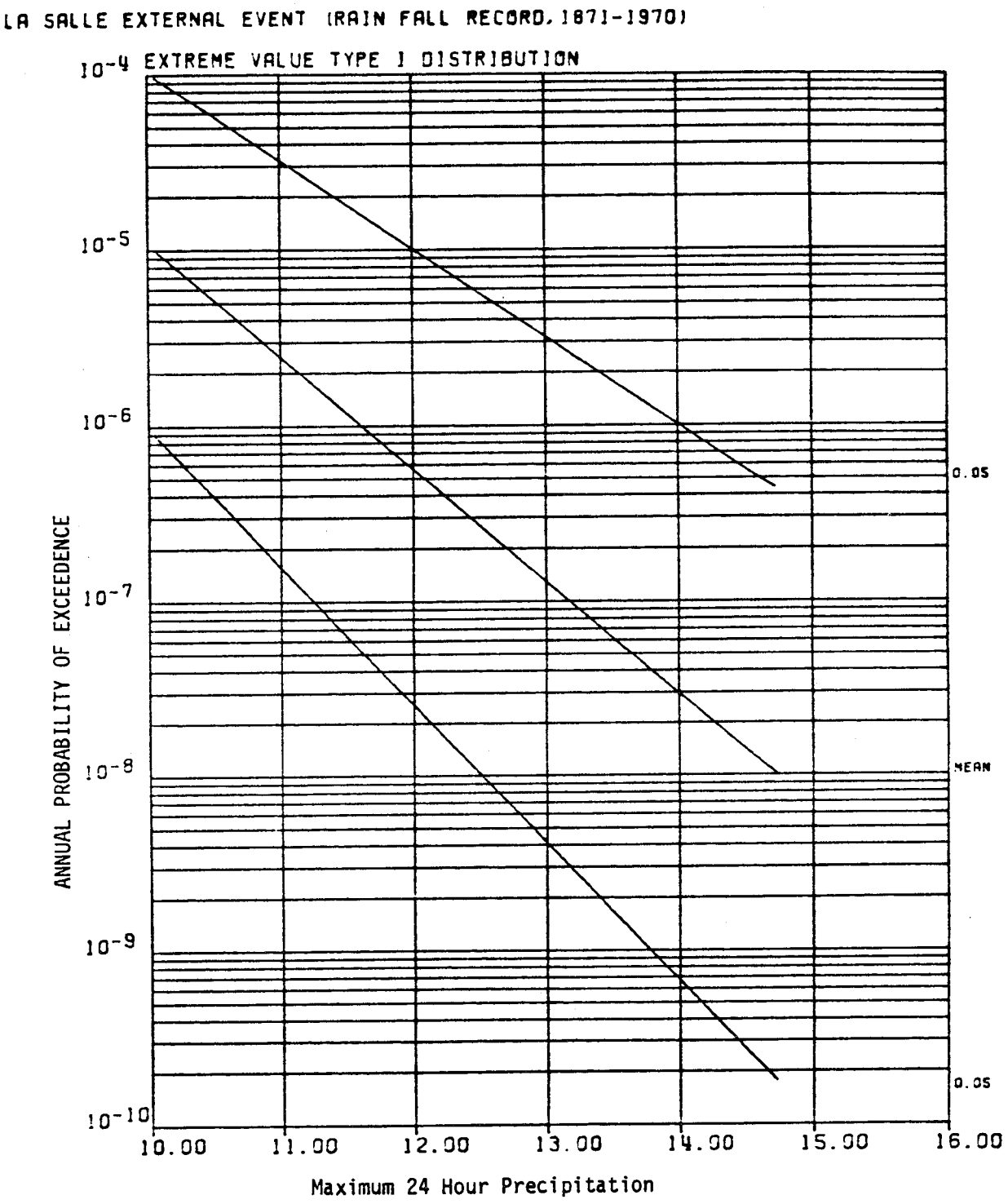

Figure 3.4-23. Extreme Value Type I Distribution Fit For Maximum Daily Precipitation

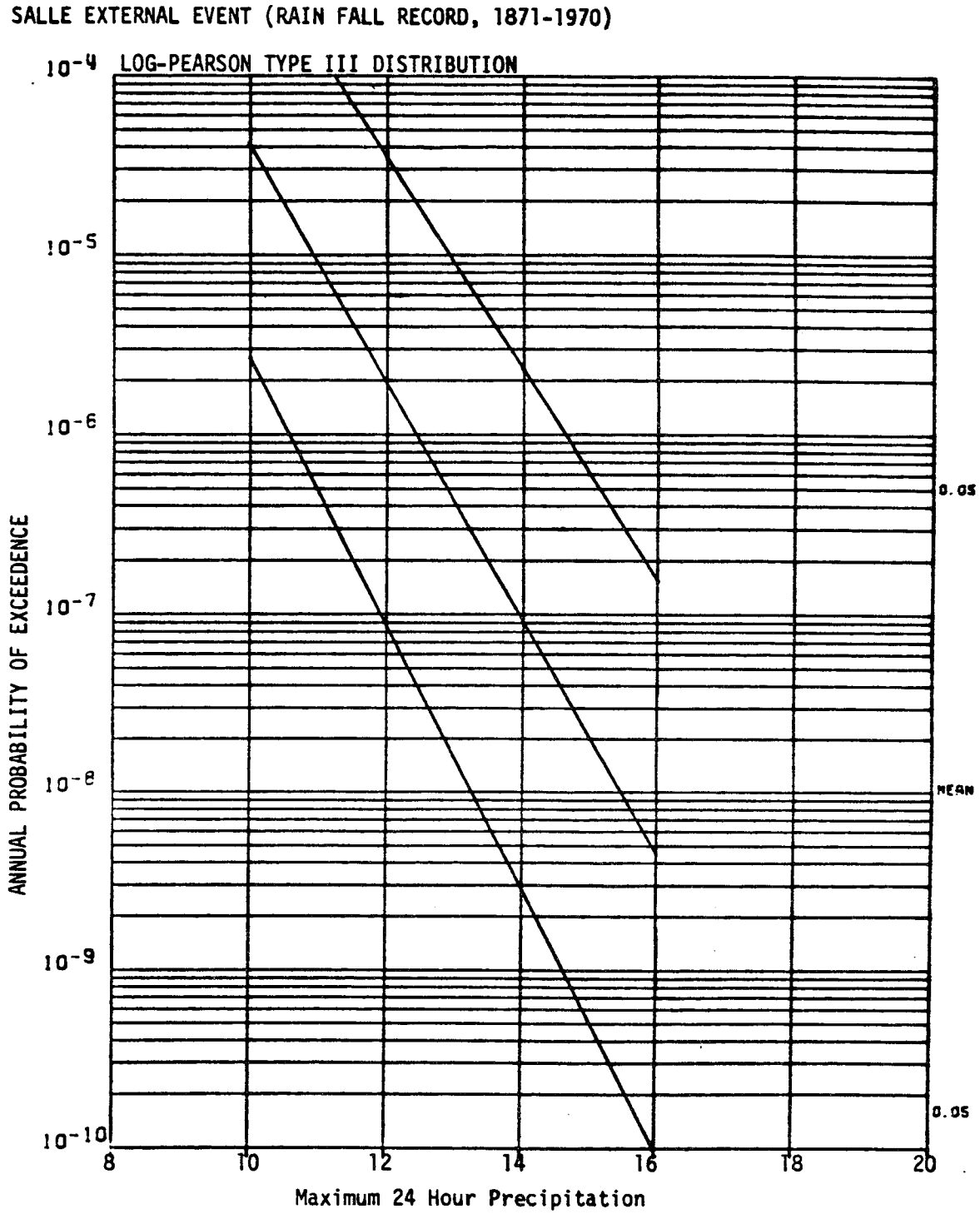

Figure 3.4-24. Log-Pearson Type III Distribution Fit for Maximum Daily Precipitation

3.5 Events Requiring Detailed PRA

Bounding analyses for the events which could not be excluded based on the initial screening process were presented in Section 3.4. These events included aircraft impact, winds and tornadoes, transportation accidents, turbine generated missiles and external flooding. Among these external events, aircraft impact and tornadoes were found to be potential contributors to the plant risk. Based on the bounding analysis for aircraft impact, the median frequency of core damage was found to be equal to 5×10^{-7}/year. Also, the uncertainty analysis showed that the 95 percent confidence bound for the frequency of damage due to aircraft impact is 10^{-6}/year. For tornadoes, the median frequency of core damage was calculated to be 3×10^{-8}/year whereas the 95 percent confidence bound was calculated to be 3×10^{-7}/year. As mentioned in Section 3.4, the bounding analyses did not account for the plant systems failures and accident sequences leading to a core damage and, therefore, was generally conservative. In light of the conservatism in the bounding analyses and also the low frequencies of core damage for aircraft impact and tornadoes, it was concluded that the external events considered in this scoping quantification study are not significant contributors to the plant risk. However, a detailed evaluation of aircraft impact risk to the LaSalle site may become necessary if the contribution of internal events to the risk is found to be less than 10^{-6}/year.

4.0 SUMMARY AND RECOMMENDATIONS

A scoping quantification study was performed for the LaSalle County Station to determine the external events which should be included in the detailed PRA study performed as part of the RMIEP program. Section 4.1 summarizes the results and Section 4.2 presents the recommendations of this study.

4.1 Summary

The scoping quantification study which was performed here considered all possible external events at the site except for internal flooding, seismic and fire events, i.e., these three events were included in a detailed external events analysis. The PRA Procedures Guide (1983) was used as a guideline for identification of all possible external events at the LaSalle site. Next, an initial screening process was carried out to eliminate some of the events from the list. For this purpose, a set of screening criteria was developed and then each external event was examined for possible elimination based on these criteria. After the initial screening process was completed, the following events were found to be potential contributions to the plant risk.

1. Military and industrial facilities accidents
2. Pipeline accidents
3. Release of chemicals in onsite storage
4. Aircraft impact
5. Extreme winds and tornadoes
6. Transportation accidents
7. Turbine generated missiles
8. External flooding

The top three events in this group were eliminated based on the analyses and information which is presented in the LaSalle FSAR.

A probabilistic bounding analysis was performed for each of the remaining five events in the above list. The degree of sophistication in the bounding analysis for each event was dependent on whether the event could be eliminated based on only a hazard analysis or a complete analysis including hazard analysis, fragility evaluation, and response analysis. However, the plant system and accident sequence analysis was conservatively neglected for these external events.

For aircraft impact, the median frequency of core damage was calculated as 5×10^{-7}/year whereas the 95 percent confidence bound was found to be 10^{-6}/year. An evaluation of the plant

structures for extreme winds and tornadoes revealed that extreme winds do not dominate the response and therefore could be eliminated from the bounding analysis. The median frequency of plant core damage due to tornadoes was calculated to be 3 x 10^{-8}/year, and its 95 percent confidence bound was found to be 3 x 10^{-7}/year. The bounding analysis for transportation accidents including toxic chemical release and chemical explosions showed that these accidents do not significantly contribute to the plant risk. For turbine generated missiles, the FSAR analysis was re-examined in light of new information regarding the generation of such missiles. It was concluded that the 95 percent confidence bound on the frequency of a plant damage state due to turbine missiles is on the order of 10^{-7}/year. The bounding analysis for external flooding showed that probability of occurrence of the probable maximum precipitation (PMP) at the site for which the plant has been designed for is indeed very low. Since the only credible mode of flooding at LaSalle is due to an intense local precipitation, this event could be eliminated from the detailed PRA study.

4.2 Recommendations

The bounding analysis of potential external events at the LaSalle site showed that only aircraft impact and tornadoes may be potential contributors to the plant risk. For aircraft impact, the 95 percent confidence bound on the frequency of core damage was calculated to be 10^{-6}/year and for tornadoes, the 95 percent confidence bound was calculated to be 3 x 10-^{7}/year. Since the bounding analysis did not consider the plant systems failures and consequence analysis, these frequencies are generally conservative. It is our judgement that none of the external events considered in this scoping quantification study is a significant contributor to the plant risk. However, if the PRA analysis for internal events should show that contribution of the internal events to the risk is less than 10^{-6}/year, then there may be a need to further examine aircraft impact and tornado events.

REFERENCES

Abbey, R. F., "Risk Probabilities Associated with Tornado Wind Speeds," Proceedings, Symposium on Tornadoes, Lubbock, Texas, June, 1976.

"Annual Review of Airport Accident Rates, Calendar Year 1980," National Transportation Safety Board, NTSB-ARG-80-1, May 1980.

Berriaud, C., Sokolovsky, A., Gueraud, R., Dulac, J., Labrot, R., and R. Avet-Flancard, "Local Behavior of the Reinforced Concrete Walls Under Missile Impact", Nuclear Engineering and Design, pp. 457-469, Vol. 45, 1978.

Biggs, J. M., Introduction to Structural Dynamics, McGraw-Hill Book Company, 1964.

Bobee, B., "The Log Pearson Type 3 Distribution and Its Application in Hydrology", Water Resources Research, Vol. II, No. 5, October 1975.

Bobee, B., "The Use of the Pearson Type 3 and Log Pearson Type 3 Distributions Revisited," Water Resources Research, Vol. 13, No. 2, April 1977.

Bush, S. H., "Probability of Damage to Nuclear Components Due to Turbine Failure," Nuclear Safety, Vol. 14, No. 3, May-June 1973.

Chang, W. S., "Impact of Solid Missiles on Concrete Barriers," Journal of the Structural Division, ASCE, Vol. 107, No. ST2, pp. 257-271, February 1981.

Changery, M. J., "Historical Extreme Winds for the United States - Great Lakes and Adjacent Regions," National Oceanic and Atmospheric Administration, NUREG/CR-2890, August 1982.

Chelapati, C. V., Kennedy, R. P. and I. B. Wall, "Probabilistic Assessment of Aircraft Hazard for Nuclear Power Plants," Nuclear Engineering and Design, 1972.

Eichler, T. V. and H. S. Napadensky, "Accidental Vapor Phase Explosions on Transportation Routes Near Nuclear Power Plants," IIT, Research Institute, Chicago, IL, NUREG/CR-0075, May 1978.

Eichler, T., Napadensky, H. and J. Mavec, "Evaluation of the Risks to the Marble Hill Nuclear Generating Station from Traffic on the Ohio River," Engineering Division, IIT Research Institute, Chicago, IL, October 1978.

Ellingwood, B., "Reliability Basis of Load and Resistance Factors for Reinforced Concrete Design," National Bureau of Standards, Washington, D.C., February 1978.

"FAA Statistical Handbook of Aviation, Calendar Year 1979," U.S. Department of Transportation, Federal Aviation Administration, December 1979.

Ferguson, P. M., Reinforced Concrete Fundamentals, Third Edition, John Wiley and Sons, 1973.

Filstein, E., and M. K. Ravindra, "Probability Analysis of Turbine Missile Hazard," Proceedings of ASCE/EMD Specialty Conference, Austin, Texas, September 1979.

Fujita, T. T. and A. D. Pearson, "Results of FPP Classification of 1971 and 1972 Tornadoes," Paper presented at the Eighth Conference on Severe Local Storms, October 1973.

Galambos, T. V. and M. K. Ravindra, "Properties of Steel for Use in LRFD," Journal of the Structural Division, ASCE, September 1978.

Garson, R. C., Catalan, J. M. and C. A. Cornell, "Tornado Design Winds Based on Risk", Department of Civil Engineering, MIT, August 1974.

General Electric Company, "Memo Report - Hypothetical Turbine Missiles - Probability of Occurrence," March 14, 1973.

General Electric Company, "Memo Report - Hypothetical Turbine Missile Data 38-Inch Last-Stage Bucket Units," March 16, 1973.

Ho, F. P. and J. T. Riedel, "Seasonal Variation of 10-Square-Mile Probable Maximum Precipitation Estimates - United States East of 105th Meridian," U. S. National Weather Service, Silver Springs, MD, NUREG/CR-1486, June 1980.

Kennedy, R. P., Blejwas, T. E. and D. E. Bennett, "Capacity of Nuclear Power Plant Structures to Resist Blast Loadings," Sandia National Laboratories, Albuquerque, NM, NUREG/CR-2462, SAND83-1250, September 1983.

Letter from Department of Transportation (FAA) to S. Hallaron, Sargent and Lundy Engineers, June 15, 1984.

"LaSalle County Station, Final Safety Analysis Report," Commonwealth Edison Company.

Markee, E. J., Beckerley, J. G. and K. E. Sanders," Technical Basis for Interim Regional Tornado Criteria," WASH 1300, U.S. Government Printing Office, Washington, May 1974.

McDonald, J. R., "A Methodology for Tornado Hazard Probability Assessment," Texas Tech University, Lubbock, TX, NUREG/CR-3058, October 1983.

Mirza, S. A. and J. G. MacGregor, "Variability of Mechanical Properties of Reinforcing Bars," Journal of the Structural Division, ASCE, May 1979.

Mirza, S. A., Hatzinikolas, M. and J. G. MacGregor, "Statistical Descriptions of Strength of Concrete," Journal of the Structural Division, ASCE, June 1979.

Niyogi, P. K. et. al., "Safety Design of Nuclear Power Plants Against Aircraft Impacts," Proceedings of Topical Meeting on Thermal Reactor Safety, Sun Valley, Idaho, July 31 - August 4, 1977.

NSAC (Nuclear Safety Analysis Center, Electric Power Research Institute), "Lightning Problems and Protection at Nuclear Power Plants," NSAC/41, December 1981.

Park, P. and T. Paulay, Reinforced Concrete Structures, John Wiley and Sons, 1975.

Patton, E. M., et. al., "Probabilistic Analysis of Low-Pressure Steam Turbine-Missile Generation Events," Battelle Pacific Northwest Laboratories, EPRI NP-2749, August 1983.

"Midland Probabilistic Risk Assessment," Consumer Power Company, Midland, MI, 1984.

Reinhold, T. A. and B. Ellingwood, "Tornado Damage Risk Assessment," National Bureau of Standards, Washington, DC, NUREG/CR-2944, September 1982.

Ravindra, M. K. and H. Banon, "Methods for External Event Screening Quantification: Risk Methods Integration and Evaluation Program (RMIEP) Methods Development," prepared for Sandia National Laboratories, NUREG/CR-4839, SAND87-7156, March 1992

"Seabrook Probabilistic Safety Study," Pickard, Lowe and Garrick, Inc., Newport Beach, California, 1983.

Semanderes, S. N., "Methods for Determining the Probability of a Turbine Missile Hitting a Particular Plant Region," Westinghouse Topical Report WCAP-7861, February 1972.

Philadelphia Electric Company, Severe Accident Risk Assessment, Limerick Generating Station, Philadelphia, PA, 1983.

Schaefer, J. T., Kelley, D. L. and R. F. Abbey, "Tornado Track Characteristics and Hazard Probabilities," Proceedings of the Fifth International Conference on Wind Engineering, Pergamon Press, New York, 1980.

Sliter, G. E., "Assessment of Empirical Concrete Impact Formulas," Journal of the Structural Division, ASCE, May 1980.

Sliter, G. E., Chu, B. B. and M. K. Ravindra, "EPRI Research on Turbine Missile Effects in Nuclear Power Plants," Transactions of 7th International Conference on Structural Mechanics in Reactor Technology, Paper J8/5, Chicago, IL, pp. 403-409, 1983.

Stephenson, A. E., "Full Scale Tornado-Missile Impact Tests," Electric Power Research Institute, RP-399, August 1976.

Solomon, K. A. et. al., "Estimate of the Hazards to a Nuclear Reactor from the Random Impact of Meteorites," UCLA-ENG-7426, March 1974.

Southwest Research Institute, "Steam Turbine Disc Cracking Experience, Volume 2: Data Summaries and Discussion," Prepared for the Electric Power Research Institute, EPRI NP-2429, June 1982.

"Tornado-Borne Missile Speeds," NBSIR 76-1050, National Bureau of Standards, April 1976.

Twisdale, L. A. and W. L. Dunn, "Tornado Missile Simulation and Design Methodology," Research Triangle Institute, NP-2005, Vol. 1, August 1981.

Twisdale, L. A. and W. L. Dunn, "Probabilistic Analysis of Tornado Wind Risks," Journal of the Structural Division, ASCE, February 1983.

Twisdale, L. A. et al., "Probabilistic Analysis of Turbine-Missile Risks," Report prepared for the Electric Power Research Institute, EPRI NP-2749, February 1983.

Uman, M. A., Understanding Lightning, Bek Technical Publications, Inc., Caraegia, Pennsylvania, 1971.

United States Water Resources Council, "Guidelines for Determining Flood Frequency," US/WRC-1121, March 1976.

USNRC, "PRA Procedures Guide," NUREG/CR-2300, January, 1983.

USNRC, Regulatory Guide 1.115, "Protection Against Low-Trajectory Turbine Missiles."

USNRC, Regulatory Guide 1.91, "Evaluations of Explosions Postulated to Occur on Transportation Routes Near Nuclear Power Plants."

USNRC, Regulatory Guide 1.78, "Assumptions for Evaluating the Habitability of a Nuclear Power Plant Control Room During a Postulated Hazardous Chemical Release."

USNRC, Regulatory Guide 1.76, "Design Basis Tornado for Nuclear Power Plants."

USNRC, "Safety Evaluation Report Related to the Operation of Perry Nuclear Power Plant Units 1 and 2," NUREG/0887, Supplement No. 3, 1983.

USNRC, "Standard Review Plan for the Review of Safety Analysis Reports for Nuclear Power Plants," NUREG-0800-75/087, 1975.

Wen, Y-K, "Note on Analytical Modeling in Assessment of Tornado Risk," Proceedings, Symposium on Tornadoes, Lubbock, Texas, June 1976.

Distribution

James Abel
Commonwealth Edison Co.
35 1st National West
Chicago, IL 60690

Kiyoharu Abe
Department of Reactor Safety
Research
Nuclear Safety Research Center
Tokai Research Establishment
JAERI
Tokai-mura, Naga-gun
Ibaraki-ken,
JAPAN

Bharat B. Agrawal
USNRC-RES/PRAB
MS: NLS-372

J. Alman
Commonwealth Edison Co.
LaSalle County Station
RR1, Box 220
2601 North 21st Rd.
Marsielles, IL 61341

George Apostolakis
UCLA
Boelter Hall, Room 5532
Los Angeles, CA 90024

Vladimar Asmolov
Head, Nuclear Safety Department
I. V. Kurchatov Institute
of Atomic Enegry
Moscow, 123182
U.S.S.R.

H. Banon
Exxon Production Research
P.O. Box 2189
Houston, TX 77252-2189

Patrick W. Baranowsky
USNRC-AEOD/TPAB
MS: 9112

Robert A. Bari
Brookhaven National Laboratories
Building 130
Upton, NY 11973

Richard J. Barrett
USNRC-NRR/PD3-2
MS: 13 D1

William D. Beckner
USNRC-NRR/PRAB
MS: 10 E4

Dennis Bley
Pickard, Lowe & Garrick
2260 University Drive
Newport Beach, CA 92660

Gary Boyd
Safety & Reliability Optimization
Services
9724 Kingston Pike, Suite 102
Knoxville, TN 37922

Robert J. Budnitz
Future Resources Associates
734 Alameda
Berkeley, CA 94707

Gary R. Burdick
USNRC-RES/RPSIB
MS: NLS-314

Arthur J. Buslik
USNRC-RES/PRAB
MS: NLS-372

Annick Carnino
Electricite de France
32 Rue de Monceau 8EME
Paris, F5008
FRANCE

S. Chakraborty
Radiation Protection Section
Div. De La Securite Des Inst. Nuc.
5303 Wurenlingen
SWITZERLAND

Michael Corradini
University of Wisconsin
1500 Johnson Drive
Madison, WI 53706

George Crane
1570 E. Hobble Creek Dr.
Springville, Utah 84663

Mark A. Cunningham
USNRC-RES/PRAB
MS: NLS-372

G. Diederick
Commonwealth Edison Co.
LaSalle County Station
RR1, Box 220
2601 North 21st Rd.
Marsielles, IL 61341

Mary T. Drouin
Science Applications International
Corporation
2109 Air Park Road S.E.
Albuquerque, NM 87106

Adel A. El-Bassioni
USNRC-NRR/PRAB
MS: 10 E4

Robert Elliott
USNRC-NRR/PD3-2
MS: 13 D1

Farouk Eltawila
USNRC-RES/AEB
MS: NLN-344

John H. Flack
USNRC-RES/SAIB
MS: NLS-324

Karl Fleming
Pickard, Lowe & Garrick
2260 University Drive
Newport Beach, CA 92660

James C. Glynn
USNRC-RES/PRAB
MS: NLS-372

T. Hammerich
Commonwealth Edison Co.
LaSalle County Station
RR1, Box 220
2601 North 21st Rd.
Marsielles, IL 61341

Robert A. Hasse
USNRC-RGN-III
MS: RIII

Sharif Heger
UNM Chemical and Nuclear
Engineering Department
Farris Engineering
Room 209
Albuquerque, NM 87131

P. M. Herttrich
Federal Ministry for the
Environment, Preservation of
Nature and Reactor Safety
Husarenstrasse 30
Postfach 120629
D-5300 Bonn 1
FEDERAL REPUBLIC OF GERMANY

S. Hirschberg
Department of Nuclear Energy
Division of Nuclear Safety
International Atomic Energy Agency
Wagramerstrasse 5, P.O. Box 100
A-1400 Vienna
AUSTRIA

M. Dean Houston
USNRC-ACRS
MS: P-315

Alejandro Huerta-Bahena
National Commission on Nuclear
Safety and Safeguards (CNSNS)
Insurgentes Sur N. 1776
C. P. 04230 Mexico, D. F.
MEXICO

Peter Humphreys
US Atomic Energy Authority
Wigshaw Lane, Culcheth
Warrington, Cheshire
UNITED KINGDOM, WA3 4NE

W. Huntington
Commonwealth Edison Co.
LaSalle County Station
RR1, Box 220
2601 North 21st Rd.
Marsielles, Il 61341

Brian Ives
UNC Nuclear Industries
P. O. Box 490
Richland, WA 99352

William Kastenberg
UCLA
Boelter Hall, Room 5532
Los Angeles, CA 90024

George Klopp [10]
Commonwealth Edison Company
P.O. Box 767, Room 35W
Chicago, IL 60690

Alan Kolaczkowski
Science Applications Int. Corp.
2109 Air Park Rd. SE
Albuquerque, NM 87106

Jim Kolanowski
Commonwealth Edison Co.
35 1st National West
Chicago, IL 60690

S. Kondo
Department of Nuclear Engineering
Facility of Engineering
University of Tokyo
3-1, Hongo 7, Bunkyo-ku
Tokyo
JAPAN

Jose A. Lantaron
Cosejo de Suguridad Nuclear
Sub. Analisis y Evaluaciones
Justo Dorado, 11
28040 Madrid
SPAIN

Josette Larchier-Boulanger
Electricte de France
Direction des Etudes Et Recherches
30, Rue de Conde
65006 Paris
FRANCE

Librarian
NUMARC/USCEA
1776 I Street NW, Suite 400
Washington, DC 80006

Bo Liwnang
IAEA A-1400
Swedish Nuclear Power Inspectorate
P.O. Box 27106
S-102 52 Stockholm
SWEDEN

Peter Lohnberg
Expresswork International, Inc.
1740 Technology Drive
San Jose, CA 95110

Steven M. Long
USNRC-NRR/PRAB
MS: 10 E4

Herbert Massin
Commonwealth Edison Co.
35 1st National West
Chicago, IL 60690

Andrew S. McClymont
IT-Delian Corporation
1340 Saratoga-Sunnyvale Rd.
Suite 206
San Jose, CA 95129

Jose I. Calvo Molins
Head, Division of P.S.A. and Human Factors
Consejo De Seguridad Nuclear
Justo Dorado, 11
28040 Madrid
SPAIN

Joseph A. Murphy
USNRC-RES/DSR
MS: NLS-007

Kenneth G. Murphy, Jr.
US Department of Energy
19901 Germantown Rd.
Germantown, MD 20545

Robert L. Palla, Jr.
USNRC-NRR/PRAB
MS: 10 E4

Gareth Parry
NUS Corporation
910 Clopper Rd.
Gaithersburg, MD 20878

G. Petrangeli
ENEA Nuclear Energy ALT Disp
Via V. Brancati, 48
00144 Rome
ITALY

Ing. Jose Antonio Becerra Perez
Comision Nacional De Seguridad
Nuclear Y Salvaguardias
Insurgentes Sur 1806
01030 Mexico, D. F.
MEXICO

William T. Pratt
Brookhaven National Laboratory
Building 130
Upton, NY 11973

William Raisin
NUMARC
1726 M. St. NW
Suite 904
Washington, DC 20036

D. M. Rasmuson
USNRC-RES/SAIB
MS: NLS-372

M. K. Ravindra [10]
EQE Inc.
2150 Bristol St., Suite 350
Costa Mesa, CA 92626

John N. Ridgely
USNRC-RES/SAIB
MS: NLS-324

Richard C. Robinson Jr.
USNRC-RES/PRAB
MS: NLS-372

Denwood F. Ross
USNRC-AEOD
MS: 3701

Christopher P. Ryder [10]
USNRC-RES/PRAB
MS: NLS-372

Takashi Sato
Deputy Manager
Nuclear Safety Engineering Section
Reactor Design Engineering Dept.
Nuclear Energy Group
Toshiba Corporation
Isogo Engineering Center
8, Shinsugita-cho, Isogo-ku,
Yokohama 235,
JAPAN

Martin Sattison
Idaho National Engineering Lab.
P. O. Box 1625
Idaho Falls, ID 83415

Louis M. Shotkin
USNRC-RES/RPSB
MS: NLN-353

Desmond Stack
Los Alamos National Laboratory
Group Q-6, Mail Stop K556
Los Alamos, NM 87545

T. G. Theofanous
University of California, S. B.
Department of Chemical and Nuclear
Engineering
Santa Barbara, CA 93106

Harold VanderMolen
USNRC-RES/PRAB
MS: NLS-372

Magiel F. Versteeg
Ministry of Social Affairs and Employment
P.O. Box 90804
2509 LV Den Haag
THE NETHERLANDS

Edward Warman
Stone & Webster Engineering Corp.
P.O. Box 2325
Boston, MA 02107

Wolfgang Werner
Gesellschaft Fur Reaktorsicherheit
Forschungsgelande
D-8046 Garching
FEDERAL REPUBLIC OF GERMANY

3141 S. A. Landenberger [5]
3151 G. L. Esch
6321 T. A. Wheeler
6400 N. R. Ortiz
6410 D. A. Dahlgren
6411 D. D. Carlson
6411 D. M. Kunsman
6411 R. J. Breeding
6411 K. J. Maloney
6412 A. L. Camp
6412 S. L. Daniel
6412 S. E. Dingman
6412 B. D. Staple
6412 G. D. Wyss
6412 A. C. Payne, Jr. [25]
6412 D. W. Whitehead
6413 F. T. Harper
6413 T. D. Brown
6419 M. P. Bohn
8524 J. A. Wackerly